IN VIVO SWELLING KINETICS OF A SERIES OF HYDROGEL POLYMERS IN THE GASTROINTESTINAL TRACT OF THE CANNULATED CANINE

by

Eliot M. Slovin

A dissertation submitted in partial fulfillment
of the requirements for the degree of

Doctor of Philosophy
(Pharmacy)

at the

UNIVERSITY OF WISCONSIN - MADISON

1997

Dedicated with all my love to

Lynn, Ayelet and Margalit

IN VIVO SWELLING KINETICS OF A SERIES OF HYDROGEL POLYMERS IN THE CANNULATED GASTROINTESTINAL TRACT OF THE CANINE

Eliot M. Slovin

Hydrogels for oral controlled drug delivery must swell at a predictable rate as they move through the various regions of the gastrointestinal tract. Residence time in these different regions, coupled with available water and local environmental conditions, can potentially influence the rate and extent of swelling.

The objective of this study is to regio-specifically study the *in-vivo* swelling behavior of four hydrogel polymers in the duodenal and ileal regions of the small intestine of cannulated canines in fasted and fed states. The four polymers were hydroxypropyl methyl cellulose, carboxylmethyl cellulose sodium salt, Carbopol 974P™, and Noveon AA1™ (polycarbophil). The fed state was generated by gavage feeding of either water or Pulmocare™. Atropine sulfate, a naturally occurring antimuscarinic known to inhibit gastric and duodenal secretions, administered intravenously allowed us to study the effect of these secretions on the polymer swelling.

Information gathered from these *in-vivo* studies, combined with data previously reported in the literature and data generated by a series of *in-vitro* studies, enabled us to design a computer generated kinetic model to describe polymer swelling and movement of fluid, spatially and temporally, through the

gastrointestinal tract using STELLA™, a simulation software package for handling compartment models.

For each of the hydrogels studied, swelling was observed to be greater in the duodenum than the ileum. *In-vivo* swelling appears not to be strongly influenced by the fluid ingested per os nor by the gastric and duodenal secretions. In addition, the extent of swelling was seen to be independent of the timing of the insertion or ingestion of the polymer relative to the migrating myoelectric complex (MMC). Through intravenous injections of atropine sulfate to shut down gastric and duodenal secretions, *in vivo* polymer swelling was seen not to be affected by the presence or absence of these gastrointestinal secretions. We therefore propose that the fluid necessary for polymer swelling is primarily derived from the aqueous mucous gel coating the epithelial cells lining the small intestine. Differences in swelling rate and extent in ileal and duodenal regions may be due to differences in the amount and thickness of mucous in the two regions.

ACKNOWLEDGMENTS

First and foremost, I would like to thank Professor Joseph R. Robinson for his continual encouragement and guidance. I sincerely appreciate his patience and interest offered me throughout the course of my graduate studies.

In addition, I wish to express my thanks to the many supportive faculty members, graduate students and other staff (of which there are too many to list individually) with whom I have associated during my stay at the University of Wisconsin for their conversations, suggestions and friendships. However, I would be remiss if I did not extend a special note of thanks to Professor Paul Bass for his time and helpful suggestions, to Professor Eberhard Rosin of the School of Veterinary Medicine for his surgical assistance, and to Mr. William Wade of Animal Care for his dedication to maintain an animal facility of the highest quality.

I also especially want to thank Mr. Brian Irons for his assistance in the design of the STELLA™ computer model as well as his patience in sharing with me his knowledge and experience of working with research canines.

I wish to gratefully acknowledge the financial support rendered by the Schering-Plough Research Institute, Kenilworth, NJ and by the Graduate School of the University of Wisconsin-Madison.

Finally, I would like to thank my wife, Lynn, and our daughters, Ayelet and Margalit, for their love and understanding

which made this work possible. Lynn, your demands have been small and your patience and understanding has been immeasurably great. Thank you.

Table of Contents

List of Tables

List of Figures

Hydrogels for oral controlled drug delivery swell as they move through the various regions of the gastrointestinal tract. Residence time in the different regions of the gastrointestinal tract, coupled with available water and local environmental conditions, can potentially influence the rate and extent of swelling. *In-vivo* polymer swelling studies have not been reported with the assumption that *in-vitro* conditions adequately reflect *in-vivo* conditions. The inability to routinely develop good *in-vivo/in-vitro* correlations raises questions about the validity of this assumption.

While the reasons for these *in-vivo/in-vitro* correlation failures are not understood fully, they may, in part, be due to the absence of specific information on the availability of fluid in the different regions of the gastrointestinal tract. Fluid composition and properties will influence the rate and extent of polymer swelling.

I.1 The Research Objective

The unpredictable, and sometimes poor, polymer performance seen for many gastrointestinal formulations is in part due to the absence of any specific information on the regional specific swelling action of hydrating polymers *in-vivo*. Most of the information that is available to the researcher has been generated from many *in-vitro* studies with a lack of specific *in-vivo/in-vitro* correlations.

The current research was undertaken to study the *in-vivo* swelling behavior of a series of hydrogel polymers in the duodenal

and ileal regions of the small intestine of the canine. The information gathered from these studies, combined with data previously reported in the literature, as well as the data generated by a series of *in-vitro* studies, enabled the design of a kinetic model that describes polymer swelling and movement of fluid spatially and temporally through the gastrointestinal tract.

I.2 Introduction

Hydrogels are materials that, when placed in excess water, exhibit the ability to swell rapidly, and retain large quantities of water in their swollen structures while not dissolving. They are three dimensional networks of hydrophilic homopolymers or copolymers crosslinked either by chemical, ionic or covalent, bonds or other cohesive forces, e.g., hydrogen bonding, van der Waals forces or hydrophobic interactions.[1,2] While polymer insolubility and the stability of shape are due to this network, swelling results from a balance between dispersion forces on the hydrated chains and cohesive forces that do not prevent the penetration of water into the polymer.[3]

The ability of hydrogels to absorb up to thousands of times their dry weight in water is due to the presence of hydrophilic groups such as -OH, -CONH, $CONH_2$, -COOH and $-SO_3H$.[4] The amount of imbibed water determines the absorption and diffusion of solutes through the hydrogel. The hydrogel character is determined by the hydrophilic monomers and the density of the polymer network.[3]

The earliest uses of hydrogels in medicine involved natural tissue that, for all practical purposes, can be classified as a hydrogel. Cellulose, as in sausage casing, behaves as a hydrogel and has had a long history of use in medicine, particularly in hemodialysis applications.[5] Use of synthetic, polymeric hydrogels specifically designed for biomedical applications was first proposed by Wichterle and Lim[6] when they described the use of poly (2-hydroxyethyl methacrylate) cross linked gels (p-HEMA) for use as surgical implants and medical devices.[5] Their physical similarity to soft tissues, resistance to hydrolysis under *in-vivo* implantation and heat sterilizing conditions, and permeability to electrolytes and metabolites were some of the properties that made these gels attractive.[7]

Many biomedical applications for hydrogels have appeared in the literature attributing both to their satisfactory *in-vivo* performance as well as their ability to be able to be fabricated into a wide range of forms. Among these are coatings for sutures and catheters,[8,9] drainage conduits for glaucoma surgery,[10] contact lenses,[6,11] artificial corneas,[12] dentures,[13] synthetic cartilage,[14] burn dressings,[15] organ prostheses[16,17] and drug delivery systems.[18,19]

There are many advantages for applying the use of hydrogels in drug delivery systems. Their swelling nature permits easy extraction of polymerization initiators, decomposition products and solvents prior to *in-vivo* use. Low hydrogel-water interfacial tension minimizes protein absorption and platelet adhesion. The soft, rubbery nature of hydrogels minimizes mechanical and frictional irritation

reducing pain and damage to surrounding tissue. Since the permeability of both hydrophilic and hydrophobic drugs, including charged solutes, depend upon the combination of copolymers, the ability to custom design the hydrogel synthesis allows for the development of unique systems for drug delivery.[5,20]

I.3 Hydrogel Swelling

In the dry state, hydrogels are usually hard and glassy. Once swollen in water or body fluids they permit the movement of drug out of the hydrogel network. Factors that influence swelling can be separated into two categories, those that are favorable for the entrance of water into the polymer network and those which resist or inhibit water influx. Some of these factors can be found listed in Table 1.[5] In addition, various factors innate to the polymer and solvent may influence the extent and rate of hydrogel swelling. Some of these can be found listed in Table 2.

The polymer gel is a cross-linked three dimensional network of polymer chains of macroscopic size. When immersed in a compatible fluid, the hydrogel expands by imbibing solvent. The cross-linking of the polymer chains prevents the gel from dissolving. The amount of swelling that occurs in the gel will depend on the cross-link density of the polymer as well as its compatibility with the solvent.[21]

Hydrogels can be neutral or ionic in nature. The driving force for swelling in neutral hydrogels arises from the water-polymer thermodynamic mixing contribution to the overall free energy.[4] The

Table 1 : Structural Factors which Influence Hydrogel Swelling

Favorable to swelling

- osmotic potential
- strong interactions with water
- high free volume
- high chain flexibility
- low cross-linking density

Resist or inhibit swelling

- weak interactions with water
- low free volume
- low chain flexibility
- high cross-linking density

Table 2 : Factors Controlling Swelling

Hydrogel Qualities

1. Hydrophilic Groups
   - polarity
   - concentration
2. Charged Groups
   - ionization
   - density
3. Physical Interactions
   - hydrophilic-hydrophobic balance
   - distribution of polar and non-polar groups

Swelling Medium Qualities

1. pH
2. medium composition
3. temperature

uncharged polymeric species is swellable due to functional groups that hydrate by forming hydrogen bonds with the imbibing water[22] thus extending the polymer chains. Water entry into the polymer network requires its expansion and consequently, an ordering of the polymer chains. Since the chains will be elongated into less entropically desirable configurations, they exert a resistive force. Swelling equilibrium occurs when the osmotic force driving water into the polymer is balanced by the resistive force exerted by the polymer chains.[4,5,22] Since increasing cross-link density has the effect of increasing the resistive force to chain elongation, the more highly cross-linked a hydrogel polymer, the lower the degree of swelling observed.[5]

The swelling of a polyelectrolyte hydrogel is unique due to the ionization ability of their functional groups. For swelling to occur, both solvent and ions must diffuse into the gel.[22] Weakly acidic or basic groups on the polymer dissociate depending upon the pH and ionic concentration of the outer solution. Counterions from the external solution to the ionized groups and the stiffness of the polymer chains increase the osmotic pressure acting to expand the hydrogel network. A volume change results.[23]

I.4 Physiochemical Effects on Swelling

I.4.1 Effect of pH on Swelling

Changing the pH of the outer solution will often cause a drastic change in the degree of swelling of the hydrogel. The sudden change occurs near the pK_a of the hydrogel.[5,24] In general, polyacid gels will be relatively unswollen at low pH due to suppression of ionization of the acidic groups. With increasing pH, the polyacid gel will swell to a greater degree.[21,25] The opposite holds for polybase hydrogels since ionization of the basic functional groups will increase as the pH decreases.[22] In other words, as summarized in Table 3, high pH is seen to decrease swelling in polybasic hydrogels while increasing the swelling of polyacidic gels.

I.4.2 Effect of Medium Composition on Swelling

The swelling behavior of hydrogels is affected by the polymeric network structure and polymer-solvent interactions. In the case of polyelectrolyte hydrogels, such as those containing weakly acidic or basic groups, sorption of the solvent is accompanied by ionization of the polymer. This ionization depends upon the ionic composition of the bulk solution.[4,26-28] In order to maintain electroneutrality in the swollen state, diffusion of mobile counterions from the swelling medium into the polymer is coupled with ionization of fixed charges and penetrant diffusion as the hydrogel swells.[4,21,27,28] This gives

Table 3 : Effect of pH on Swelling

Neutral hydrogels - no effect

Ionic hydrogels

- Low pH
  - decreases swelling of polyacids
  - increases swelling of polybases
- High pH
  - increases swelling of polyacids
  - decreases swelling of polybases

rise to a difference between the osmotic pressure of freely mobile ions in the gel and the outer solution that contributes to the increase in hydrogel swelling.[21,28]

In other words, when an initially glassy, non-ionized hydrogel is inserted into an electrolyte solution, the polymer absorbs water and ionizes. This, in turn, leads to an influx of counterions. In the case of polyacid polymers, positive ions would be carried into the swollen network by the infusing external solution. These positive counterions replace protons released from the ionized carboxylic acid groups. The movement of these counterions contributes to the swelling kinetics of the hydrogel.[4,22,26] It is therefore recognized that the overall rate of swelling is controlled by the rate of ion exchange and the ionic equilibrium.[4] It is also noted that the ionic forces depend only on the ionic composition of the solvent and on the concentration of fixed ionizable groups in the gel.[28]

I.4.3 Effect of Temperature on Swelling

Some ionic and non-ionic hydrogels undergo volume-phase transition with temperature. This sudden volume change has been found to be reversible and dependent upon both the degree of ionization and the stiffness of the polymer chains.[4,29-32]

When polymers swell in solvents, there is usually a negligible or small positive enthalpy of mixing or dilution. Although a positive enthalpy change opposes the process, the large gain in entropy drives it. In aqueous polymer solutions, the opposite is often observed.[4,29]

This behavior, associated with a polymer phase separation as the temperature is raised to a critical value, often referred to as the "lower critical solution temperature" (LCST).[4,29-33]

In general, networks that show lower critical solution temperatures usually shrink as the temperature is raised above the LCST. Lowering the temperature below the LCST results in hydrogel swelling.[23,31,34,35] Above the phase transition temperature, it is believed that polymer networks undergo both inter- and intramolecular hydrophobic interactions between the alkyl groups of the polymer. This induces an aggregation of the polymer network.[31,36] At temperatures below the lower critical solution temperature, hydrophilic gels are hydrated and expanded. With increasing temperature the polymer rapidly begins to dehydrate and becomes more hydrophobic. This thermally induced dehydration promotes rapid shrinking and collapse of the polymer network.[23,31] In addition, it has been observed that as the number of ionizable groups increases, the volume change at the transition increases and the transition temperature rises.[23,27,34]

I.5 Physiological Effects on Swelling

In addition to the physiological aspects affecting swelling behavior of hydrogel polymers, there are also a number of physiological aspects of the gastrointestinal tract that need to be considered. Figure 1[37] graphically presents a number of factors an

Figure 1 : Schematic Representation of Physiological Factors Influencing Hydrogel Swelling.

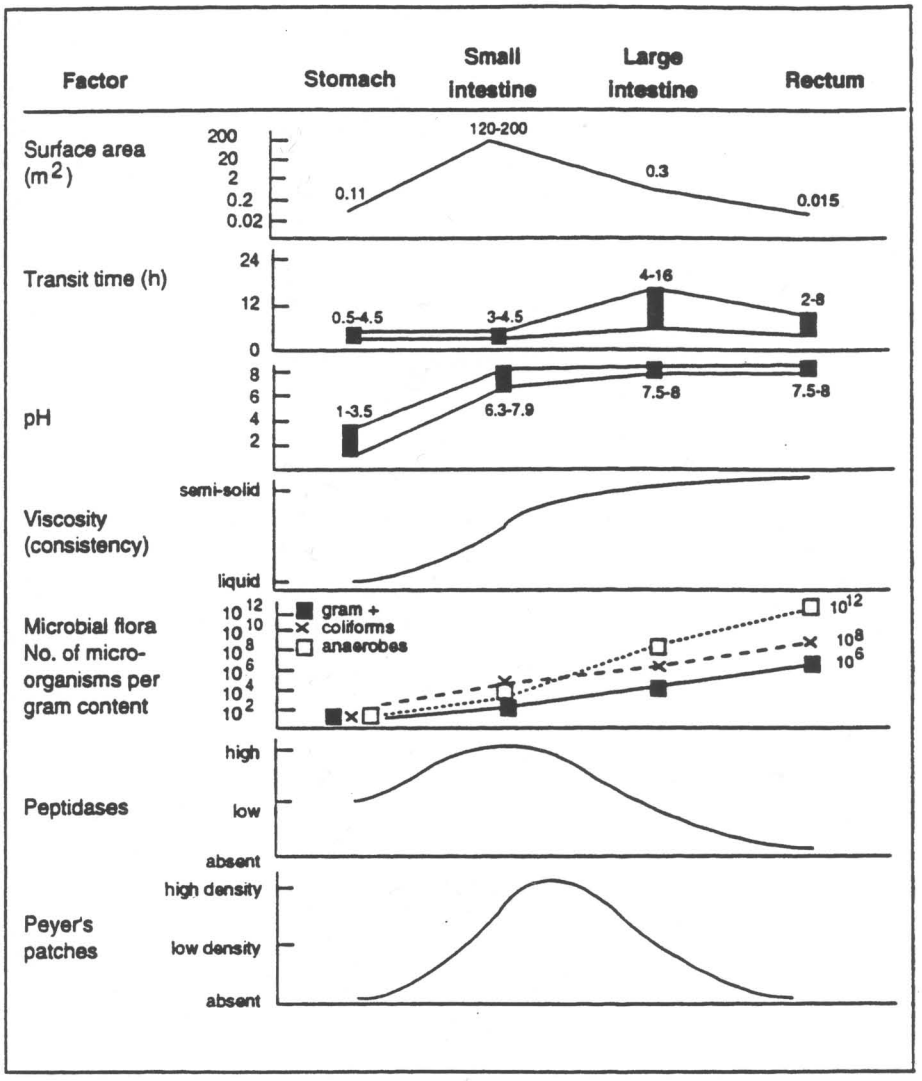
Factor
Stomach
Small intestine
Large intestine
Rectum
Surface area (m^2)
200
20
2
0.2
0.02
0.11
120-200
0.3
0.015
Transit time (h)
24
12
0
0.5-4.5
3-4.5
4-16
2-8
pH
8
6
4
2
1-3.5
6.3-7.9
7.5-8
7.5-8
Viscosity (consistency)
semi-solid
liquid
Microbial flora No. of micro-organisms per gram content
10^{12}
10^{10}
10^{8}
10^{6}
10^{4}
10^{2}
gram +
coliforms
anaerobes
10^{12}
10^{8}
10^{6}
Peptidases
high
low
absent
Peyer's patches
high density
low density
absent

ingested hydrogel delivery system would encounter that has the potential of affecting the rate and extent of its swelling.

The human small intestine represents a tube of approximately 6 meters in length with an average diameter of 5 centimeters. Due to the presence of about 3000-6500 microvilli projecting 0.75-1.5 microns into the intestinal lumen from each epithelial cell,[38] surface area is estimated to be between 120 and 200 square meters.[37,39]

Gastric transit time depends upon several factors such as the fed state of the subject and the composition of the meal ingested.[40] While a wide range has been observed, fasted gastric emptying times in normal humans have been measured to be 77 ± 19 minutes.[41] Postprandially, i.e., after a meal, small intestinal transit has been consistently observed to be between 3-5 hours regardless of whether the subjects were fasted or had ingested a light meal.[42-47]

The pH varies markedly along the gastrointestinal tract. Gastric pH is seen to be quite acidic with a pH ≈ 1.5 in the fasted human. Postprandially, gastric pH is initially seen to rise to near neutral pH due to a buffering effect of the ingested meal. This gradually declines to pre-meal acidic level over a period of 60-90 minutes.[48] Gastric contents enter the duodenum where they mix with bile and bicarbonate ions from pancreatic secretions and the duodenal mucosa. This leads to a rise to about pH 6 in the proximal jejunum and remains fairly constant throughout the small intestine, rising only slightly until the ileum where the pH is approximately 7.4.[49,50]

As the lumenal contents move through the small intestine, the viscosity of lumenal contents increases steadily due to absorption and reabsorption of water and nutrients. This conservation of fluid is counter productive for a swelling hydrogel delivery system.

As shown in Table 4, microbial flora and peptidases populate the small intestine of the human. More than 60 bacterial species have been isolated from the human intestine with viable titers of 10^3 microorganisms per gram content in the stomach, duodenum jejunum and upper ileum. This count increases to 10^9 counts per gram in the distal ileum.[39,51,52] In addition, as the result of microbial activity, exotoxins, enzymes, endotoxins and liberated enzymes are also found in the small intestine. The function of enzymes is to hydrolyze large macromolecules to di-, tri-, and oligomeric constituents. While this is not, in general, a major concern for classic hydrogel systems, recently a growing assortment of enzyme-degradable hydrogels crosslinked with substrates susceptible to enzyme-catalyzed hydrolysis have been developed based on their presence in the gastrointestinal tract. Among these modified hydrogels are those that have been prepared crosslinked with albumin,[1,53,54] gelatin,[55,56] starch,[57,58] and amylose.[59]

Fluid required by a swelling hydrogel polymer may be seen to come from a number of sources in the normal human small intestine. As shown in Table 4, normal body secretions from salivary glands, stomach, liver, pancreas and intestinal tract present over 7000 milliliters of fluid daily into the upper gastrointestinal tract, most of which is in the form of bile, mucous discharge, and gastric,

Table 4 : Biopharmaceutical Data of the Upper Gastrointestinal Tract

ANATOMICAL UNIT	ENZYMES and EXOCRINE SECRETIONS[39,60]	AMOUNT OF SECRETION[61] (ml/day)
Mouth cavity	Ptyalin Maltase Mucin	Saliva: 1200
Stomach	Pepsin Lipase Renin Hydrochloric acid Mucin	Gastric Fluid: 2000
Duodenum	Bile Trypsin Chymotrypsin Amylase Maltase Lipase Nuclease Bicarbonate Mucin	Bile: 700 Pancreatic Juice: 1200
Jejunum	Erepsin Amylase Maltase Lactase Sucrase Mucin	Intestinal Fluid: 2000
Ileum	Lipase Nuclease Nucleotidase Enterokinase Mucin	--

intestinal and pancreatic secretions. In addition, the average adult ingests approximately 800 grams of food and 1500 milliliters of water daily.[60] Prior to its reabsorption, all of this fluid would be available to a hydrogel delivery system as it resides in the lumen of the small intestine.

Often overlooked, another source of available water is the mucous gel coating of the epithelial cells. The mucous layer is present as a thin, but continuous translucent gel cover adherent to the mucosal epithelial surface. Generally heterogeneous, the thickness of the mucous layer ranges from less than 100μm to 500μm.[62] While the epithelial mucous is normally assigned the roles of mechanical protection and lubrication, it also functions in maintaining and controlling water balance of the epithelial mucosa.[63] The composition of mucous is predominately water (95%), with the remainder being glycoprotein, sloughed epithelial cells, proteins, electrolytes, and bacteria.[64] This high hydration level is maintained by an equilibrium of water movement between the lumen, epithelial cells, lymph, circulatory system and the mucous gel layer. When in intimate contact with a hydrogel, the mucous gel would easily be able to supply the water needed for swelling.

I.6 Hydrogel Polymers

Swelling kinetics of four hydrogel polymers was studied in permanently cannulated gastrointestinal tracts of canines. The four polymers were hydroxypropyl methyl cellulose, the sodium salt of

carboxylmethyl cellulose, Carbopol 974P™ and Noveon AA1™ (polycarbophil).

Two of the four polymers, hydroxypropyl methyl cellulose and the sodium salt of carboxylmethyl cellulose, are cellulose derivatives while the other two, Carbopol 974P™ and Noveon AA1™ (polycarbophil), are derivatives of polyacrylic acid. The choice of polymers allowed examination of various polymer characteristic differences and their effect on *in-vivo* swelling. These differences included molecular weight, degree of ionization, hygroscopicity, covalent versus non-covalent cross-linking, and electrolyte and pH sensitivities.

I.6.1 Carboxymethyl cellulose sodium salt

The cellulose ether, carboxymethyl cellulose sodium salt, (NaCMC) is a linear, long-chain, anionic polysaccharide that is rapidly soluble in both hot and cold water. It is physiologically inert and non-toxic. As shown in Figure 2, NaCMC is composed of anhydroglucose units with β -1,4 linkages. The degree of polymerization, i.e., average number of glucose units per molecule, may vary from 100 to 3500 corresponding to molecular weights of 20 to 700 kilodaltons.[65-67]

Figure 2: Structures of Hydroxypropyl methyl cellulose and Carboxymethyl cellulose sodium salt

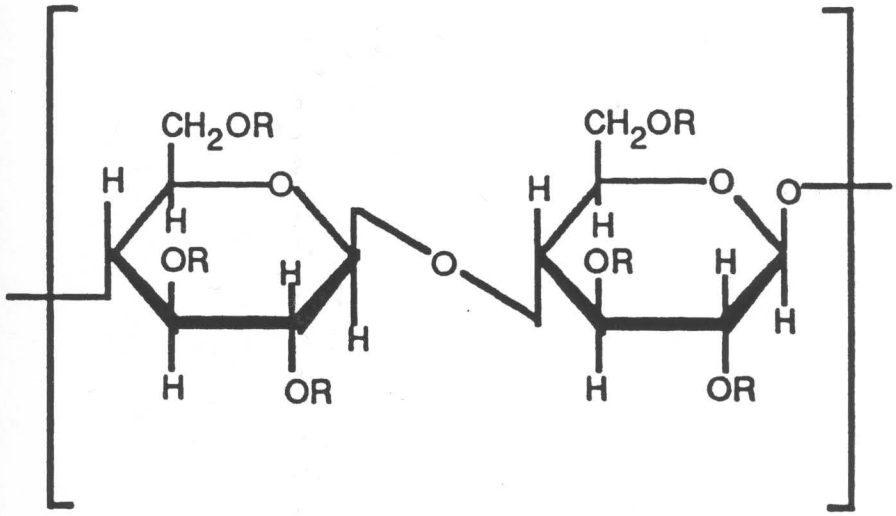

Hydroxypropyl methylcellulose (HPMC) $\overset{OH}{|}$

R = H, CH_3, $CH_2\overset{OH}{|}CH\,CH_3$

Sodium carboxymethylcellulose (CMC)

R = H, $CH_2\underset{O}{\overset{||}{C}}ONa$

I.6.1.1 Solubility

Solubility of NaCMC in water is obtained when the degree of substitution, the average number of carboxymethyl groups per anhydroglucose unit, is above 0.4 with solubility increasing with higher degree of substitution.[67] As the pH is reduced, NaCMC, with a pK_a of 4.0-4.7, gradually reverts from the salt to the insoluble free acid form.[66,68,69]

I.6.1.2 Viscosity

The viscosity of carboxymethyl cellulose solutions increases with degree of substitution, molecular weight and concentration. While reversible, increasing temperature reduces the viscosity of the solution. The apparent viscosity is independent of pH and is relatively stable over the pH range of 4-10, decreasing slightly above pH 10 and increasing slightly below pH 3.[66]

I.6.1.3 Compatibility

Carboxymethyl cellulose solutions are compatible with most water soluble nonionic and anionic polymers and solvents. Its compatibility with salts depends upon the ability of the cation to form a water soluble salt. Generally, monovalent cations form soluble salts with NaCMC, divalent cations are borderline and trivalent cations form insoluble salts. The effect of the particular

salt varies with the salt, its concentration, pH and the degree of substitution of the carboxymethyl cellulose.[66,67] Generally, divalent cations are not seen to form gels.[66,67]

I.6.2 Hydroxypropyl methyl cellulose

The cellulose ether, hydroxypropyl methyl cellulose, (HPMC) is a linear, long chained, nonionic polysaccharide. It is physiologically inert and non-toxic. It is not absorbed from the gastrointestinal system. HPMC does not interfere with and is inert to metabolism by enzymes and resident microorganism of the gastrointestinal tract.[70-74]

The structure of hydroxypropyl methyl cellulose, as shown in Figure 2, is very similar to carboxymethyl cellulose discussed above. Both are composed of anhydroglucose units with β - 1,4 linkages and the degree of substitution determines the properties of the polymer.[73,75] The degree of polymerization range in order of magnitude of 170-900, corresponding to molecular weights of 30 to 170 kilodaltons.[70]

I.6.2.1 Solubility

It has been found that maximum water solubility occurs within a range of degree of substitution of 1.64-1.92.[69,70,75,76] Lower degree of substitution gives products soluble only in alkali, whereas

a higher degree of substitution produces materials soluble only in organic solvents.[76]

An unusual property of hydroxypropyl methyl cellulose is that it is soluble in cold water and insoluble in hot water.[75-78] Upon heating above a certain temperature, the polymer thickens and forms a structured gel. This inverse solubility-temperature behavior is often referred to as thermal gelation.[69,74,78] The temperature at which this transition occurs is dependent upon the degree of substitution and the ratio of methoxyl and hydroxypropoxyl groups.[69,76,79]

Thermal gelation of HPMC aqueous solutions is believed to be caused by the hydrophobic interaction between molecules containing methoxyl groups. At lower temperatures, molecules in a solution state are hydrated and little polymer-polymer interaction occurs other than simple entanglement. As the temperature rises, the viscosity is initially lowered and the polymer molecules gradually lose their water of hydration. When enough dehydration of the polymer occurs, a polymer-polymer association takes place and the polymer chains lock, causing the formation of a firm, high viscosity gel.[69,78-81] This gelation phenomenon is reversed upon cooling.[79,74]

Thermal gelation is seen to be a function of the type and amount of substitution. It is also affected by polymer concentration and the presence of other water-soluble materials in solution, e.g., electrolytes, sorbitol, sucrose, and glycerol, which usually causes a lowering of the gelation temperature. Conversely, the gelation

temperature has been seen to be raised by ethanol, propylene glycol and polyethylene glycol.[75,76,78,79]

I.6.2.2 Viscosity

In conjunction with the solubility-temperature phenomena, a similar effect is seen to occur in viscosity. Whereas most soluble polymers decrease in viscosity as the temperature is increased, the opposite is seen for HPMC. The viscosity of an aqueous solution of the polymer will initially decrease upon heating; however, when the transition temperature is reached, the solution will gel, thus resulting in a substantial increase in viscosity.[73,76,77,79,81]

Various other factors contribute to the viscosity of hydroxypropyl methyl cellulose. As mentioned above, the amounts and ratios of methoxyl and hydroxypropoxyl groups, as well as the presence of water soluble materials, affect the thermal gelation point. By the same mechanism the viscosity is also affected. Increasing polymer molecular weight has been seen to lower the gelation temperature of HPMC, thereby resulting in a higher than expected viscosity and gel strength.[69,78-81] In addition, increasing the concentration of the polymer increases the viscosity and strength of the gel.[75,80]

Since hydroxypropyl methyl cellulose is nonionic, its solutions are relatively insensitive to changes in pH, showing no effect on viscosity in the pH interval of 3-11.[69,74,75,78,80] In addition, viscosity is seen to be highly tolerant to the presence of electrolytes.

While a gradual decrease in viscosity is sometimes seen with increasing electrolyte concentration, HPMC is much less sensitive than ionic water-soluble polymers. The effect appears to be more due to the competition for available water than an ion-polymer interaction. This effect is particularly seen with the addition of certain surfactants, in particular the sulfates and sulfonates. In general, the prediction of the magnitude or direction of the effect of additives on the viscosity is not possible with any degree of accuracy.[75]

I.6.2.3 Compatibility

Being nonionic, hydroxypropyl methyl cellulose is not affected by ordinary concentrations of electrolytes and other solutes. Neither is it precipitated from solution as insoluble salts in the presence of multivalent cations. However, HPMC may be salted out when the concentration of electrolytes or other solutes exceeds certain limits. This is caused by competition of the electrolytes for water, lowering the hydration of the polymer that, in turn, may result in its precipitation.[73,79-81]

I.6.3 Carbopol 974P™ and Noveon AA1™ (polycarbophil)

Carbopol 974P and Noveon AA1 (polycarbophil) are synthetic, hydrophilic polymers composed of polyacrylic acid loosely cross-linked with polyalkenyl ethers (allyl sucrose or allyl pentaerythritol)

or divinyl glycol, respectively.[82-84] The basic structure of these compounds is shown in Figure 3.

They are non-toxic and pharmacologically and physiologically inert. While they are not seen to be metabolized by enzymes and micro-organisms native to the gastrointestinal tract,[76,82,85-87] recent studies have shown that polycarbophil inhibits protease activity in the gastrointestinal tract.[88,89] In addition, they are not subject to hydrolysis nor oxidation.[76]

I.6.3.1 Molecular Weight and Particle Size

These macromolecules are very high molecular weight polymers with an estimated range of 740,000 to 4-5 million.[83] They are produced as flocculated powders of primary particles averaging 0.2 micron in diameter. Determined by Coulter Counter, the flocculated powders have an average size of 2-7 microns.[82,87] Like many other macromolecules, they are not absorbed from the gastrointestinal tract. On the other hand, they do not interfere with intestinal absorption.[85,86,90]

I.6.3.2 Physical and Chemical Properties

Carbopol 974P and Noveon AA1 (polycarbophil) are insoluble in water, dilute acids, and common organic solvents.[82,85,86] Due to the carboxylic acid groups on the polymer backbone, the pH of a 1% aqueous dispersion of the polymers is 2-4.[91,92]

Figure 3 : Structures of Carbopol 974P™ and Noveon AA1™. R_3 represents the cross-link of the polymer.

$R_1 = R_2 = R_4 = H$.

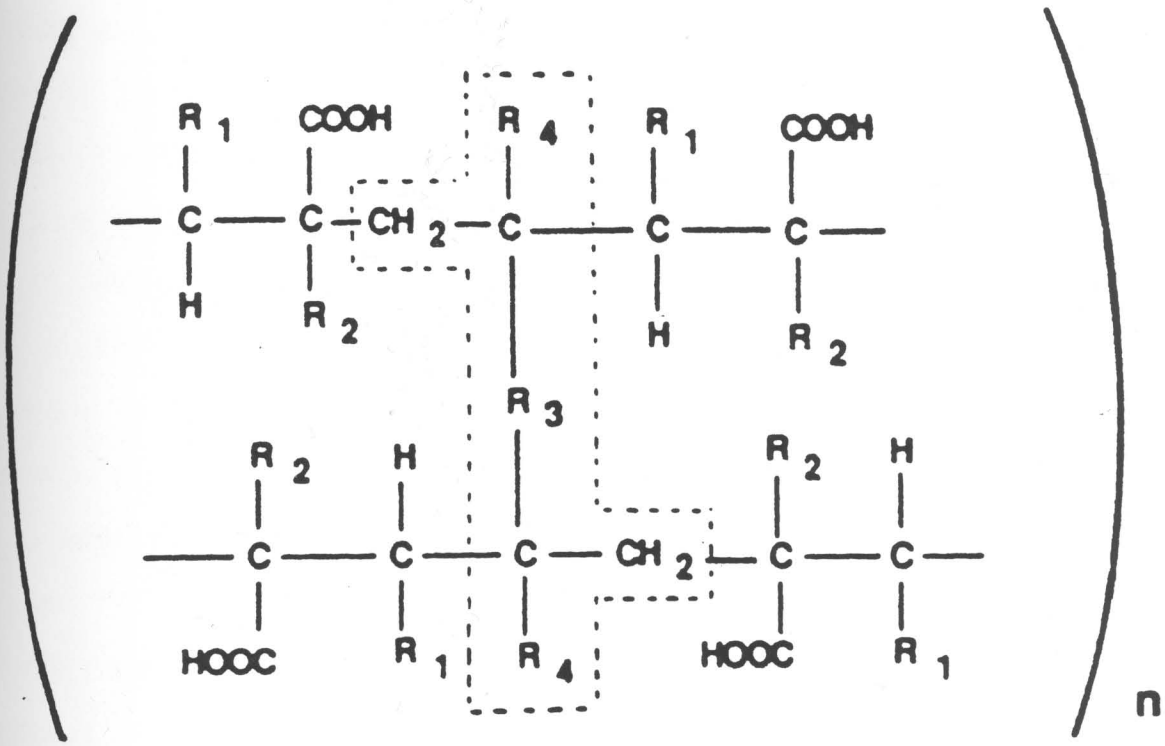
R 1
COOH
R 4
R 1
COOH
CH 2
H
R 2
H
R 2
R 3
R 2
H
R 2
H
CH 2
HOOC
R 1
R 4
HOOC
R 1
n

These macromolecules readily swell in water. At low pH, the carboxylate groups of the polymer are highly protonated, resulting in little electrostatic charge repulsion, and relatively little swelling compared to the neutralized system. When exposed to a pH environment above 4-6, the polymers are observed to form gels in water by swelling 100 - 1000 times their original volume compared to only 15-35 times at low pH (pH 1-3).[82,93-96] While there is a disagreement in the literature over the assignment of values for the pK_a of these compounds (4.7 - 4.9[97,98] and 6.0 ± 0.5[82,99]),it appears that, in alkaline pH at or above its pK_a, swelling results from the ionization of the polymers' carboxylate groups. The reason for this is that the ionization establishes an electrostatic repulsion which tends to expand the polymer network. Water, absorbed from the bulk solution following Donnan equilibrium phenomenon, further promotes polymer swelling.[82,95,100] If used as a drug delivery system, these polymers exhibit "quasi-enteric" behavior providing slow release in low pH of the stomach, but quickly release the drug when the pH is increased in the intestines.[87,95]

I.6.3.3 Viscosity and Electrolyte Sensitivity

At the beginning of hydration, a hydrogel with high viscosity develops. As the network further hydrates, the resultant viscosity decreases. Thus, the lower the degree of hydration, the higher the viscosity of the hydrogel.[100,101], Viscosity can be increased by

increasing the concentration of polymer, increasing the pH of the medium, or decreasing the water of hydration.

It also has been observed that viscosity increases very rapidly with concentration, but is inversely influenced by electrolyte concentration.[100,101] Electrolytes tend to reduce the viscosity of Carbopol and polycarbophil gels by the Donnan equilibrium phenomenon. Hydration depends upon the establishment of a net osmotic pressure across the polymer network. The net osmotic pressure decreases as the ionic strength of the external medium increases. The result is a decrease in the degree of hydration.[99,101]

The macromolecules, due to their anionic character, are seen to strongly interact with soluble salts to decrease the degree of swelling. In addition, they tend to form precipitates with divalent, polyvalent and large monovalent cations.[76,99,101]

I.7 Animal Model

In experimental studies there are a number of factors that govern the choice of which animal species is to be used. These factors include (1) ease of handling, housing, maintenance in a normal environment and cost, (2) experience in terms of past use by other laboratories and investigators, (3) life span of the animal, (4) the biochemical or physiological system to be studied or suspected to be affected, (5) the anatomy or structural characteristics of the animal in relation to the study and (6) presence or absence of physiological response systems similar to those in humans.[102]

More specifically, characteristics of an ideal animal model for gastrointestinal studies need to include (1) physiological characteristics of the gastrointestinal system similar to that of humans, (2) convenient and direct means for introduction of the system to be studied without unduly disturbing the animal, (3) availability for chronic and acute studies of long duration in an unanaesthetised state, and (4) reproducible and frequent sampling and repeated studies on the same animal.

The relatively large size and longevity of the canine are advantageous for sequential studies in individual animals. Their temperament and ability to be caged for long periods without significant health or physiological changes are often the basis for their selection.[103] The canine has often been used as a model for human drug absorption, bioequivalence, and renal metabolism and clearance.[104,105]

The physiology of the gastrointestinal tract has a direct bearing on the design of drug delivery systems. Among these many factors, the most relevant to our present study are motility, transit, and pH. It is important to note that, in general, the comparison of animal and human gastrointestinal physiology is further complicated by the enormous variability of the values quoted in the literature. The values given in the following discussion have been, as often as possible, verified by a number of different sources. In those cases in which differences in values have been found, the data have been either reported individually or as a range.

I.7.1 Anatomy

The small intestine, a long coiled tube extending from the pylorus of the stomach to the ileocaecal valve where it joins the large intestine, is seen to be very similar in the canine and the human. In each it is divided into duodenum, jejunum, and ileum. A comparison of the lengths of these regions is shown in Table 5. These values are only approximate due to the lack of any definite gross, microscopic or developmental manifestations to mark the divisions between the various regions.[106] Bile and pancreatic ducts, major and accessory, open into the duodenum about 5-10 cm from the pylorus.[107,108]

The intestinal wall is composed of four layers, an outer serosal layer, a muscular layer, the submucosa and an inner mucosal layer. Histologically, it is very similar in humans and canines.[106-108,113] In each, the primary functional layer of the small intestine is the mucosa, where materials come into contact with an absorptive and digestive surface. While the mucosal cells are able to absorb large quantities of materials from the intestinal lumen, cellular secretions aid in the digestion of these materials. Also, it is through this mucosal layer that the ducts of the pancreas and the biliary system of the liver discharge into the lumen to add their digestive capabilities.[107,113]

On the basis of the above, except for the shorter canine ileal length, the human and canine small intestine are very similar anatomically and histologically.

Table 5 : Comparison of Small Intestinal Length in the Human and Canine.

	Human[38,107]	Canine[106]
Duodenum	20-30 cm	25 cm
Jejunum	250 cm	250-350 cm[103, 109]
Ileum	350 cm	15-30 cm[106,110]
Total length	≈ 650 cm	≈ 5 times body length[108,109,111] (≈ 300 - 400 cm)
Lumen diameter	≈ 4 cm	2.5-3.5 cm[112]

I.7.2 pH

The luminal content pH varies markedly along the gastrointestinal tract. Differences, as well as fluctuations, in pH may strongly affect the rate and extent of dosage form performance, e.g., polymer swelling. It is therefore important to be able to compare the usual range of values in the animal model and human and understand how it varies under normal physiological conditions.

Numerous studies have examined the pH in the upper gastrointestinal tract using various techniques with subjects representing a wide variation of ages.[48-50,114-117] This is important since increasing age has been seen to be associated with changes in gastrointestinal pH.[48,49,103,114,118] In general, no differences due to gender have been seen in gastric or duodenal pH studies.[49]

The acidic gastric content enters the duodenum where it mixes with bile, bicarbonate ions from pancreatic secretions and the duodenal mucosa. This leads to a rise in pH from about 2 in the stomach to about 6 in the proximal jejunum.[49,50] The pH is seen to be maintained fairly constant at this level through the small intestine until the ileum at which point it is further raised to approximately pH 7.4.

Table 6 is a summary of some of the many literature values available for human and canine gastric and intestinal pH. Much of the variation observed in this table results from different experimental

Table 6 : Comparison of Gastrointestinal pH in the Human and Canine.

	Human		Canine
	fasted	fed*	fasted
Stomach	1.1-1.6[118]	3.9-5.5[118]	1.8±0.1[119]
	1.3-2.1[41]	6.4-7.0[49]	1.5±0.04[120,121]
	1.0-2.5[50]		1.9±0.2[122]
Duodenum	4.9-6.0[123]	4.3-6.3[50]	6.2[124]
	6.2-6.7[118]	6.0-6.7[49]	5.5-6.5[125]
	5.8-6.5[49]	6.4-6.7[118]	6.1±0.1[121]
	5.8-7.1[126]		6.2±0.1[127]
Jejunum	4.8-6.8[126]	6.63-7.41[50]	7.3±0.09[119]†
	4.65-5.70[123]		
	5.5-6.5[128]		
Ileum	7.5[124]	7.49[50]	7.5[124]
	7.4[119]		

* pH very dependent upon meal ingested[13]

† pH measured at "mid small bowel"

protocols, such as the age of subjects, method of measurement, and duration of study.

I.7.2.1 Gastric pH

Gastric acid production has been measured in both man and dog. Results have shown that basal secretory rates are low in the dog, but peak gastric response to stimuli is considerably higher than in humans.[120] Gastric pH in either species is seen to be quite acidic. As shown in Table 6, the fasted gastric pH in both species is around 1.5.

Postprandially, gastric pH in humans is seen to initially rise due to the near neutral pH buffering effect of the ingested meal. Gradually, over a period of 60-90 minutes, it declines and returns to the acidic pre-meal level.[49] In the canine, the initial buffering effect of the ingested meal is much less pronounced and the pH is seen to vary from 0.5 to 3.5 (mean 2.1 ± 0.04).[121] This lack of early elevation in canine pH is probably due to stimuli induced higher peak gastric output that, in humans, does not occur until approximately an hour post-meal.[129]

Overall it appears that the fasting pH is very similar in both species. However, initial peaking in pH seen postprandially in humans is absent in canines, but this difference disappears usually within an hour.

I.7.2.2 Intestinal pH

The higher pH of the small intestine is mainly due to pancreatic bicarbonate secretions. While the concentration of bicarbonate in pancreatic secretion is similar in the two species, in the fasted state, basal gastric acid secretion is lower in the canine. As a result, the canine intestinal pH consistently appears to be about 1 pH unit higher, as shown in Figure 4.[119] This difference harbors a potential problem in analyzing and comparing the performance and behavior of a dosage form. However, in a study evaluating enteric coating in vivo using a Heidelberg pH capsule coated with hydroxypropyl methylcellulose phthalate,[125] the onset of disintegration in the canine upper intestine was seen to be 14.2 ± 2 minutes comparing well with the 5 minutes reported for disintegration in humans of tablets with the same coating.[130]

While limited data are available for postprandial pH in either species, observations have shown that the duodenal pH decreases more rapidly and to a greater extent in the canine.[120,131] This is most likely due to gastric emptying of chyme that is expected to be more acidic in dogs due to earlier and higher peak acid output.

For ileal pH, very little data are available, but, as shown in Table 2, studies performed have shown that the pH in both species is essentially the same regardless of whether the subject is fed or fasted.[50,119,124]

Figure 4 : The Mean and SEM of the intestinal pH-time profile of (•) dogs and (o) humans.

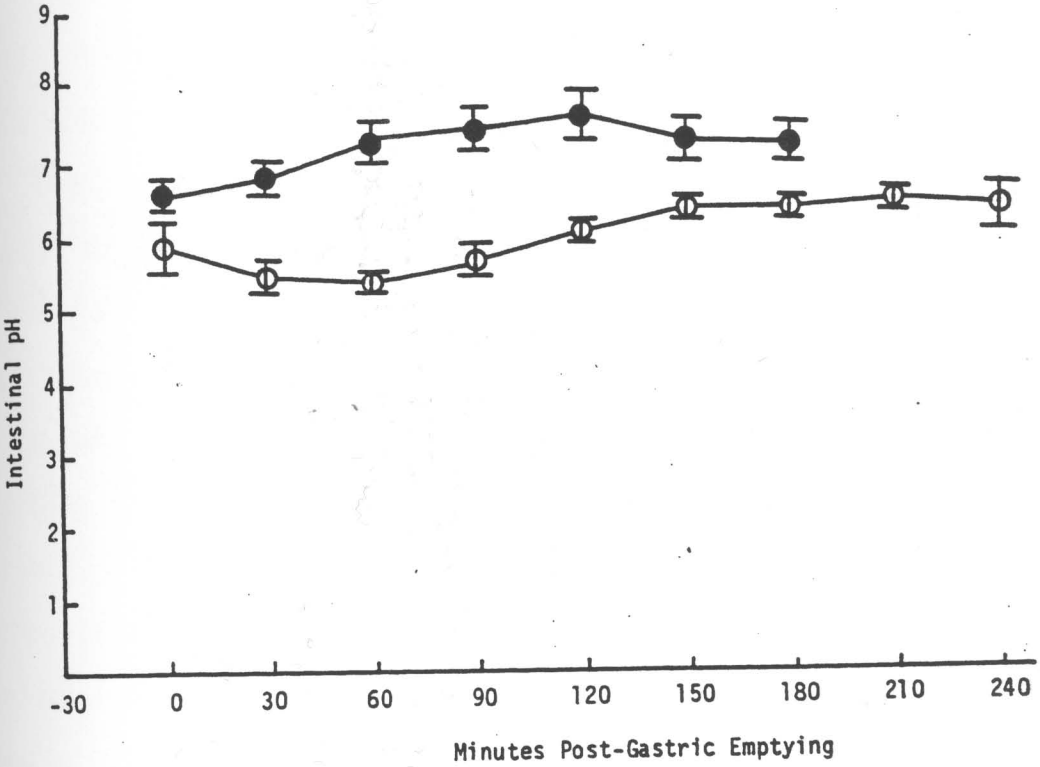
9
8
7
6
5
4
3
2
1
Intestinal pH
-30
0
30
60
90
120
150
180
210
240
Minutes Post-Gastric Emptying

I.7.3 Motility

An important factor to consider when comparing the gastrointestinal system of canines and humans is the gut motility. Motility is the characteristic feature of the gastrointestinal tract responsible for the shear forces applied to any material within it.

The cyclic pattern of gastrointestinal motility originates in the foregut and propagates to the terminal ileum.[132] It is well documented that there are two modes of gastrointestinal motility patterns seen both in man and animals. These patterns, classified as the digestive or fed state and the interdigestive or fasted state, have been fully characterized and shown to be very similar in humans and canines.[133-135] The motility pattern of the fasted state, commonly referred to as the migrating myoelectric (or motor) complex, is most often referred to by the letters, MMC. The MMC is organized into cycles of alternating active and quiescent periods and can be divided into four distinct phases: Phase I-a quiescent period of minimal or no electrical activity and contractions; Phase II-a period of random action potentials (spikes) and intermittent contractions that move in an aboral direction along the small intestine; Phase III-a period of regular spikes and contractions at a maximal frequency; and Phase IV-a transitional period between Phase III and Phase I. Thus in the fasted state, spike and contractile activity ranges from resting to maximal amplitude and frequency. Phase III is often referred to as the "housekeeper wave" whose primary function is to clear all

indigestible material from the stomach and small intestine.[132,133,136,137]

When food, liquid or solid, is ingested, the MMC is disrupted. The duration of the disruption depends upon meal composition as well as caloric content, with fatty meals causing the greatest effect.[132,136] While the cyclic pattern is replaced by the appearance of a continuous pattern of spike potentials and contractions throughout the whole small intestine, it is primarily reflected in the constant emptying of chyme from the stomach into the duodenum.[138] The change occurs almost immediately after the ingestion of food.[136]

The motility pattern of the fed and fasted states is described in Table 7 with a pictorial description shown in Figure 5.[138]

I.7.3.1 Gastric Residence Time

Gastric residence time depends upon several factors such as whether the material administered is liquid or solid, the volume or particle size administered as well as the chemical and osmotic properties of the meal.[40] As described above, the variation of the fasted versus the fed state has also been seen to significantly affect the gastric residence time.

Table 7 : Characteristics of the GI Motility Patterns in the Dog

Fasted State

Phases	Duration	Characteristics
I	30-60 min	-quiescence
II	20-40 min	-irregular contractions -medium amplitude but can be as high as phase III -bile secretions begins -onset of gastric discharge of administered fluid of small volume usually occurs before that of particle discharge -onset of particle and mucus discharge may occur during the latter part of phase II
III	10-20 min	-regular contractions (4-5 contractions/min) with high amplitude -mucus discharge continues -particle discharge continues
IV	0-5 min	-irregular contractions -medium descending amplitude -often absent

Fed State

Phase	Duration	Characteristics
one phase only	as long as food is present in the stomach	-regular, frequent contractions -amplitude is lower than phase III -4-5 contractions/min

Figure 5 : A pictorial representation of typical motility patterns in the interdigestive (fasted) and digestive (fed) states.

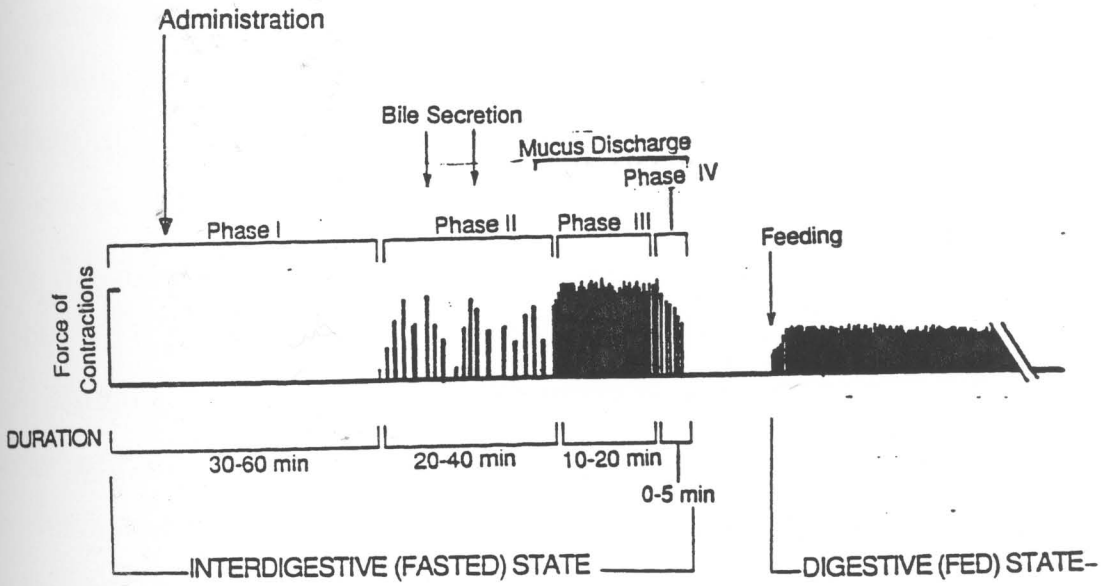
Administration
Bile Secretion
Mucus Discharge
Phase IV
Phase I
Phase II
Phase III
Feeding
Force of Contractions
DURATION
30-60 min
20-40 min
10-20 min
0-5 min
INTERDIGESTIVE (FASTED) STATE
DIGESTIVE (FED) STATE

I.7.3.1.1 Fasted State

Studies of fasted gastric motility have been performed in both the canine and the human.[139,140] Phase III activity studies in man and canine have shown that the duration of the activity is essentially identical at 18.6 ± 4 and 19 ± 2 minutes, respectively. The interval between two Phase III cycles, i.e., the length of a MMC, was measured to be 112.5 ± 19 minutes for humans and 106 ± 8 minutes for the canine.[137,141]

Gastric residence time, determined as the length of time a Heidelberg radiotelemetry capsule remained in the stomach, was determined in both species.[41,121] While a wide range was observed, it was determined that the average emptying time was the same with values of 74 ± 27 and 77 ± 19 minutes in the canine and healthy human respectively.

It therefore appears that the motility patterns observed for the fasted canine and human are very comparable.

I.7.3.1.2 Postprandial or Fed State

I.7.3.1.2.1 Liquid Emptying

In considering the emptying of liquid from the stomach, a series of different scenarios needs to be considered. The first is the emptying of non-nutrient liquids. The elimination of ingested water or saline from the stomach during the fasted state follows first

order kinetics without disrupting the fasting motility pattern unless ingested volume is greater than 150 ml.[142,143] Half emptying times have been shown to be 8-12 minutes[143] and 8-15 minutes[131,144] in canines and humans, respectively. Increasing viscosity or administering hyperosmotic solutions results in a reduced gastric emptying rate.[145,146]

The second scenario is the emptying of nutrient liquids. In these circumstances it has been shown that fasting motility patterns in canine and human subjects is interrupted and elimination appears to be much more linear due to a feedback mechanism in the duodenum. Half emptying times have been determined to be 75 minutes in humans for a 25% glucose solution.[147] Similar effects have been reported for the canine.[148]

When fluids are ingested with a solid meal, there is a tendency for the liquid emptying rate to be reduced.[149-152] Unfortunately, due to the failure of using identical meal and fluids in the two species, no direct quantitative human - canine comparison of the liquid emptying can be made.[120] A similar pattern has been reported in which the half-emptying times increase in proportion to the size of the meal or, in other words, the larger the meal, the slower the gastric emptying.

I.7.3.1.2.2 Solid Meal Emptying

The fed motility pattern is initiated upon ingestion of a solid meal of a certain size and consistency with emptying rates being very

dependent upon the size and composition of the meal.[149,153] Due to the failure of studying identical meals in the two species, direct quantitative human versus canine comparison of the gastric emptying cannot be made. In general, there is a tendency that the rate of emptying a solid meal in canines is slower than in humans.

It has also been observed that the rate of gastric emptying of digestible solids increases with decreasing particle size in both the human and dog.[154-156] On the other hand, large non-digestible particles are not emptied until the return of the interdigestive state and phase III of the MMC.[151,157,158] There is a clear meal size dependency on the time for Phase III to return after feeding, and it is seen to be longer in the canine than in the human.

I.7.3.2 Small Intestine Transit Time

The interdigestive and digestive motility patterns govern the movement of chyme and other material through the small bowel. During phase I of the MMC cycle, liquids and solids move through the small intestine slowly, if at all. Movement is mainly governed by phase III activity for solids and phase II activity for liquids.[138] The speed of the migration of the housekeeper wave decreases as it moves down the small intestine and with it the force to move the material within it.[159] In general it appears that, in humans, small intestinal transit time appears to be consistently 3-5 hours independent of particle size when the subjects were fasted or had

ingested a light meal.[42-47] In the fed state, the transit time was shown to be relatively short at about 2 hours.[160]

The Heidelberg telemetry capsule was used to study intestinal transit times by observing the abrupt pH rise when the capsule passes into the cecum.[120] This study showed that the transit time in dogs, with a small intestine about half the length of humans, was less than half of that in man, albeit, with highly variable data. The canine transit time was seen to be 111 ± 17 minutes (range: 15 - 206) while in the human it was 238 ± 14 minutes (range: 180-300). Similar results have been reported for transit studies of pellets and tablets.[44,161] The times required to traverse the small bowel is 1.3 and 3.8 hours for the pellets and 2.6 and 3.1 hours for the tablets in canines and humans respectively.

1.7.4. Summary

In conclusion, the gross anatomy and physiology of the gastrointestinal tract in humans and dogs are very similar. This is seen in the motility patterns, gastric pH, and the gastric emptying of liquids. The higher intestinal pH in canines is the main difference between the species in the fasted state.

The meal emptying rate and the subsequent return of the fasting motility pattern are seen to be slower in canines. However, the emptying rate relative to particle size and meal viscosity appears to correlate well between the two species. Gastric and intestinal pH in the postprandial phase appear to be more acidic in the dog. Therefore

caution might be necessary in predicting the performance of enteric coated delivery systems in humans based upon the data accumulated in dogs. However, as shown in the study on the coated Heidelberg capsule mentioned above,[125] this caution may not be warranted.

II. STATEMENT OF THE PROBLEM

Hydrogels for oral controlled drug delivery must swell at a predictable rate as they move through the various regions of the gastrointestinal tract. Residence time in the different regions of the gastrointestinal tract, coupled with available water and local environmental conditions, can potentially influence the rate and extent of swelling. *In-vivo* polymer swelling studies have not been reported and it has been assumed that *in-vitro* conditions adequately reflect *in-vivo* conditions. The inability to routinely develop good *in-vivo /in-vitro* correlations raises questions about the validity of this assumption.

The reasons for these *in-vivo /in-vitro* correlation failures are not fully understood but may in part be due to the absence of specific information on the availability of fluid in the different regions of the gastrointestinal tract. Fluid composition and properties influence the rate and extent of polymer swelling.

The unpredictable, and often poor, polymer performance seen for many gastrointestinal formulations are in part due to the absence of any specific information on the regional specific swelling action of hydrating polymers *in-vivo*. Most of the information that is available to the researcher has been generated from *in-vitro* studies without *in-vivo/in-vitro* correlations.

The current research was undertaken to study the *in-vivo* swelling behavior of a series of hydrogel polymers in the duodenal and ileal regions of the cannulated small intestine of the canine. The

information gathered from these studies, combined with data previously reported in the literature, as well as the data generated by a series of *in-vitro* studies, enabled the design of a kinetic model that describes polymer swelling and movement of fluid, spatially and temporally, through the gastrointestinal tract.

Specifically the aim of this study was to examine the swelling kinetics of four hydrating polymers, hydroxypropyl methyl cellulose, the sodium salt of carboxylmethyl cellulose, Carbopol 974P™, and Noveon AA1™ (polycarbophil), in the gastrointestinal tract of permanently cannulated canines. The four model polymers were placed into dialysis tubing of known volume and surface area that, in turn, were inserted into either the duodenal or ileal regions of the small intestine and swelling was studied as a function of time. These hydrogel polymers, chosen because of their differences in chemical and physical nature, were also studied under a series of *in-vitro* situations and the results of the two series were compared.

In addition, a computer generated model using STELLA,™ a simulation software package for handling compartment models, was developed to mimic the temporal and spatial movement of fluid as well as the swelling of an orally ingested polymer delivery system through the human gastrointestinal tract.

III. GENERAL EXPERIMENTAL PROCEDURE

III.1 Materials

Noveon AA1™ (polycarbophil) and Carbopol 974P™ were a gift from B.F. Goodrich Company (Breckville, OH). Carboxymethyl cellulose sodium salt (NaCMC, Sigma Chemical Company, St. Louis, MO) and hydroxypropyl methyl cellulose (HPMC, Aldrich Chemical Company, Milwaukee, WI) were obtained commercially and used as received without further treatment. Pulmocare™, a high calorie, high fat, low carbohydrate liquid food was donated by the Ross Products Division of Abbott Laboratories (Columbus, OH). Atropine sulfate (0.4 mg/ml) was obtained from Eli Lilly and Company (Indianapolis, IN). All other chemicals were either reagent or analytic grade and were used as received. All solutions were prepared with water freshly purified with a Synbron / Barnstead Nanopure II water purification system. Solution osmolarities were determined by a Wescor 5500 vapor pressure osmometer (Wescor, Logan, UT).

Three female mongrel hounds weighing between 17 and 27 kg were used throughout the study. Lighting was maintained on a twelve hour alternating cycle. The animals were fed a regular diet without any restrictions on the amount of water consumed.

III.2 Methods

III.2.1 Preparation of Sample

Polymer swelling kinetics were studied using 18 mm flat diameter Spectra/Por 3 regenerated cellulose dialysis membrane (Spectrum, Houston, TX) with a molecular weight cut off (MWCO) of 3500 Dalton. For each study, 155 mg of the desired polymer was inserted into a weighted (Eagle Claw split shot sinkers, Size #4, Taiwan) piece of dialysis tubing that was sealed at one end by 3-0 silk braided thread (Ethicon, Inc., Somerville, NJ). The second end of the tubing was then tied 4.0 cm from the first knot and trimmed to an overall length of 5.0 cm. This provided a constant surface area of 7.23 cm^2 and a constant internal volume of 4.15 cm^3 for all of the samples used throughout this study.

A 30 cm piece of nylon line (Eagle Claw, monofilament fishing line, 20 lb. test, Brazil) was attached to one end of the dialysis bag permitting insertion, anchoring and recovery of the sample. The entire set up was weighed just prior to insertion of the polymer containing tubing into the medium of the study (*in-vivo* or *in-vitro*).

III.2.2 Statistical Analysis

All results are expressed as the mean ± standard error of the mean (SEM). Statistical analyses were performed using Statworks™ v. 1.2 (Cricket Software, Philadelphia, PA) and Statview™ v.1.0 (Brain

Power, Inc., Calabasa, CA). Differences were considered significant when $p < 0.05$.

IV. *IN-VITRO* STUDIES

IV.1 Swelling as a Function of Surface Area

The swelling nature of Noveon AA1 (polycarbophil) in water and isoosmotic phosphate and citrate buffers[162] was studied in a series of dialysis membranes (Spectra/Por 3 regenerated cellulose dialysis membrane, Spectrum, Houston, TX) of various diameters. The diameters ranged from 11.5 mm to 28.6 mm which corresponds to surface areas of 7.23 cm^2 to 19.75 cm^2.

IV.1.1 Experimental

The dialysis tubing set up was prepared as described earlier. The tubing containing 155 mg of the polymer, polycarbophil, was weighed just prior to being placed into 100 ml of a stirred solution of either water, isoosmotic citrate buffer pH 4.8,or isoosmotic phosphate buffer pH 7.2.[1] The studies were conducted over a period of a minimum of 24 hours. The amount of fluid sorbed by the polymer was measured by removing the tubing from the test solution, drying the excess external fluid by gently tapping with a paper towel, and then weighing. The above process was executed in less than two minutes to minimize evaporation loss. The grams of fluid sorbed, i.e., the weight increase, divided by the weight of the dry polymer to yield

---

[1]both made isoomotic with mannitol

a normalized degree of hydration. The degree of hydration was plotted as a function of time and is shown in Figures 6 through 8. The rates of fluid sorbed is presented in Table 8. Each point on the graph represents the mean ± SEM of at least four individual measurements.

IV.1.2 Results

It is apparent from the figures and table that there is a direct relationship between the surface area of the tubing and the kinetics and extent of the amount of fluid sorbed by the polymer, polycarbophil. The greater the surface area, the more fluid sorbed.

From this information it was decided to use 11.5 mm diameter tubing as the standard of size, surface area and volume for both the *in-vitro* and *in-vivo*. portions of this study. The diameter of the dialysis membrane permitted the movement of fluid into the swelling polymer which, after the eight hour study, occupied a volume less than the maximum of the fully expanded tubing.

IV.2 *In-vitro* Swelling Studies

In order to correlate *in-vivo* information to *in-vitro* experiments more easily performed in the normal laboratory environment, polymer swelling was studied in a series of solvent systems chosen in an attempt to mimic the various pH conditions a polymeric drug delivery system would encounter in the gastrointestinal tract. These were water, simulated gastric fluid (pH

Figure 6 : *In-vitro* Swelling of Noveon AA1™ (polycarbophil) as a function of Surface Area. Dialysis medium is water. Degree of Hydration = (gms of fluid sorbed) / (weight of dry polymer).

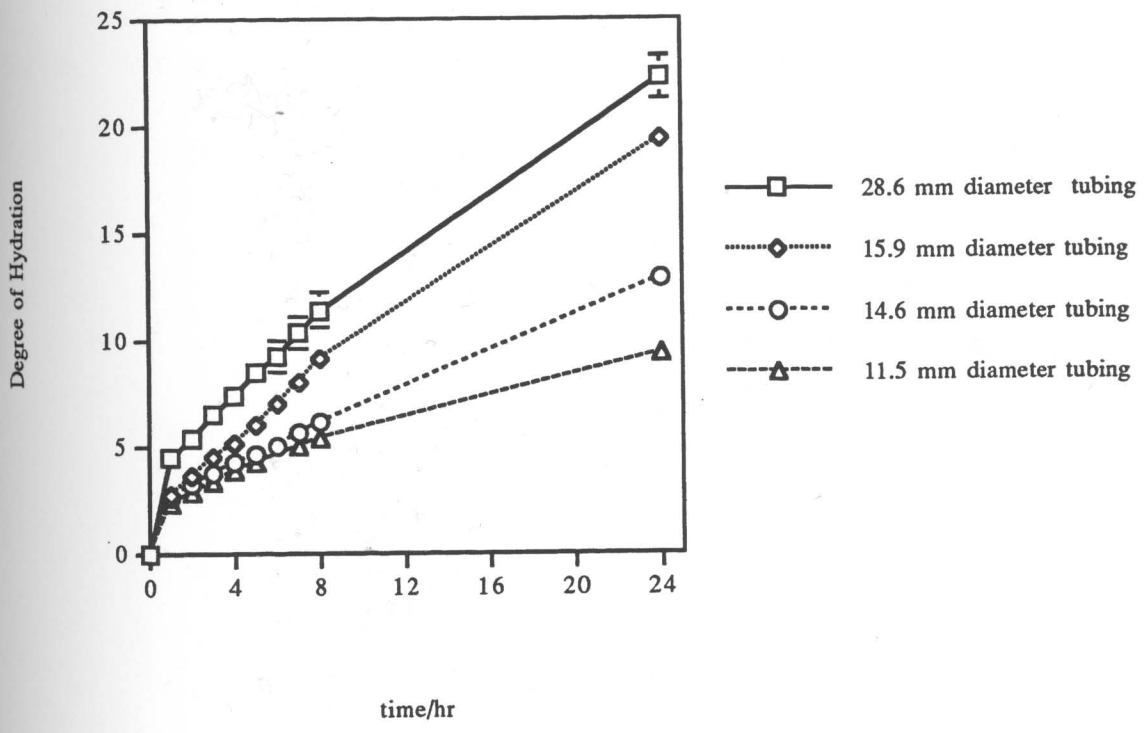
Degree of Hydration
25
20
15
10
5
0
0
4
8
12
16
20
24
time/hr
28.6 mm diameter tubing
15.9 mm diameter tubing
14.6 mm diameter tubing
11.5 mm diameter tubing

Figure 7 : *In-vitro* Swelling of Noveon AA1™ (polycarbophil) as a function of Surface Area. Dialysis medium is pH 4.8 Citrate Buffer . Degree of Hydration = (gms of fluid sorbed) / (weight of dry polymer).

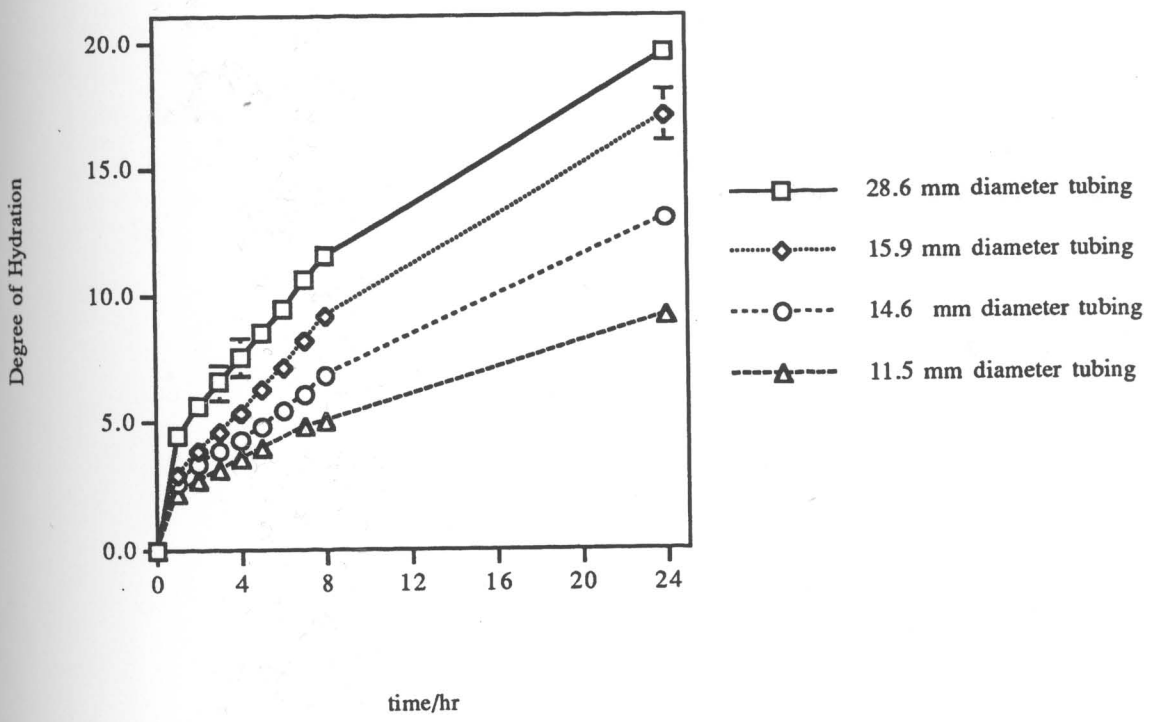
Degree of Hydration
20.0
15.0
10.0
5.0
0.0
0
4
8
12
16
20
24
time/hr
28.6 mm diameter tubing
15.9 mm diameter tubing
14.6 mm diameter tubing
11.5 mm diameter tubing

Figure 8 : *In-vitro* Swelling of Noveon AA1™ (polycarbophil) as a function of Surface Area. Dialysis medium is pH 7.2 Phosphate Buffer . Degree of Hydration = (gms of fluid sorbed) / (weight of dry polymer).

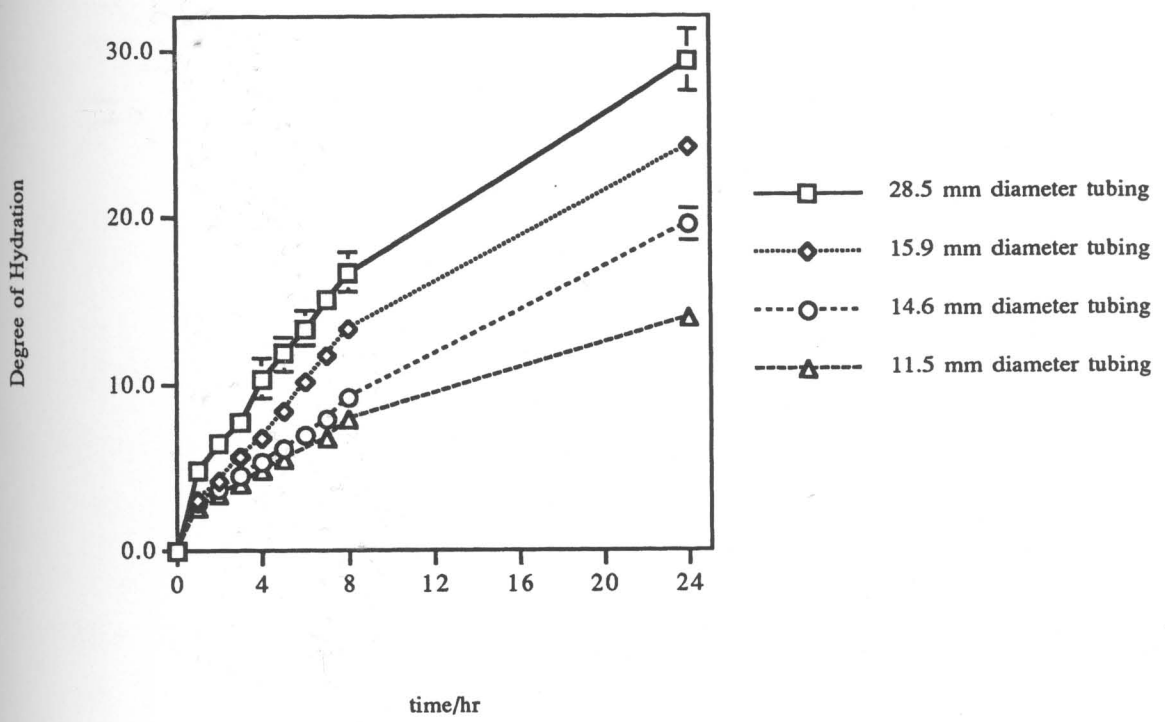
Degree of Hydration
30.0
20.0
10.0
0.0
0
4
8
12
16
20
24
time/hr
28.5 mm diameter tubing
15.9 mm diameter tubing
14.6 mm diameter tubing
11.5 mm diameter tubing

Table 8 : Comparison of Rates of Water Sorption for Noveon AA1™ (polycarbophil) in a Series of Dialysis Membranes of Different Diameters. Rates are reported in gm/hr.

Tubing Diameter/mm	Water	Citrate Buffer	Phosphate Buffer
11.5	0.0659	0.0635	0.113
14.6	0.0753	0.0898	0.134
15.9	0.136	0.135	0.229
28.6	0.149	0.154	0.267

1.2),[163] isoosmotic citrate buffer (pH 4.8), duodenal secretions (pH 6.3),[2] isoosmotic phosphate buffer (pH 7.2), and simulated intestinal fluid (pH 7.5).[164]

IV.2.1 Experimental

The dialysis tubing set up was prepared as described earlier, weighed then placed into 100 ml of the solution medium of interest. The studies were followed for at least 24 hours, periodically removing the tubing, drying the excess external fluid by lightly tap drying with paper toweling, and then weighing. The tubing was weighed within two minutes of being removed from the buffer in order to minimize loss due to evaporation. All studies were performed at ambient temperature.

IV.2.2 Results and Conclusions

The results of these in-vitro studies are presented in Figures 9 through 12. Each point on the graphs represents the mean ± SEM of at least four individual experiments. Statistical analysis of each of the four compounds was done to ascertain patterns in the swelling behavior of the polymers.

---

[2] combined fractions collected from three fasted canines.

Figure 9 : *In-vitro* Swelling Kinetics of Hydroxypropyl methyl cellulose in a series of buffer media. Degree of Hydration = (gms of fluid sorbed) / (weight of dry polymer). Each point on the graph represents the mean ± SEM of at least four measurements.

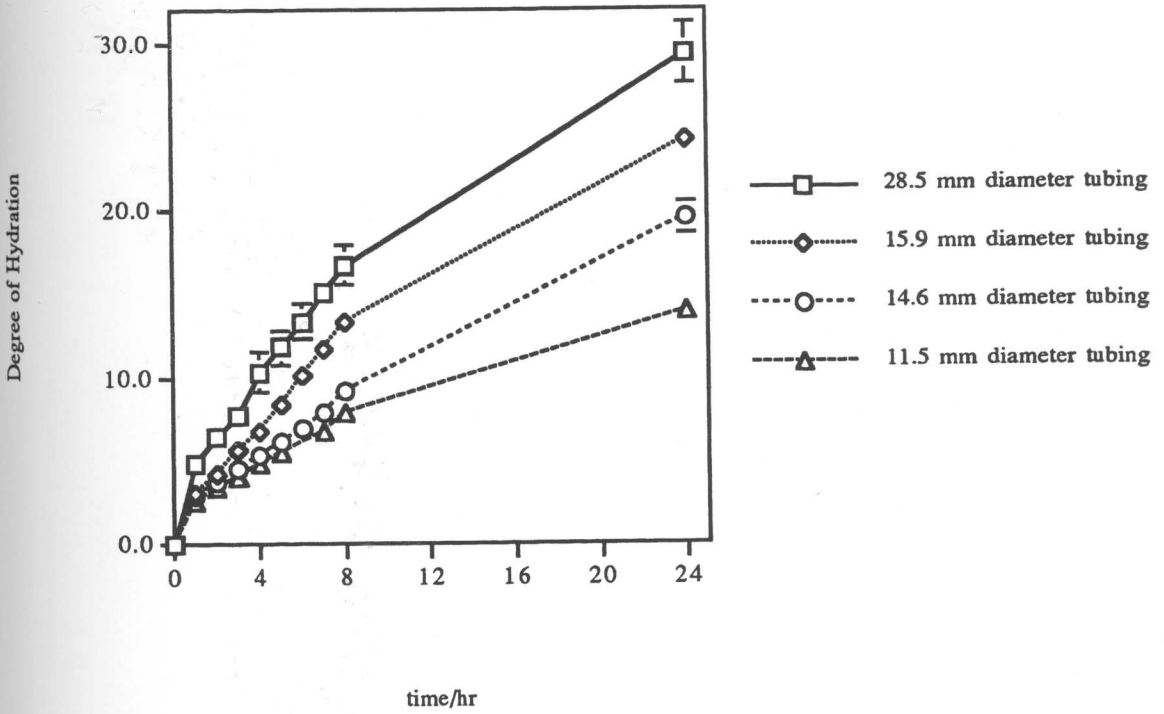
Degree of Hydration
30.0
20.0
10.0
0.0
0
4
8
12
16
20
24
time/hr
28.5 mm diameter tubing
15.9 mm diameter tubing
14.6 mm diameter tubing
11.5 mm diameter tubing

Figure 10 : *In-vitro* Swelling Kinetics of Carboxymethyl cellulose sodium salt in a series of buffer media. Degree of Hydration = (gms of fluid sorbed) / (weight of dry polymer). Each point on the graph represents the mean ± SEM of at least six measurements.

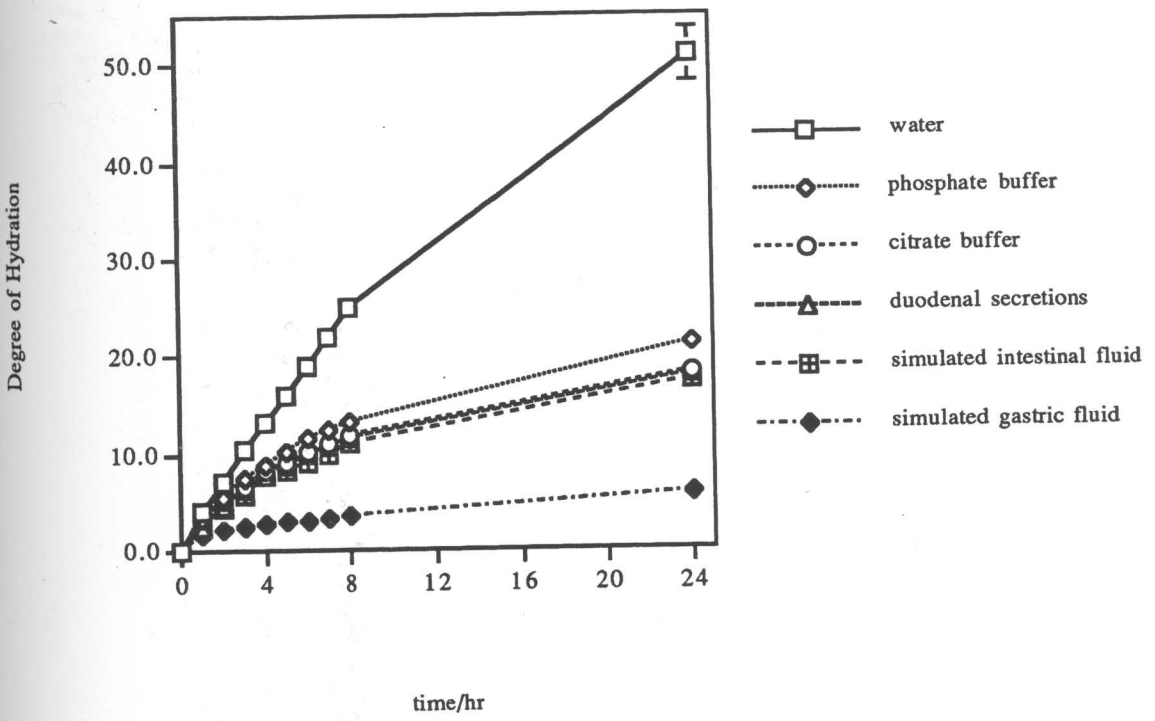
Degree of Hydration
50.0
40.0
30.0
20.0
10.0
0.0
0
4
8
12
16
20
24
time/hr
water
phosphate buffer
citrate buffer
duodenal secretions
simulated intestinal fluid
simulated gastric fluid

Figure 11 : *In-vitro* Swelling Kinetics of Carbopol 974P™ in a series of buffer media. Degree of Hydration = (gms of fluid sorbed) / (weight of dry polymer). Each point on the graph represents the mean ± SEM of at least six measurements.

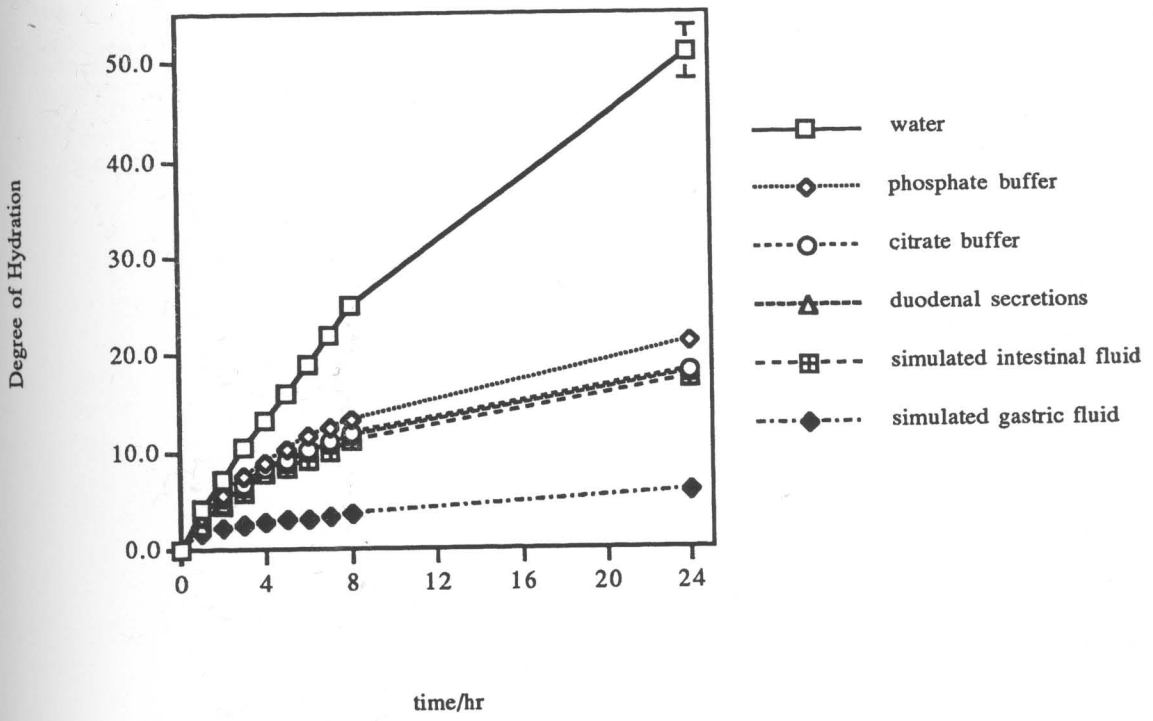
Degree of Hydration
50.0
40.0
30.0
20.0
10.0
0.0
0
4
8
12
16
20
24
time/hr
water
phosphate buffer
citrate buffer
duodenal secretions
simulated intestinal fluid
simulated gastric fluid

Figure 12 : *In-vitro* Swelling Kinetics of Noveon AA1™ (polycarbophil) in a series of buffer media. Degree of Hydration = (gms of fluid sorbed) / (weight of dry polymer). Each point on the graph represents the mean ± SEM of at least six measurements.

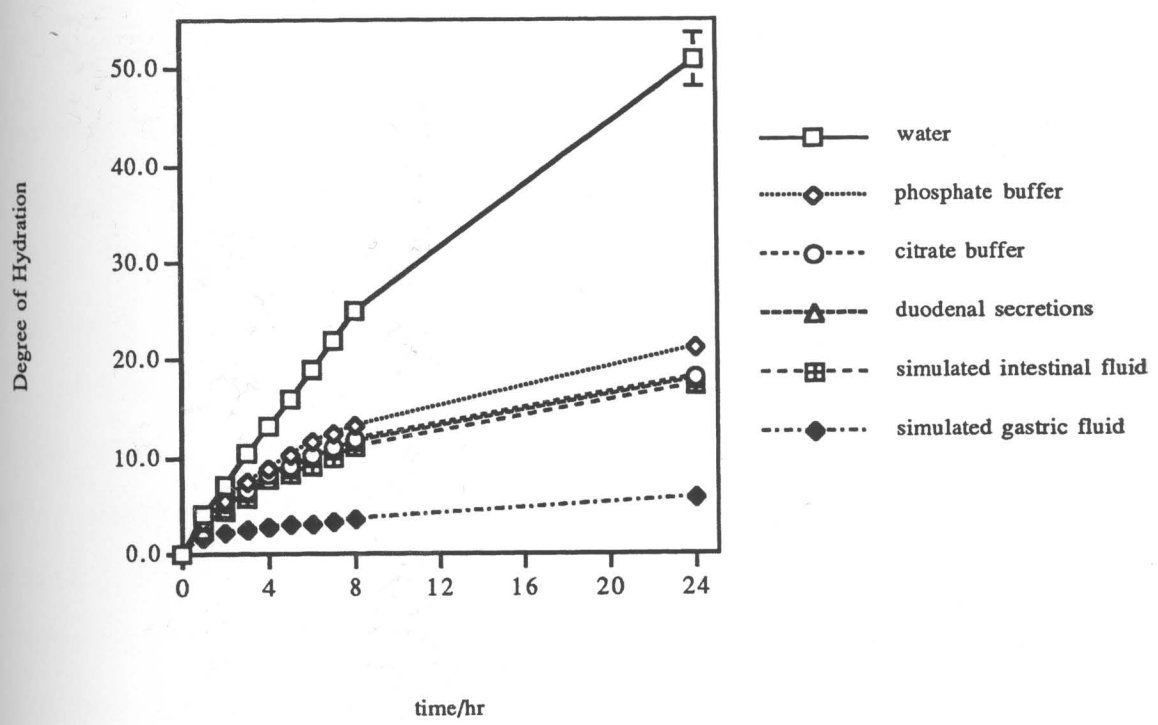
Degree of Hydration
50.0
40.0
30.0
20.0
10.0
0.0
0
4
8
12
16
20
24
time/hr
water
phosphate buffer
citrate buffer
duodenal secretions
simulated intestinal fluid
simulated gastric fluid

IV.2.2.1 Hydroxypropyl methyl cellulose

As can be seen in Figure 9, during the initial eight hours of hydration, the extent of swelling in water, ≈ 6.8 times dry polymer weight, was slightly more than in any of the other media, ≈ 5.3-6.0 times. In addition, water was the only medium whose swelling curve was seen to be statistically different.

An examination of the initial slope, i.e., for the first six hours of the study, showed, at the 99% significance level, that the rate of water uptake by HPMC was the same irrespective of the media studied. As would be expected for a neutral polymer, pH and ionic effects do not appear to affect the swelling behavior of the hydroxypropyl methyl cellulose.

IV.2.2.2 Carboxymethyl cellulose sodium salt

It has often been observed that ionizable hydrogel polymers tend to swell more when they are ionized. This point is supported by examination of the extent and rate of swelling pictured in Figure 10 in which the rate and extent of swelling for carboxymethyl cellulose differed are seen to be dependent upon the medium used.

In simulated gastric fluid, pH 1.2, the extent, ≈ 3.5 times dry polymer weight, and the rate of swelling were significantly less than in any other medium. It appears that the acidic nature of the solution protonates the free carboxylate groups, which results in an overall minimizing of the repulsive force of the negatively charged ionized

form. The hydration effect of the diffusing water molecules is lowered, resulting in reduced swelling.

When the diffusing medium was pure water, the extent, ≈ 25 times dry polymer weight, and rate of swelling were seen to be statistically more than in any other system studied. The remaining solutions were seen all grouped together, with similar swelling rates and extents, 10.9 - 13.3 times dry polymer weight. At 95% confidence, NaCMC swelled slightly better in the pH 7.2 phosphate buffer than in the other media, but still only about half of that seen in water alone. It appears that with a pKa of approximately 4.0 - 4.7 a large portion of the carboxylic acid groups would be ionized in the media studied (pH range 4.8-7.5). The more ionized the polymer, the greater the effect of hydration, and the better the swelling.

IV.2.2.3. Carbopol 974P™ and Noveon AA1™ (polycarbophil)

The hydrogel polymers Carbopol and Noveon are very similar both chemically and structurally. Both polymers are large, with molecular weights ≈ 2 x 10^6 daltons, and covalently cross-linked with high density of carboxylic acid groups. As with NaCMC, these polymers demonstrated the least swelling in acidic simulated gastric fluid (pH 1.2). In this medium it would be expected that essentially all of the carboxylic groups of the polymer backbone are protonated. As seen in Figures 11 and 12, the extent of swelling of Carbopol and Noveon, at eight hours, was seen to be 3.4 and 3.1 times the original dry polymer weight, respectively. In addition, each simulated gastric

fluid curve was statistically significant from that in any of the other media studied.

The only other statistically different curve was that generated in the pH 7.2 phosphate buffer swelling study. During the initial eight hours of the study in this buffer, Carbopol and Noveon sorbed enough fluid to result in weight increases of 6.6 and 7.8 times dry polymer weight, respectively. Since the pH 7.2 buffer is as much as 2.5 pH units above the pKa of either polymer, it would be expected that the functional groups of the polyacid hydrogels would be more than 95% ionized. As has already been noted, the repulsive forces of the carboxylate anions generated help to promote expansion of the polymer matrix, allowing water to diffuse in and hydrate the negatively charged moiety. Increased swelling would result.

The remaining studies resulted in weight increases of 4.5-5.5 and 3.5-5.1 times original dry polymer weight for Carbopol and Noveon respectively.

With the patterns described above, no pH effect appears to consistently explain all of the trends seen in Table 9. While a positive swelling effect was seen for NaCMC, Carbopol and Noveon in the pH 7.2 phosphate buffer studies, a similar effect in simulate intestinal fluid at pH 7.5 was not observed. The question is why?

Hydrogel swelling responds to changes in many environmental conditions. Most prominent are temperature, pH, ionic strength, salt type and solvent. Any and all of these would be expected to influence the extent and rate of swelling.

Table 9 : *In-vitro* Extent of Polymer Swelling. Degree of Hydration at t = 8 hours.
Degree of Hydration = (weight of fluid sorbed) / (weight of dry polymer).

Polymer	Water	Phosphate Buffer	Citrate Buffer	Duodenal Secretions	Simulated Intestinal Fluid	Simulated Gastric Fluid
HPMC	6.8	5.5	5.6	5.6	6.0	5.3
NaCMC	25	13.3	11.8	11.6	10.9	3.5
Carbopol	5.4	6.6	4.8	4.5	4.9	3.4
Noveon	5.3	7.8	5.1	4.5	3.7	3.1

In our studies, temperature and solvent, which was mainly water, were fairly constant throughout the study. However, differences in the media may have arisen from the components of the buffers. Pancreatin, porcine pancreatic enzymes, (Sigma Chemical Company, St. Louis, MO) , monobasic potasium phosphate and sodium hydroxide in the simulated intestinal fluid,[164] citric acid, sodium hydroxide and mannitol in the citrate buffer, pepsin, porcine gastric enzymes, (Amend Drug and Chemical Co., Irvington, NJ), sodium chloride, and hydrochloric acid in the simulated gastric fluid,[163] and potasium and sodium phosphate in their mono- and dibasic forms in the phosphate buffer demonstrate the diversity of components that made up the solutions of this study. Comparing these solutions to pure water or the multiple unknown components that make up the duodenal secretions leaves many questions as to how one can compare these complex mixtures. A calculation of the ionic strengths of the citrate and phosphate buffers showed values that were similar (0.147 M versus 0.188 M).

Another point that needs to be considered is the variety of osmotic pressures of the different media. While citrate and phosphate buffers were made isoosmotic (≈ 295 mosmols/kg) with mannitol, the simulated intestinal fluid and the collected duodenal secretions were hyperosmotic at ≈ 400 mosmols/kg. The simulated gastric fluid prepared had an hypoosmotic pressure of 215 mosmols/kg and pure water is naturally hypoosmotically with a value nearly zero.

The differences in osmolarity of the solutions may account for the variety of results seen. It is probable that the hypoosmotic water may be driven into the polymer by virtue of an osmotic gradient across the dialysis membrane. This would account for the strong influence seen in the swelling results of each of the polymers. The differences, albeit not always statistically significant, seen for the isoosmotic phosphate pH 7.2 and the hyperosmotic simulated intestinal fluid pH 7.5 may also be accounted for due to this gradient. That is, while it would be expected that the rates and extents of swelling would be the same due to similar pH's, differences in the water movement due to the osmotic pressure disparity of the two solutions might account for the differences seen. This is especially apparent for the polyacrylic acids, Carbopol and Noveon, where pH would be expected to have a naturally strong effect on the chemical nature of the polymer. While the isoosmotic phosphate buffer showed greater swelling than would be expected, the hypoosmotic water demonstrated greater swelling results than any of the buffers with higher osmotic pressures.

In the case of simulated gastric fluid, while osmolarity of the solution (215 mosmols/kg) would be expected to enhance swelling, acidity of the buffer demonstrated a stronger influence resulting in a reduction of swelling.

IV.3 pH Study

To answer the question of what effect is exerted by the diffusing solution on the polymer, as well as what effect the polymer exerts on the diffusing solution, led us to attempt to measure changes in local pH as the solution diffuses into the polymer. Measurements of pH were carried out using a flexible pH electrode (Model MI-506, flexible pH electrode, Microelectrodes Incorporated, Bedford, NH) with a total length of 3 meters, a 1.6 mm O.D., 1.3 mm tip diameter and 1 mm pH sensitive tip length. The local pH was measure via a previously calibrated microelectrode inserted into the center of the dry polymer contained in a 11.5 mm diameter dialysis tubing. The tubing was secured at each end with 3-0 braided silk threads and trimmed so that each study was performed with a dialysis membrane of constant surface area (7.23 cm^2).

The tubing was placed in 80 ml of either pH 4.8 citrate or pH 7.2 phosphate buffer and monitored Corning Model 5 pH Meter, Corning Scientific Products) as a function of time. The result of these studies is shown in Figures 13 through 20. Each curve on the graph represents a separate study.

It is important to note that what we see in the figures is an empirical measurement consistent with what would be expected in a pH measurement. However, it is also important to remember that we are not measuring an aqueous solution, the most commonly pH studied system, but instead we are studying a system that may be described

Figure 13 : *In vitro* pH Study of Hydroxypropyl methyl cellulose in isoosmotic Citrate Buffer pH 4.8. Each curve represents a separate study.

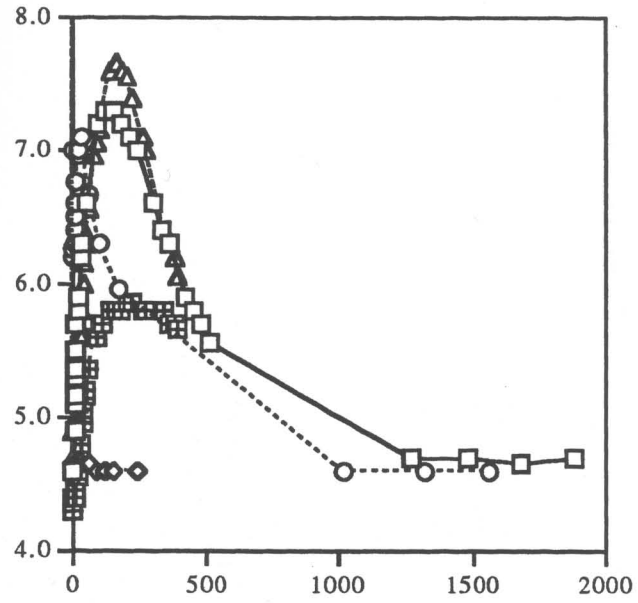
8.0
7.0
6.0
5.0
4.0
pH
0
500
1000
1500
2000
time / min

Figure 14 : *In vitro* pH Study of Carboxymethyl cellulose sodium salt in isoosmotic Citrate Buffer pH 4.8. Each curve represents a separate study.

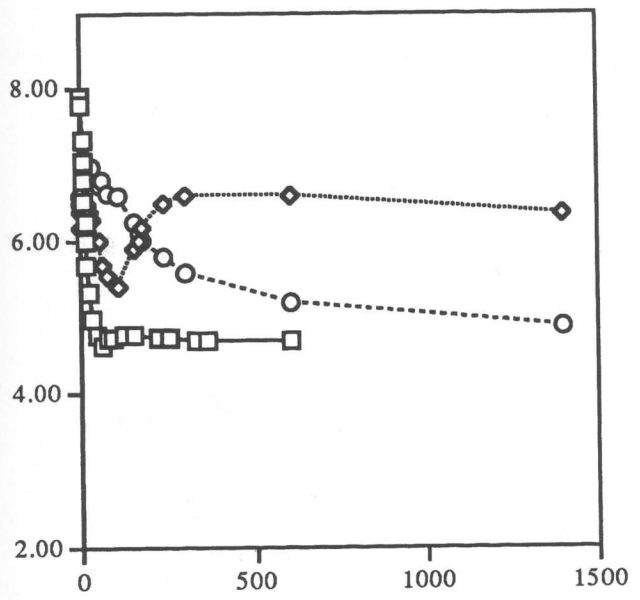
8.00
6.00
4.00
2.00
pH
0
500
1000
1500
time / min

Figure 15 : *In vitro* pH Study of Carbopol 974P™ in isoosmotic Citrate Buffer pH 4.8. Each curve represents a separate study.

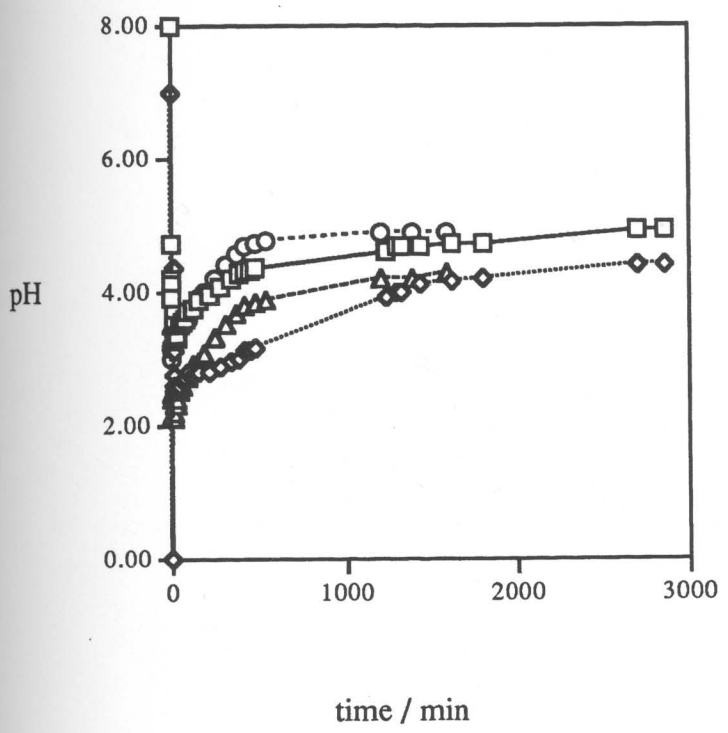
8.00
6.00
4.00
2.00
0.00
pH
0
1000
2000
3000
time / min

Figure 16 : *In vitro* pH Study of Noveon AA1™ (polycarbophil) in isoosmotic Citrate Buffer pH 4.8. Each curve represents a separate study.

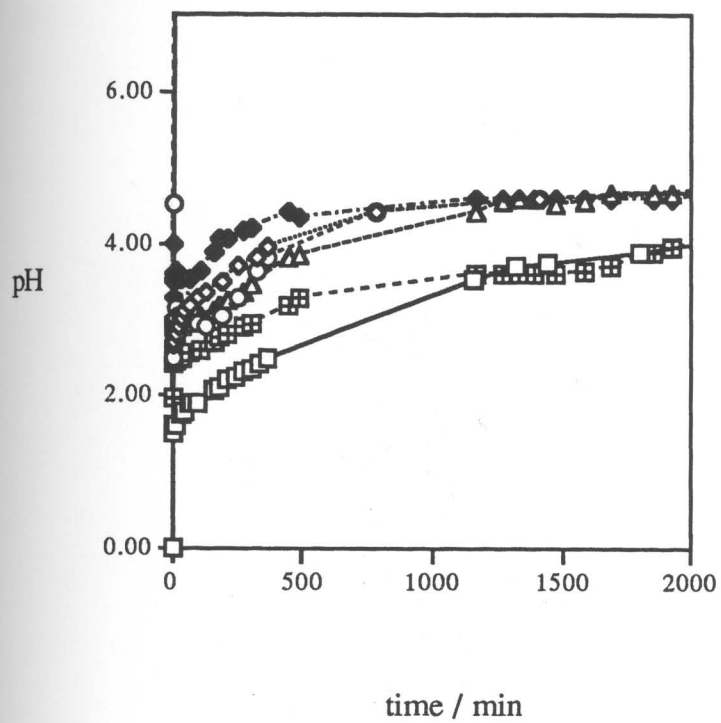
6.00
4.00
2.00
0.00
pH
0
500
1000
1500
2000
time / min

Figure 17 : *In vitro* pH Study of Hydroxypropyl methyl cellulose in isoosmotic Phosphate Buffer pH 7.2. Each curve represents a separate study.

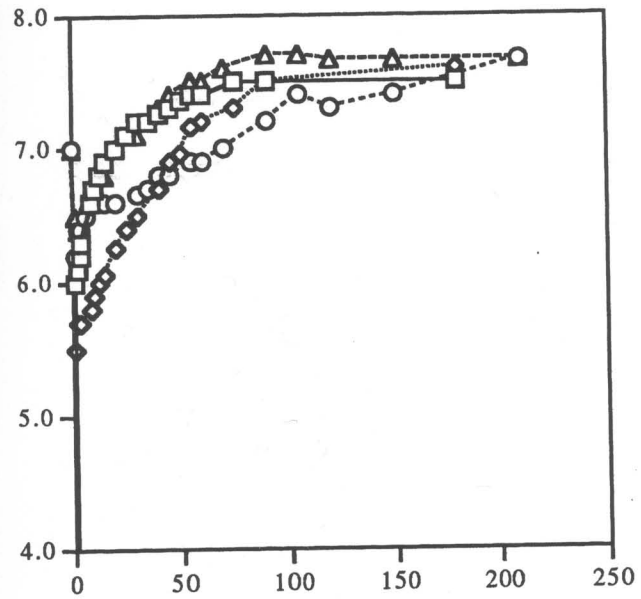
8.0
7.0
6.0
5.0
4.0
pH
0
50
100
150
200
250
time / min

Figure 18 : *In vitro* pH Study of Carboxymethyl cellulose sodium salt in isoosmotic Phosphate Buffer pH 7.2. Each curve represents a separate study.

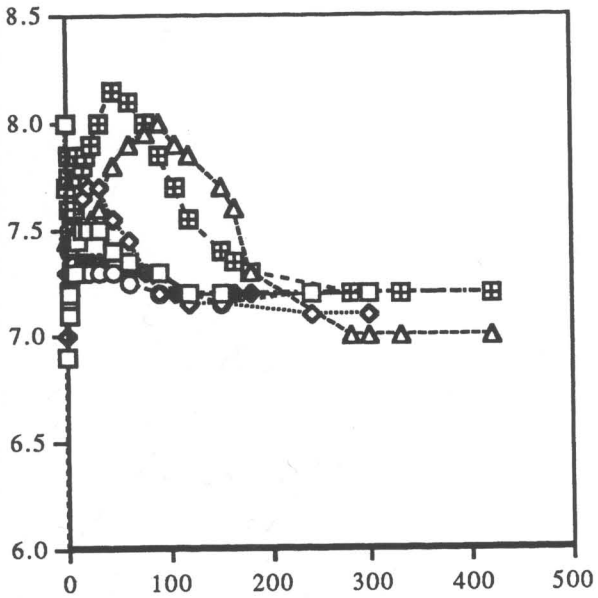
8.5
8.0
7.5
7.0
6.5
6.0
pH
0
100
200
300
400
500
time / min

Figure 19 : *In vitro* pH Study of Carbopol 974P™ in isoosmotic Phosphate Buffer pH 7.2. Each curve represents a separate study.

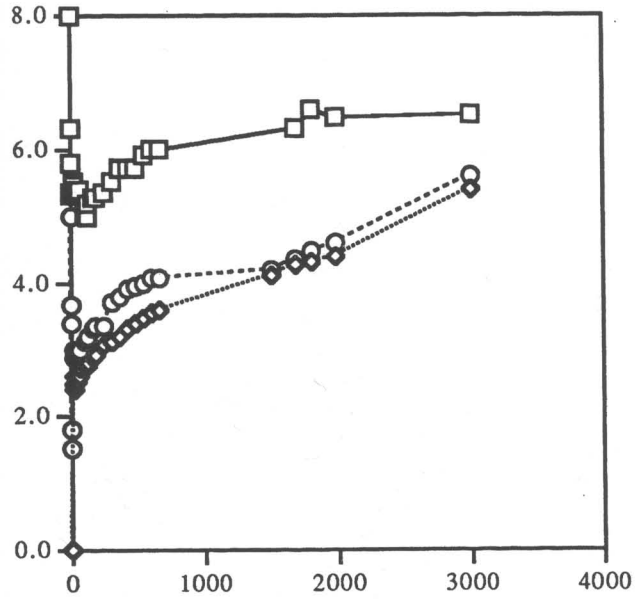
8.0
6.0
4.0
2.0
0.0
pH
0
1000
2000
3000
4000
time / min

Figure 20 : *In vitro* pH Study of Noveon AA1™ (polycarbophil) in isoosmotic Phosphate Buffer pH 7.2. Each curve represents a separate study.

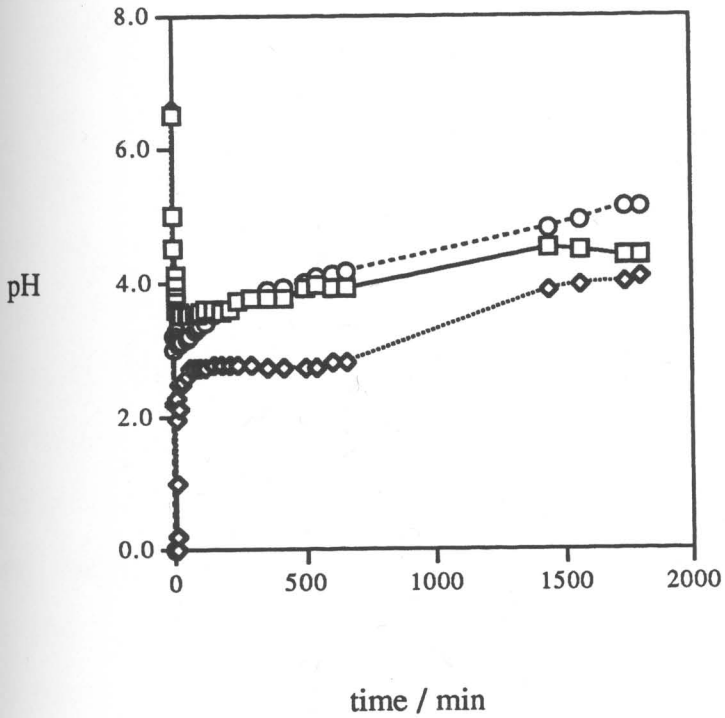
8.0
6.0
4.0
2.0
0.0
pH
0
500
1000
1500
2000
time / min

as "two solvents," polymer and buffer, which, especially during early swelling, can at best be considered a very concentrated aqueous mixture.

In examining the figures, the observation is made that the curves generated for each of the four polymers asymptote towards the pH of the buffer, albeit it may take a long time to achieve. It is also noted that a very prominent characteristic is that the pH curve approaches this asymptote from either the acidic or basic direction reflecting the innate chemical nature of the polymer studied. That is, Carbopol and Noveon asymptote from a lower pH, reflecting the polyacrylic acid groups of their structures. The pH of a 1% solution has been measured to be 2-4.[91,92] In fact, neither polymer ever reached pH 7.2 when diffused with phosphate buffer even after 50 - 80 hours. This is most likely due to the large number of acid groups within the chemical structure of the polymers.

Carboxymethyl cellulose asymptotes from higher pH due to the conjugate base behavior of its carboxylate ions. This is reflected in the fact that a 1% solution of NaCMC has a pH of 7.4 - 8.0. (Aldrich Chemical Company, personal communication) The chemically neutral HPMC asymptotes relatively quickly to the pH of the buffer solution from a more neutral pH. This fits what would be expected as reflected by its 1% solution pH of 5.5 - 7.5. (Aqualon, personal communication)

In summary, it appears that the microclimate surface pH innate to the polymer species, originating from the functional groups making

up its chemical structure, acts as a buffer to minimize and retard the effect of the diffusing solution.

V. *In vivo* Studies

V.1 Background

A number of direct and indirect techniques have been used to examine the gastrointestinal disposition of drugs and delivery systems in humans and animals. Among these techniques, the methods most frequently used are x-rays,[110] scintigraphy,[43,160,161,165] intubation,[166,167] as well as the classic drug concentration-versus-time blood sampling studies.

Radiographic (x-ray) examinations have yielded great advances in the knowledge of anatomy, physiology and pathology of the gastrointestinal tract since its first use in 1904.[110] Unfortunately, to obtain sharp, contrast-rich x-ray pictures electron dense substances such as barium sulfate must be ingested. This in turn alters the natural state of the gastrointestinal tract. Scintigraphy involves the addition of a radioactive isotope to the formulation of whatever is being studied. These isotopes usually have short half lives that thereby limit the complexity of the study performed.

Intubation, most often in concert with regional intestinal perfusion, has several drawbacks, not the least of which being that a tube approximately 200 cm long and 5 mm in diameter needs to be guided from the mouth to the point of interest in the intestine and remain in place for the entire period of the study. The discomfort to the subject as well as the non-physiological condition of the constant presence of the tube limits the use of this method.

The approach used in our studies was a direct technique using a permanently implanted cannula. Although the technique is in general not applicable to humans, an implanted cannula provides a direct visualization of the nature of the discharge from the stomach or intestines of the canine. It permits direct and simple introduction of materials into a specific region of the dog's intestines while permitting the collection of material (perfusate, secretions, etc.) after it passes through selective regions of the small intestine.

In addition, the long life of a permanent indwelling cannula permits the repetitious use of the same animal for many studies. We can thereby minimize the number of subjects and many sources of experimental variability, such as anesthesia effects, surgical trauma, and inter-animal variability.

V.1.1 Cannula

A modified Thomas type cannula[168] was constructed according to the modification of Rubinstein, et. al.[169] These modifications, through the use of polymeric and stable plastic material, create a cannula that is light weight, does not corrode and is easy to manipulate and maintain. The design extends the useful lifetime of the cannula and reduces the incident of leakage and infection.[142] The components of the cannula can be seen in Figure 21.

Figure 21 : Components of the Cannula. Clockwise direction: teflon plug (I) with the center drilled stainless steel wire (II), aluminum cap (III), Acetal Extension (IV), aluminum locking ring (V), Acetal slotted washer (VI), and Acetal cannula (VII).

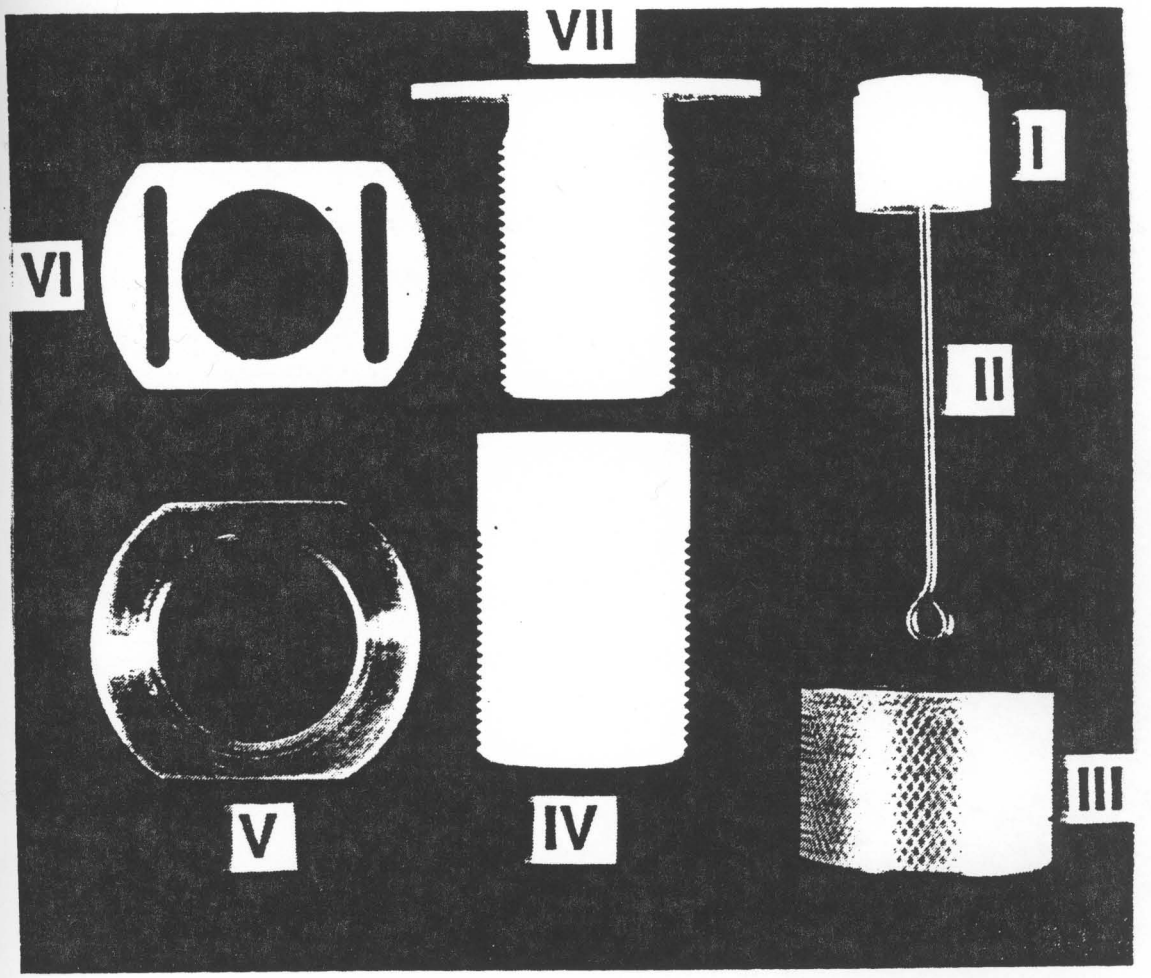
VII
I
VI
II
V
IV
III

The body of the cannula is constructed from Acetal (Delrin AF-Blend, E.I. DuPont) Homopolymer (Polymer Corporation, Reading, PA). The cap (III) is made of aluminum and the plug wire (II) is stainless steel. The stem is mainly composed of two parts: the cannula (VII) and an extension (IV). The cannula contains an oval tubular plate that fits into the opening of the intestinal incision and, once inserted, prevents the cannula from sliding out. The stem is threaded on its surface so that a slotted Acetal washer (VI) can be screwed on from outside the intestinal wall. The purpose of this washer is to fix the cannula to both the omentum and the visceral abdominal wall. When exteriorized, only a few millimeters of the lower edge of the cannula (VII) are exposed outside the skin. The extension (IV) which is threaded on both sides of the body wall, is them screwed onto the top of the cannula. The overlapped area between the two segments is about 4 millimeters. The extension is also threaded on its outer surface so that the aluminium cap (III) can be screwed outside the body wall.

A 15 mm Teflon plug (I) is fitted snugly to the tubular opening of the cannula. It has a 1 mm peripheral groove at the edge so that it cannot slide above the surface of the plate and into the intestine. A stainless 1 mm diameter steel wire (II) drilled into the center of the plug allows easy insertion or retraction from the stem. The total length of the plug and the wire match the length of the cannula and its extension when tightly fitted. The aluminum cap locks the cannula and prevents the plug from sliding out.[169]

The dimensions of the cannulae used throughout this study are summarized in Table 10.

V.1.2 Implantation of the Cannula[3]

The technique for the implantation of the cannulae (The University of Wisconsin Physical Plant Machine Shop, Madison, WI) was similar for each of the three female dogs used throughout these studies. Under thiopental anesthesia, a ventral midline was made from cranial to the umbilicus to the pubis to expose the abdominal cavity. A four centimeter incision was made in the anti-mesenteric portion of the intestine in the duodenum and the ileum. The incision in the duodenum was 20 cm distal to the pylorus and in the ileum, 20 cm proximal to the ileocecal junction. The foot plate of the Acetal cannula was inserted into the intestinal lumen and secured by a 3-0 Vicryl purse string stitch. One addition simple interrupted stitch was used to close the intestinal incision around the cannula.

A fenestration was made in the omentum through which the cannula was passed. The omentum was positioned over the enterotomy and the Acetal slotted washer was threaded onto the cannula and placed adjacent to the intestinal wall.

The cannula was placed through the abdominal wall through an opening made by a stab incision through the wall in the right flank region, caudal to the thirteenth rib and ventral to the abaxial

---

[3]modified from the surgical report of E. Rosin, D.V.M. of the School of Veterinary Medicine, University of Wisconsin.

Table 10 : Dimensions (mm) of the Intestinal Cannulae[170]

O.D. cannula	21
I.D. cannula	17
O.D. extension	26
I.D. extension	21
Diameter of tubular opening	15
Total length closed	73
Tubular head thickness	1
Tubular head length	42
Slotted washer length	40
Slotted washer width	21

muscles. The Acetal slotted washer, threaded onto the cannula and positioned adjacent to the omentum and intestine, was sutured to the peritoneal surface of the abdominal wall with two 2-0 nylon simple interrupted stitches. The cannula extension was threaded over the cannula placed through the abdominal wall. The lumen of the cannula was closed with the Teflon plug and held in place by the aluminum cap.

The skin was closed around the cannula with one or two 2-0 nylon simple interrupted stitches. The abdominal insertion was closed as follows: abdominal wall closed with 0 Maxon placed in simple continuous pattern; subcutaneous tissue closed with 3-0 Vicryl placed in simple continuous pattern; and the skin closed with a subcuticular stitch of 3-0 Vicryl and skin staples.

The animals were allowed a recovery period of at least three weeks before initiating any studies. The dogs were trained to stand quietly, supported by modified Pavlov slings, (Alice King Chatham Medical Arts, Hawthorne, CA) for periods of study of up to nine hours and to accept oral administration of liquids and solids by natural swallowing.

The placement of the cannulae can be seen in the photograph in Figure 22.

Prior to each experiment, the canines were deprived of food, but not water, for at least sixteen hours, overnight.

Figure 22 : Photographic Representation of the Cannulated Dog. The lower cannula shown is permanently implanted into duodenum 20 cm distal to the pylorus and the upper cannula shown is implanted into the ileum 20 cm proximal to the ileocaecal junction.

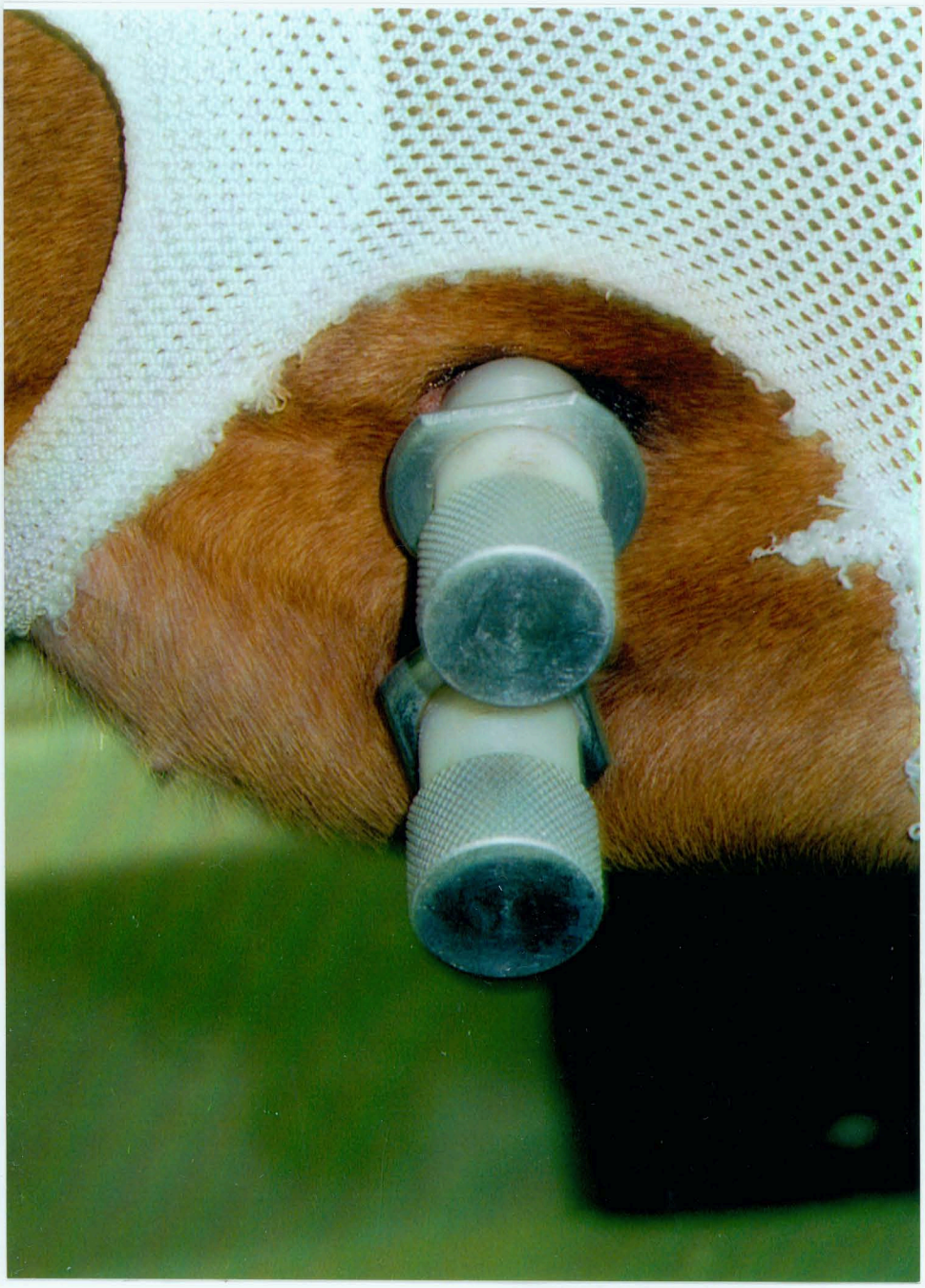

V.1.3 Sample Preparation

The dialysis tubing set up was prepared as described in the General Experimental section. The polymer containing tubing was weighed just prior to being inserted into the intestinal region of interest through the appropriate cannula (duodenum or ileum) during, phase I of the migrating myoelectric complex (MMC), except where otherwise noted. The cannula was closed by insertion of a #9 size cork that simultaneously secured the tail portion (≈ 5 cm) of the 30 cm piece of nylon line attached to the inserted dialysis tubing.

V.2 Transit Study

While the pattern of fluid transit through the duodenum has been well documented in the fasted dog,[142,143,156,170] we realized that to determine the effect of different feeding regimens on the rate of polymer swelling it would be necessary to understand the pattern and rate of emptying of material from the stomach and through the intestine. The following graphs, Figures 23 - 26, describe the appearance of material in the duodenal cannula after water or Pulmocare™ was fed to the fasted canine by a gavage tube.

To acquire this information, the three dogs were fasted for at least 16 hours the night prior to the study. In the morning the dogs were placed standing in the Pavlov slings and their duodenal cannulae were opened. The effluent from the cannula was collected and, once it was ascertained that the dogs were truly in the fasted state, as

Figure 23 : Study of the volume eluted after 300 ml water was administered as a bolus by gavage tube directly into the stomach of the canine. Each curve represents the pattern of a different dog.

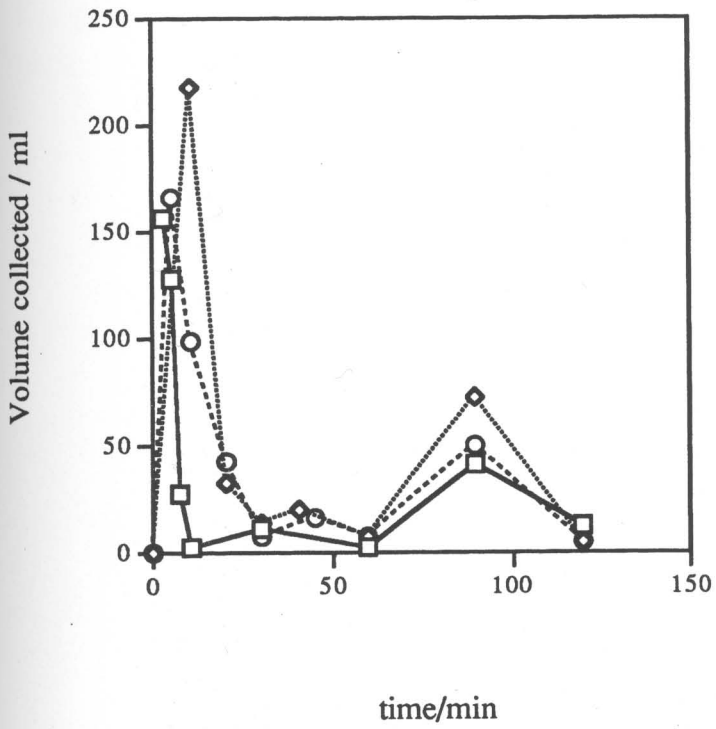
250
200
150
100
50
0
0
50
100
150
Volume collected / ml
time/min

Figure 24 : Study of the cumulative volume eluted after 300 ml water was administered as a bolus by gavage tube directly into the stomach of the fasted canine. Each curve represents the pattern of a different dog.

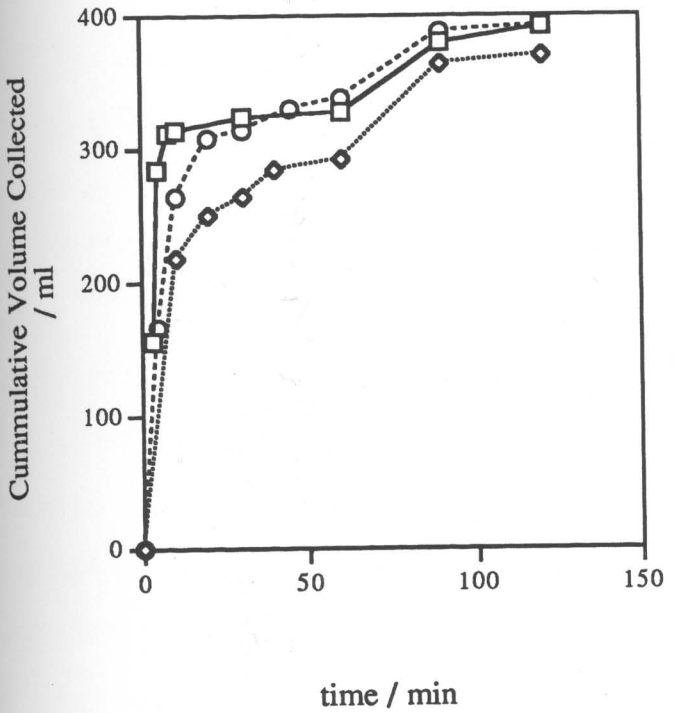
Cummulative Volume Collected / ml
400
300
200
100
0
0
50
100
150
time / min

verified by passing of two phase III patterns of the MMC, was the study begun.

Twenty minutes after the cessation of phase III activity, i.e., during phase I of the MMC, either 300 ml of doubly distilled water or a can of Pulmocare™, 8 fluid ounces, 237 ml, equilibrated at room temperature was fed into the stomach of each of dog through a gavage tube. The timing of the transit of the material was begun upon the completion of the administration of the fluid.

The effluent was collected in sampling bags hung from the opened cannulae and the volume collected was measured in a graduated cylinder. The results are presented graphically as volume collected and cumulative volume collected as a function of time.

In comparing the graphs of these two studies it is important to note the difference in time scale of the transit of the different materials. In the water fed study, essentially all that was administered to the animal eluted in less than forty-five minutes. Also, the amount collected corresponded well with the 300 ml of fluid that was fed to the animal. The return to the fasted state was quite rapid for each dog. The appearance of the phase III housekeeper wave returned approximately ninety minutes after the ingestion of water.

Pulmocare™ elution and collection are graphically shown in Figures 25 and 26. While only approximately 240 ml of fluid was administered to the canines, more than twice that amount was collected over the five hours of the study. A volume of 300 ml was collected within the first hour. It was also observed that, as opposed

Figure 25 : Study of the volume eluted after 8 oz (237 ml) Pulmocare™ was administered as a bolus by gavage tube directly into the stomach of the fasted canine. Each curve represents the pattern of a different dog.

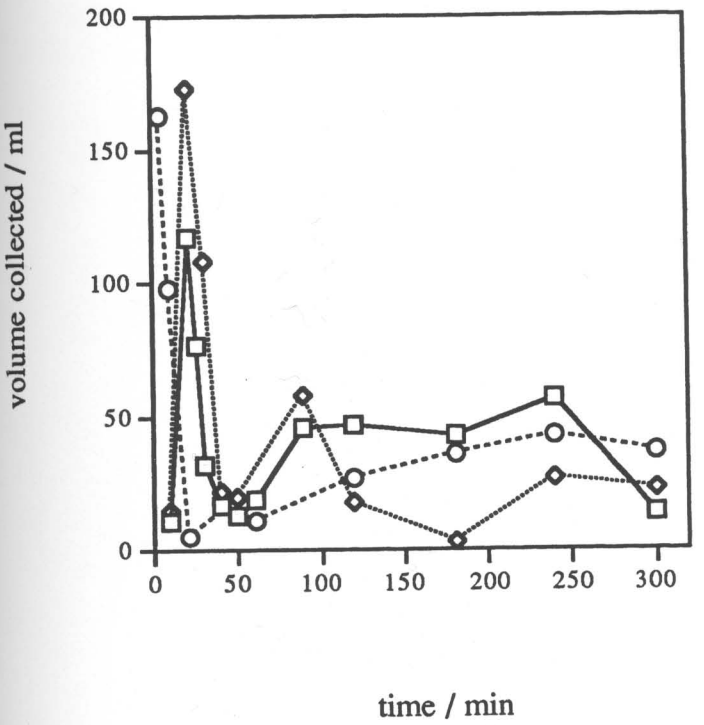
volume collected / ml
200
150
100
50
0
0
50
100
150
200
250
300
time / min

Figure 26 : Study of the cumulative volume eluted after 8 oz (237 ml) Pulmocare™ was administered as a bolus by gavage tube directly into the stomach of the fasted canine. Each curve represents the pattern of a different dog.

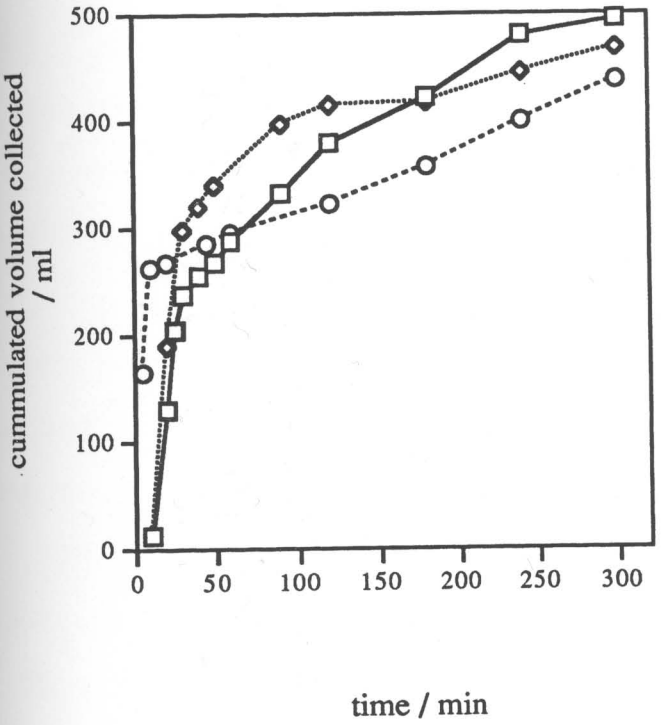
cummulated volume collected / ml
500
400
300
200
100
0
0
50
100
150
200
250
300
time / min

to what was seen in the water study, the dogs never returned to the fasted state over the five hour period of the study.

This observation was not unexpected. Pulmocare™ is by design a high fat (55.1% of the caloric distribution), hyperosmotic (≈525 mosmol/kg) liquid food product. High fat content meals have been shown to increase stomach residence time of meals[143,171] and consequently reduce the emptying rate. The consequence of hyperosmolality is an increase in duodenal and gastric secretions in an attempt to bring the osmolarity of the fluid closer to the isoosmotic conditions most preferred by the intestinal tissues.

In summary, what we see is that when water is ingested, it quickly passes through the pylorus and into the duodenum without the addition of much, if any, additional secretions. It would therefore be expected that a swelling polymer in the duodenum would likely have only a brief period of exposure to the water as it passes. In turn, we would expect that oral intake of water would exert, at best, only a small effect upon the polymer.

On the other hand, Pulmocare™ results in a prolonged flowing of fluid into the duodenum. One would expect that the ingestion of Pulmocare™, or any similarly high fat meal, would result in the duodenally based polymer to be exposed to a greater amount of fluid for a longer duration of time. We would therefore expect the conditions to better promote swelling in a polymer located in the duodenum

V.3 In vivo Swelling Studies

In-vivo swelling studies were executed in the dogs under both fasted and fed conditions. If the study was to be performed under fasted conditions, the dialysis tubing was inserted into the cannula of interest during phase I of the MMC without any further manipulations. However, if swelling was to be studied under fed conditions, water or Pulmocare™ would then be administered directly into the stomach via gavage tube . The liquid was injected at a rate such that all material was administered within two minutes. Total time from insertion of the dialysis tubing to the completion of liquid administration was less than five minutes.

At the appropriate time, the cannula was opened and the dialysis tubing was removed from the intestine. Excess intestinal material was gently wiped from the tubing with paper toweling and the tubing was then weighed. Total time between removal to weighing was kept to under a minute to minimize any loss due to evaporation. Three to five repetitions of each experiment, i.e., each time point, were conducted for each canine. The results from the three dogs were pooled and the mean and standard error were calculated. The degree of hydration, i.e., the grams of fluid sorbed divided by the weight of the dry polymer, was plotted as a function of time. The results are shown in Figures 27 - 30.

It is clear from these figures that there is a distinct difference in the degree of fluid uptake by the polymer in the duodenum versus uptake of fluid in the ileum. Independent of whether the canine was

Figure 27 : *In-vivo* swelling kinetics of Hydroxypropyl methyl cellulose in the cannulated dog. Degree of Hydration = (gms of fluid sorbed) / (weight of dry polymer). Each point on the graph represents the mean ± SEM of at least six measurements.

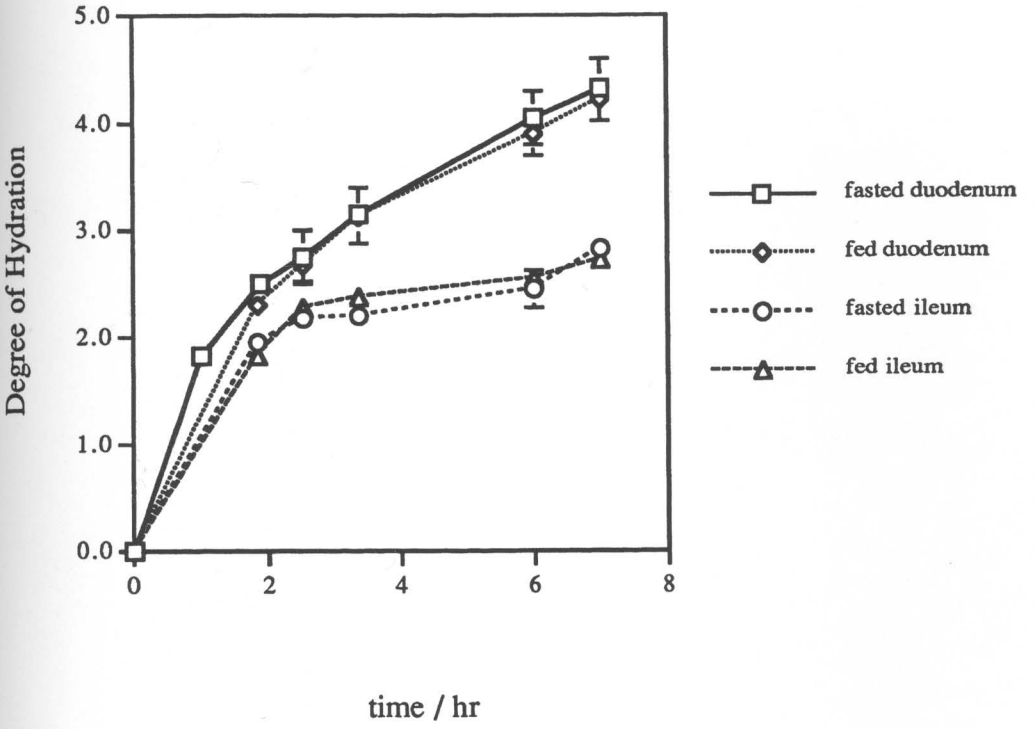
5.0
4.0
3.0
2.0
1.0
0.0
Degree of Hydration
0
2
4
6
8
time / hr
fasted duodenum
fed duodenum
fasted ileum
fed ileum

Figure 28 : *In-vivo* swelling kinetics of Carboxymethyl cellulose sodium salt in the cannulated dog. Degree of Hydration = (gms of fluid sorbed) / (weight of dry polymer). Each point on the graph represents the mean ± SEM of at least six measurements.

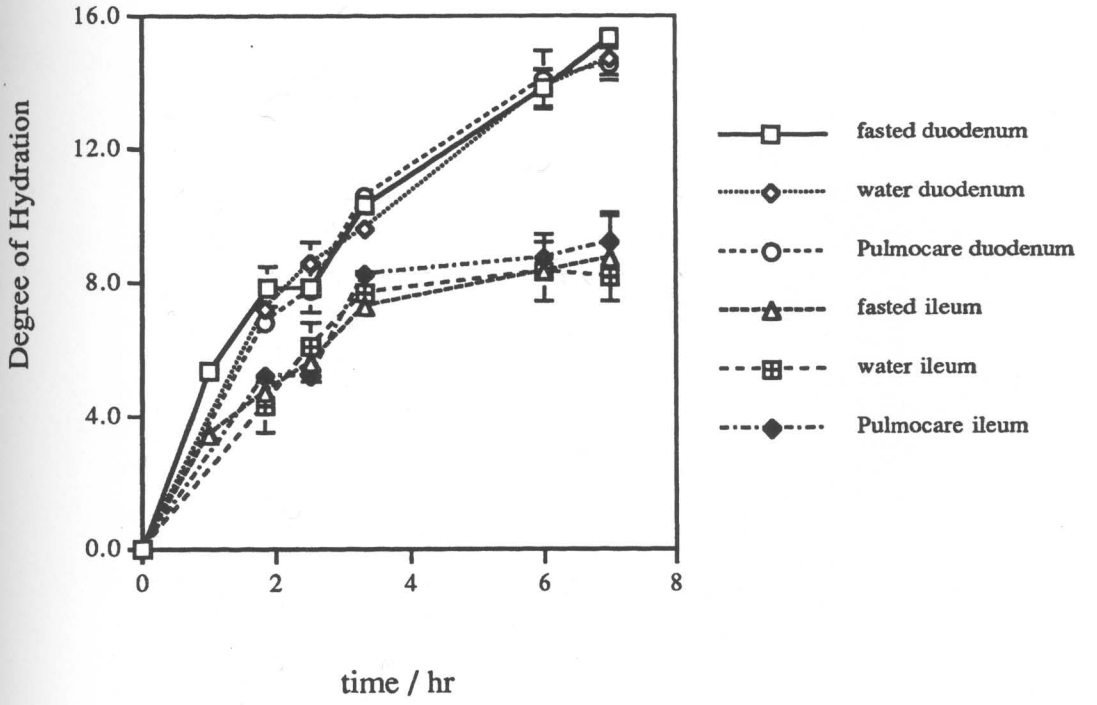
Degree of Hydration
16.0
12.0
8.0
4.0
0.0
0
2
4
6
8
time / hr
fasted duodenum
water duodenum
Pulmocare duodenum
fasted ileum
water ileum
Pulmocare ileum

Figure 29 : *In-vivo* swelling kinetics of Carbopol 974P™ in the cannulated dog. Degree of Hydration = (gms of fluid sorbed) / (weight of dry polymer). Each point on the graph represents the mean ± SEM of at least six measurements.

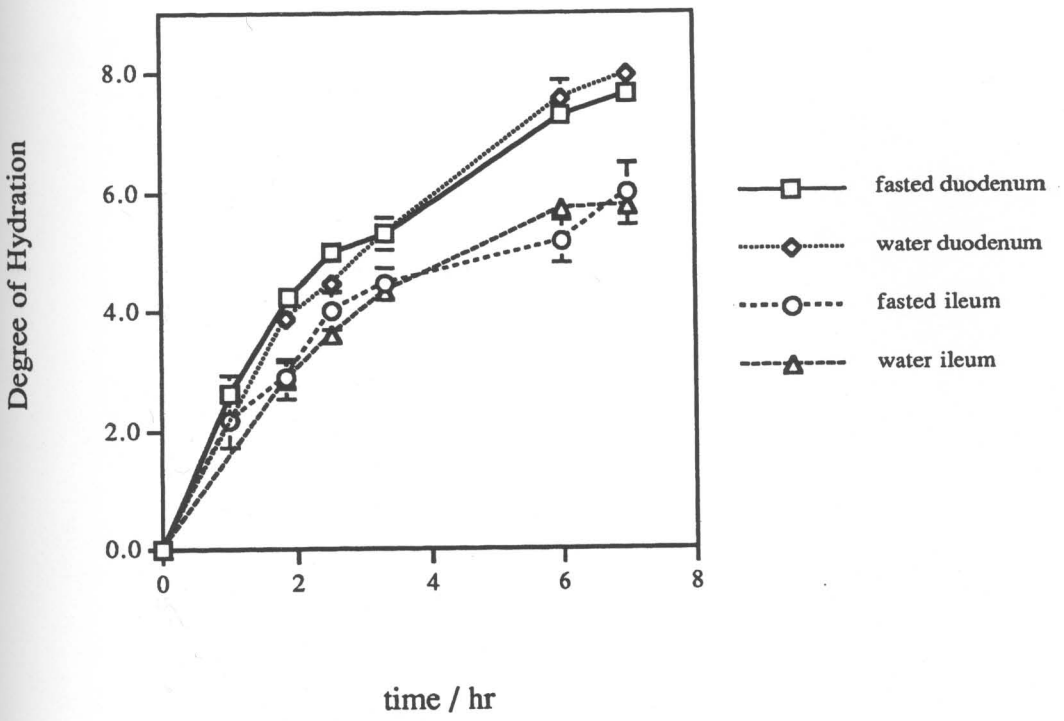
Degree of Hydration
8.0
6.0
4.0
2.0
0.0
0
2
4
6
8
time / hr
fasted duodenum
water duodenum
fasted ileum
water ileum

Figure 30 : *In-vivo* swelling kinetics of Noveon AA1™ (polycarbophil) in the cannulated dog. Degree of Hydration = (gms of fluid sorbed) / (weight of dry polymer). Each point on the graph represents the mean ± SEM of at least six measurements.

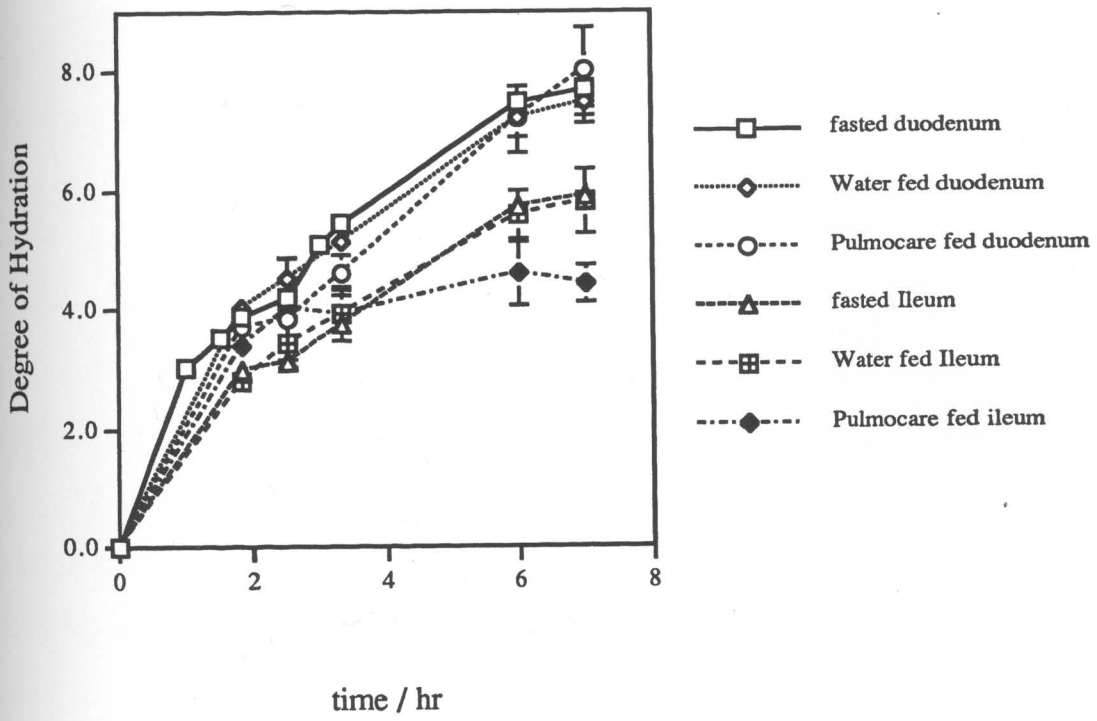
Degree of Hydration
8.0
6.0
4.0
2.0
0.0
0
2
4
6
8
time / hr
fasted duodenum
Water fed duodenum
Pulmocare fed duodenum
fasted Ileum
Water fed Ileum
Pulmocare fed ileum

fed or fasted, each polymer significantly sorbed more water in the duodenum than in the ileum. This is shown in the following table, Table 11, in which the degree of hydration at 7 hours is recorded for each polymer and each study condition.

It appears that the swelling of the polymer is governed much more by its regional position within the intestine than by the fluid it is exposed to. Considering differences in the total amount of fluid, and the time of fluid transit for the three conditions of feeding (fasted, water, and Pulmocare™), this result was surprising.

The following two figures, Figures 31 and 32, are composite graphs of the swelling of the four polymers in the fasted canine. The difference in fluid sorption is evident, with the highest degree of swelling in either the ileum or the duodenum seen for carboxymethyl cellulose sodium salt and the least for hydroxypropyl methyl cellulose. Not surprisingly Carbopol 974P™ and Noveon AA1,™ compounds of similar chemical structure and nature, were statistically identical with respect to the rate and extent of swelling and whose swelling curves were found to lie between those seen for NaCMC and HPMC.

V.4 Phasic Motility Dependence

In order to establish whether the timing of insertion of the polymer with respect to phasic motility might have any effect on the extent or rate of swelling, a study was designed in which the polymer

Table 11 : Comparison of *In-Vivo* Extent of Swelling for each of the polymers after 7 hours in the cannulated canine. Degree of Hydration = (weight of fluid sorbed) / (weight of dry polymer).

	Duodenum			Ileum		
Polymer	Fasted	Water	Pulmocare	Fasted	Water	Pulmocare
HPMC	4.32	4.22	N.A.*	2.82	2.72	N.A.
NaCMC	15.39	14.71	14.57	8.70	8.20	9.18
Carbopol	7.66	7.98	N.A.	5.97	5.75	N.A.
Noveon	7.68	7.46	8.00	5.90	5.82	4.41

* N.A. = not available. Study not performed.

Figure 31 : Comparison of *in-vivo* swelling kinetics of four hydrogel polymers in the duodenum of the cannulated dog. Degree of Hydration = (gms of fluid sorbed) / (weight of dry polymer).

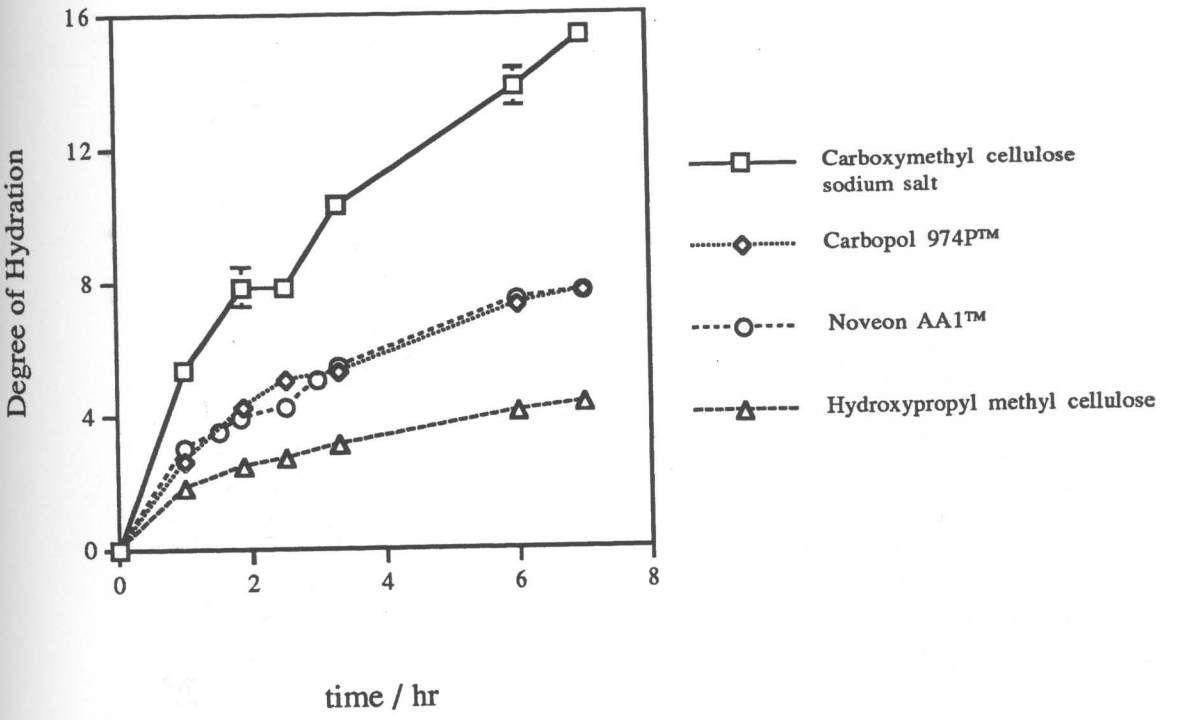
Degree of Hydration
16
12
8
4
0
0
2
4
6
8
time / hr
Carboxymethyl cellulose sodium salt
Carbopol 974P™
Noveon AA1™
Hydroxypropyl methyl cellulose

Figure 32 : Comparison of *in-vivo* swelling kinetics of four hydrogel polymers in the ileum of the cannulated dog. Degree of Hydration = (gms of fluid sorbed) / (weight of dry polymer).

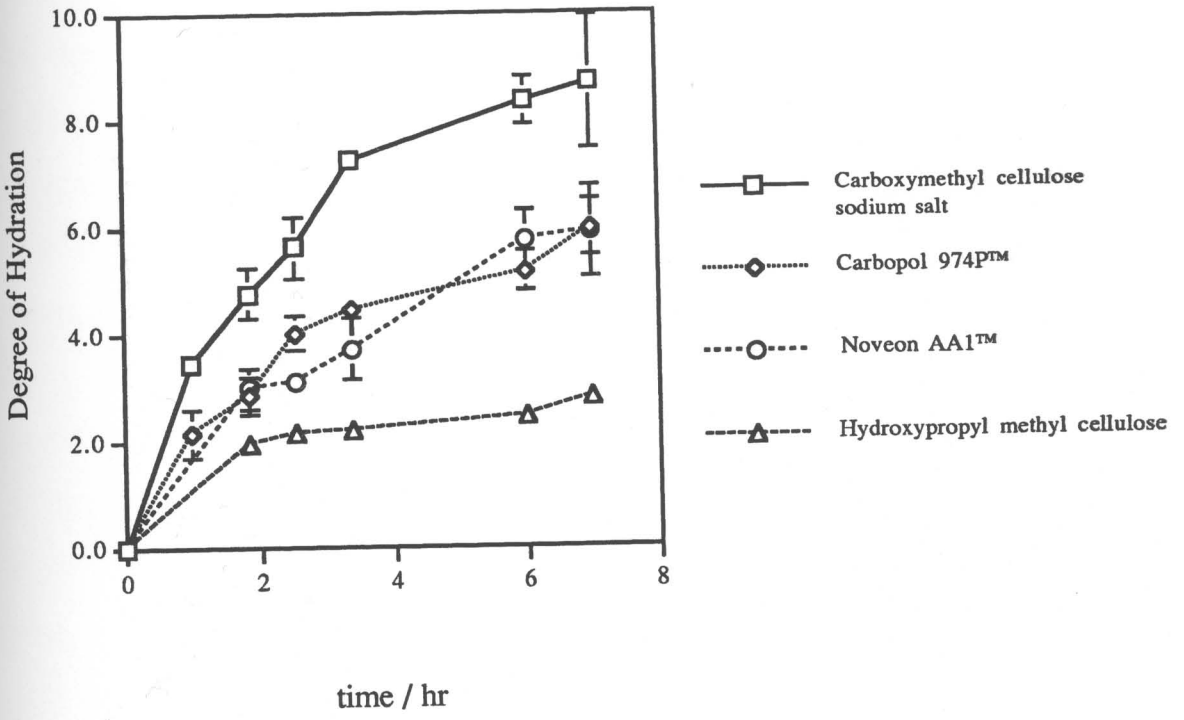
10.0
8.0
6.0
4.0
2.0
0.0
0
2
4
6
8
Degree of Hydration
time / hr
Carboxymethyl cellulose sodium salt
Carbopol 974P™
Noveon AA1™
Hydroxypropyl methyl cellulose

was inserted either approximately ten or sixty minutes prior to the onset of the phase III housekeeper wave.

In preparation for this study, the dogs were fasted for at least 16 hours overnight. In the morning the dogs were placed in the sling harnesses, the duodenal cannulae opened and the effluent observed for evidence of phasic activity. After the passage of two phase III housekeeper waves, to insure true fasted conditions, the dialysis tubing set up with 155 mg of Noveon AA1™ (polycarbophil) was inserted either twenty minutes after the cessation of phase III activity (i.e., during phase I, the quiescent or quiet phase) or eighty minutes after the cessation of the previous phase III, which would correspond to late phase II.

The results of these studies are shown in Figure 33. From this plot it is easily deduced that the swelling observed is independent of the motility pattern of the canine. There was no significant difference seen between phase I and late phase II insertion of the polymer. The timing of the insertion did not affect the amount of fluid sorbed by the polycarbophil filled dialysis tubing.

V.5 Oral Ingestion of Dialysis Tubing

The question of how an orally ingested hydrogel delivery system would behave compared to a device placed directly into the duodenum led us to design the following experiment.

Two canines were fasted overnight for at least 16 hours. In the morning the animals were placed in the Pavlov-type slings, their

Figure 33 : Swelling kinetics dependence on gastric motility. Comparison of Noveon AA1™ (polycarbophil) swelling after insertion of sample during phase I and late phase II of the MMC.

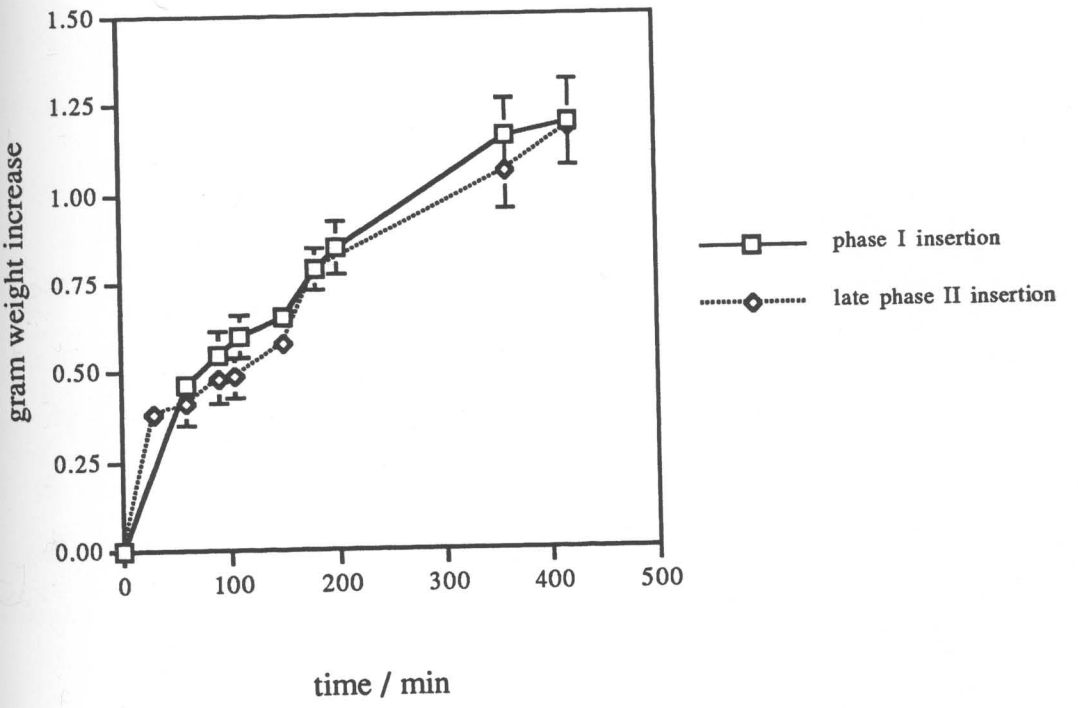
1.50
1.25
1.00
0.75
0.50
0.25
0.00
gram weight increase
0
100
200
300
400
500
time / min
phase I insertion
late phase II insertion

duodenal cannulae opened and the effluent observed to establish that the animals were indeed fasted, verified by two phase III housekeeper waves of the MMC. The study was then begun using the dialysis tubing set up previous described filled with 155 mg of Noveon AA1™ (polycarbophil).

During phase I, i.e., 20 minutes after the cessation of activity of the second phase III, the weighed tubing was swallowed by the canine after being placed in the back of the throat and washed down with 50 ml of water equilibrated to room temperature. The volume of 50 ml was used because it is below the threshold of ≈ 150 ml where a fasted canine is converted to the fed state.[142] The use of only 50 ml of water assures that the canine remains in the fasted state.

The tubing, allowed to freely pass from the stomach into the small intestine, was collected at the opened duodenal cannula. The time the dialysis tubing exited from the cannula was noted and the tubing weighed. The weight increase was normalized to the degree of hydration and plotted as a function of the time the tubing took to pass from the stomach to the duodenal cannula. The resulting graph is depicted in Figure 34. (Note: t=0 corresponds to the time the dialysis tubing was washed into the stomach with the 50 ml of water.)

While an obvious linear relationship exists between weight increase and gastrointestinal residence time of the tubing, there are clear inter-animal differences. The reason for these differences may be due to the age (2.5 years versus 1 year), size (23 kg versus 17 kg) or differences in the time length of the phases of the MMC of each animal especially in phases I and II. (The total MMC cycle of

Figure 34 : *In vivo* swelling study in the canine. Oral ingestion of Noveon AA1™ (polycarbophil) filled dialysis tubing collected at duodenal cannula.

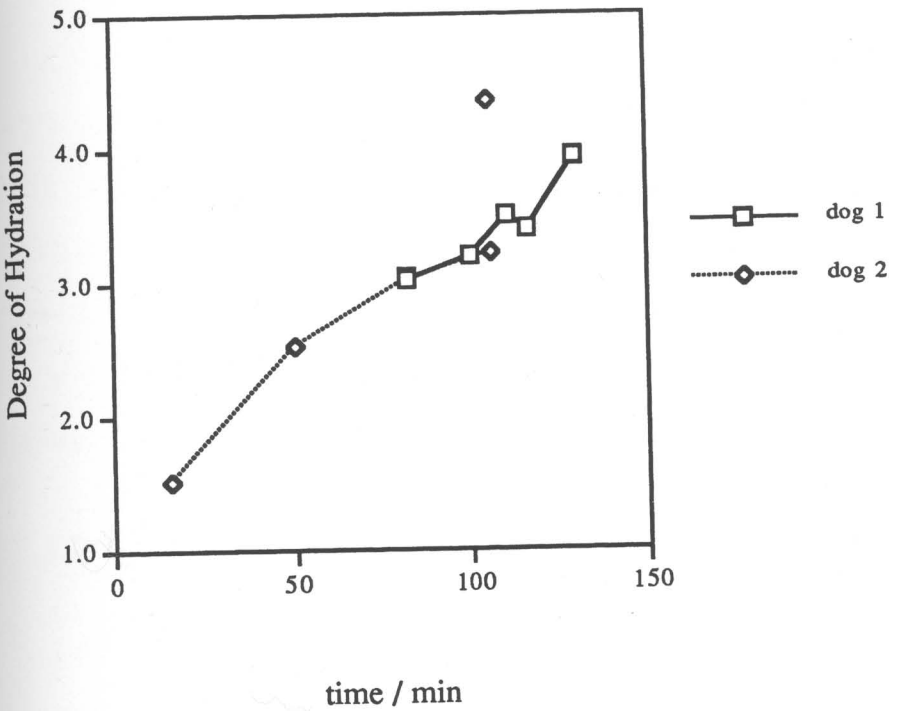
5.0
4.0
3.0
2.0
1.0
Degree of Hydration
0
50
100
150
time / min
dog 1
dog 2

animal has been found to be essentially identical in each canine, ≈ 125 minutes.)

When the results of a swelling study for polycarbophil directly inserted into a duodenal cannula was overlaid onto Figure 34, the orally ingested experiment, no significant difference was seen as shown in Figure 35. From this experiment we conclude that swelling appears to be linearly dependent upon the time the polymer is resident to the gastrointestinal tract, i.e., the in vivo time, and not related to a specific canine.

V.6 Loss on Drying

An attempt to determine the relative amount of fluid in the different intestinal regions led us to examine the loss-on-drying of material collected from the ileal and duodenal cannulas. The canines were studied in both the fasted, i.e., 16+ hours without food, but free access to water, and fed, i.e., free access to food and water, states.

The canines, either fed or fasted, were placed in sling restraints and samples were collected from the intestine through the opened cannulae. Access to the contents of the intestinal lumen was accomplished through the use of a long handled spatula.

The material, on pre-weighed aluminum weighing pans, were placed into an oven at 100° C and heated until constant weight. The results, calculated as the percent of weight lost upon drying, were pooled by region. The mean and standard deviation for each study, as

Figure 35 : *In vivo* swelling study in the canine. Oral ingestion of Noveon AA1™ (polycarbophil) filled dialysis tubing collected at duodenal cannula compared to similarly filled tubing inserted directly into duodenal cannula.

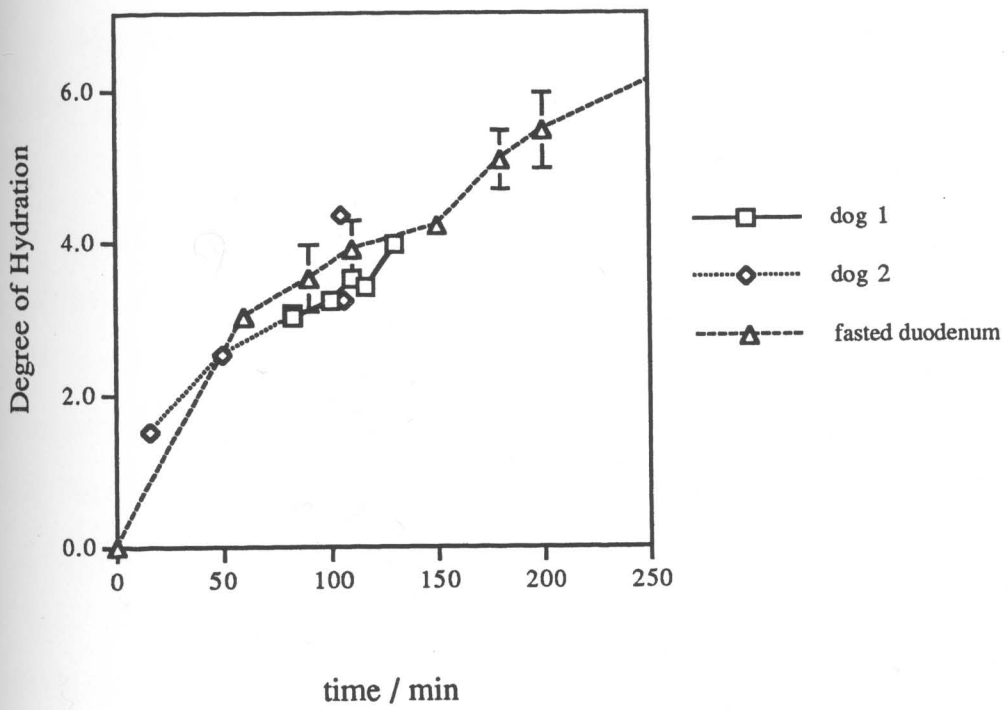
Degree of Hydration
6.0
4.0
2.0
0.0
0
50
100
150
200
250
time / min
dog 1
dog 2
fasted duodenum

well as the results of an unpaired Student's t-test analysis, is shown in Table 12.

For the small sample studied the percent of water lost upon drying was found to be significantly different for the regio-specific sampling for fasted, but not fed animals. In addition, we found that the percent lost upon drying was significantly different for the canines in the fasted state when compared to their fed states. Albeit, it is important to note that, in absolute terms, the differences in the values for the fasted ileum and the fed duodenum and ileum were not very different (89.6% versus 86.8%).

We conclude from this study that while there may be a difference in fluid content in the material isolated from the lumen of the fasted canine, with more fluid found in the duodenum than the ileum, the difference in absolute terms does not seem to be very large. It is difficult to imagine that this is the primary source of the rate and extent of swelling differences described in earlier studies. The consistent differences seen in the regio-specific swelling (duodenum > ileum) are not fully explained by the very small differences in lumenal fluid content. These differences must be the result of a more defining property of the gastrointestinal tract.

V.7 Swelling Study with Atropine Sulfate

Atropine sulfate is an antimuscarinic agent that competitively inhibits the actions of acetylcholine at muscarinic receptors of the autonomic effector sites as well as inhibiting the action of

Table 12 : Loss on Drying.

	Region	n	weight loss	Standard Deviation	Statistical Significance
Fasted	duodenum	8	96.8%	1.17	yes; $p < 0.001$
	ileum	7	89.6%	1.34	
Fed	duodenum	12	86.8%	2.73	no
	ileum	4	86.8%	1.07	

acetylcholine on smooth muscle lacking cholinergic innervation.[172] These actions include vasodilation, drying of the mouth, increase in heart rate, inhibition of contraction of the gastrointestinal tract, ureter and bladder, and the reduction of, and often temporarily abolish the salivary, bronchial, gastric, intestinal, nasal and sweat gland secretions.[172-180] In larger doses atropine sulfate causes dilatation of the pupils and paralysis of accommodation.[180]

These properties allowed us to design our next experiment. We wanted to observe the swelling kinetics of a polymer inserted into the duodenal and ileal regions without the influences of gastric or intestinal secretions and gastrointestinal motility. Atropine sulfate (50μg/kg) was administered to the fasted canine as an intravenous bolus thirty minutes prior to insertion of the dialysis tubing. Subsequently, bolus booster injections of 30 μg/kg were given at intervals of thirty minutes for two hours. The study was then continued for four hours, i.e., six hours total, without any additional atropine. The total atropine sulfate injected into each animal per study was 200 μg/kg. A wash out period of at least 72 hours was permitted between studies.

In addition, a series of studies was performed in which the initial bolus dose was 100μg/kg followed by the booster injections at 30 minutes intervals for a total of 250 μg/kg. However, this was seen to be toxic to two of the three canines demonstrated by their restlessness and excitement as well as CNS depression. In deference to the well being of the canines, the initial bolus injection was lowered to 50 μg/kg, a dose still higher than the literature value for

the minimum required to shut down the secretory and motility patterns.[172-179]

Carboxymethyl cellulose sodium salt was the polymer chosen for this study. Since we wanted to be able to measure the effect of reduced fluid secretion on swelling, we chose the polymer that had previously shown the greatest sorption capacity under normal conditions. The hydration curves generated in the atropinized animals were compared to curves similarly generated in fasted, non-atropinized animals. The result of these studies is shown in Figure 36 and Table 13. Each time point on the curves corresponds to the mean ± standard error of a pool of at least three studies per canine, i.e., a minimum of nine data points.

The curves are essentially superimposable. The only significant difference seen was for the ileum at t = 6 hours at which time, the swelling curve for the non-atropinized canines is seen to deviate from linearity as opposed to swelling curves for the atropinized animals which did not. This deviation was observed under both fed and fasted conditions.

In this experiment we have demonstrated that the intestinal secretions are not a major source of fluid for polymer swelling. Combining this with the observation that lumenal contents were also not a major contributor of fluid for swelling, led us to search for what could be the major source of the swelling inducing fluid.

It appears that the mucous lining coating the epithelial cells of the gastrointestinal tract is most likely the source for swelling fluid. Mucous is by nature 95% water and is kept fully hydrated

Figure 36 : *In-vivo* swelling kinetics of carboxymethyl cellulose sodium salt in the atropine sulfate dosed canine . Degree of Hydration = (gms of fluid sorbed) / (weight of dry polymer).

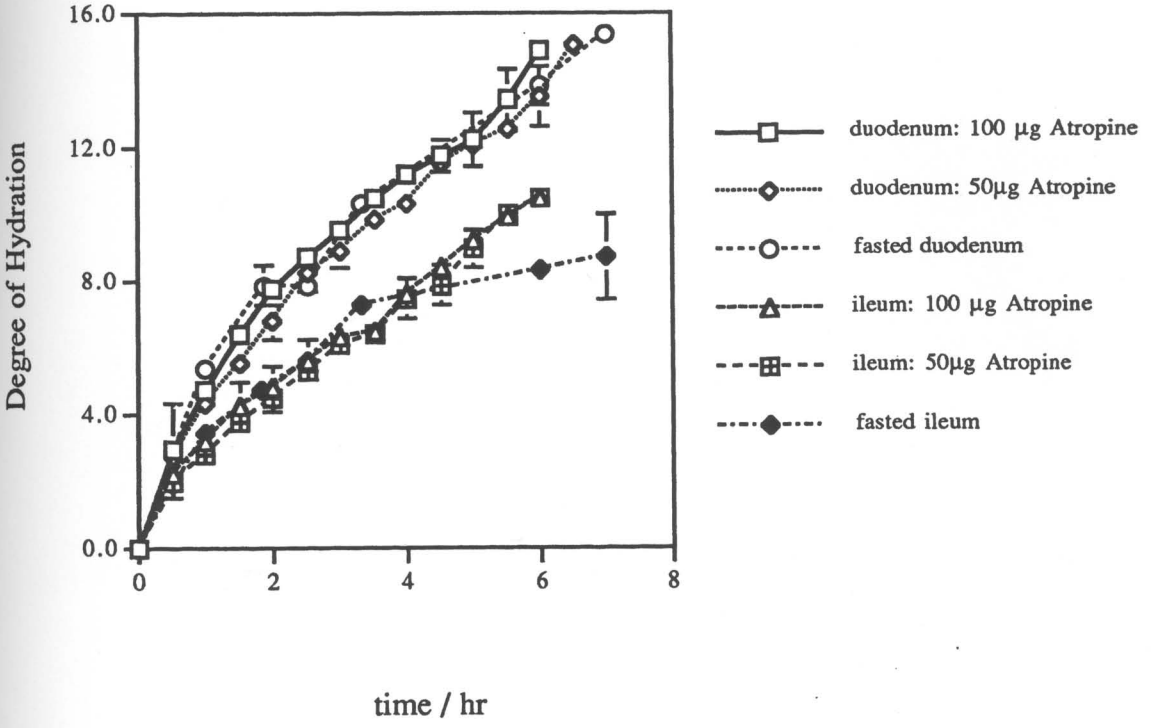
16.0
12.0
8.0
4.0
0.0
0
2
4
6
8
Degree of Hydration
time / hr
duodenum: 100 µg Atropine
duodenum: 50µg Atropine
fasted duodenum
ileum: 100 µg Atropine
ileum: 50µg Atropine
fasted ileum

Table 13 : Comparison of the extent of swelling under fasted, fed and atropinized conditions after six hours in the cannulated canine. Degree of Hydration = (weight of fluid sorbed) / (weight of dry polymer).

	Duodenum				Ileum			
Polymer	Fasted	Water	Pulmocare	Atropine	Fasted	Water	Pulmocare	Atropine
HPMC	4.06	3.90	N.A.*	N.A.	2.45	2.54	N.A.	N.A.
CMC	13.82	13.83	14.09	13.55	8.34	8.30	8.76	10.50
Carbopol	7.27	7.58	N.A.	N.A.	5.17	5.70	N.A.	N.A.
Noveon	7.47	7.22	7.19	N.A.	5.73	5.58	4.58	N.A.

* N.A. = not available. Study not performed.

through a dynamic equilibrium with water being supplied from the epithelial cells, the vascular bed and the lymphatic system.[181-184] It is not difficult to envision that an orally administered polymeric delivery system, residing within a collapsed intestine, would be in continuous, intimate contact with the mucous layer lining the epithelial cells. It would therefore be very reasonable to assume that this intimate contact would result in the transfer of the fluid required for polymer hydration. This assumption, that the mucous layer is the major source of swelling fluid, might also explain the difference in the rate and extent of swelling seen between the duodenal and ileal studies.

Studies on the intestinal tract of the rat[185-188] have determined the thickness of the mucous gel layers in various regions of the intestinal tract. The mucous gel was found to be thickest in the duodenum decreasing gradually from the upper duodenum to the terminal ileum.[187,188] In addition, it has been observed that the mucous secretion rate was significantly higher in the upper regions of the small intestine.[186]

Taken together, this evidence implies that a polymeric delivery system would be in contact with a greater amount of mucous in the duodenum than an identical delivery system situated in the ileum More mucous implies more water available for hydration. Therefore, the result expected is exactly what has been observed. The rate and extent of swelling of identical polymers would be greater in the duodenal region of the small intestine than in the ileum.

V.8 *In vivo* pH Study

As we were interested in what effect is exerted *in vitro* by the diffusing buffer solutions on the polymer, similarly we were interested in the effect exerted *in vivo*. This led us to try to measure changes in the microclimate pH caused by diffusion of intestinal fluid in the non-anesthetized canine. To accomplish this we used a previously calibrated flexible pH microelectrode inserted into the center of the dry polymer contained in a 11.5 mm diameter dialysis tubing set up secured at each end with 3-0 silk threads. The dialysis membrane was trimmed so that a constant surface area of 7.23 cm^2 was used throughout the study.

The rear leg of each fasted canine was shaven and a skin reference electrode (3M Medical Red Dot Monitoring Electrodes, 3M Medical-Surgical Division, St. Paul, MN) was applied. The entire study was performed with the animals restrained in sling harnesses.

The dialysis tubing set up was inserted into the duodenal cannula twenty minutes after cessation of a second phase III housekeeper wave, i.e., during phase I of the MMC. The pH was monitored as a function of time. The result of these studies is shown in Figures 37 through 40. Each curve on the graph represents a separate study.

In these figures we observe patterns in the polymer microclimate similar to what was observed in the *in vitro* studies, albeit with very large inter- and intra-animal variability. This variability may be due to (1) slight variations in insertion during

Figure 37 : *In vivo* pH study of Hydroxypropyl methyl cellulose in the unaesthetized canine. Each curve represents a separate study.

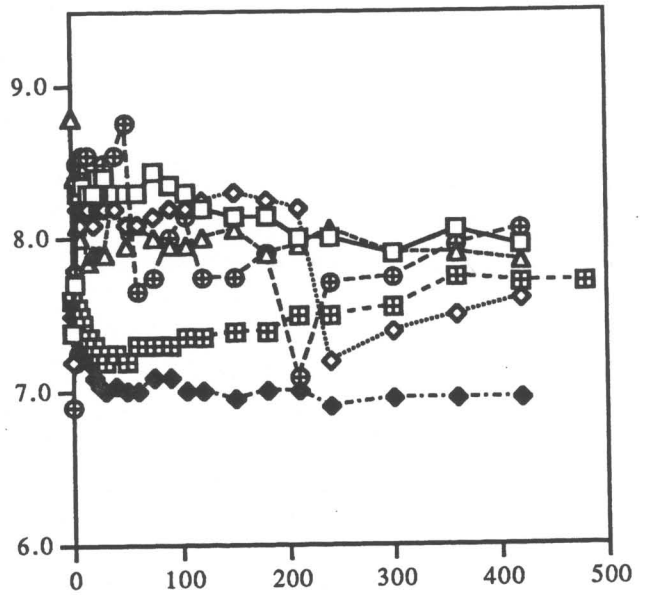
9.0
8.0
7.0
6.0
pH
0
100
200
300
400
500
time / min

Figure 38 : *In vivo* pH study of Carboxymethyl cellulose sodium salt in the unaesthetized canine. Each curve represents a separate study.

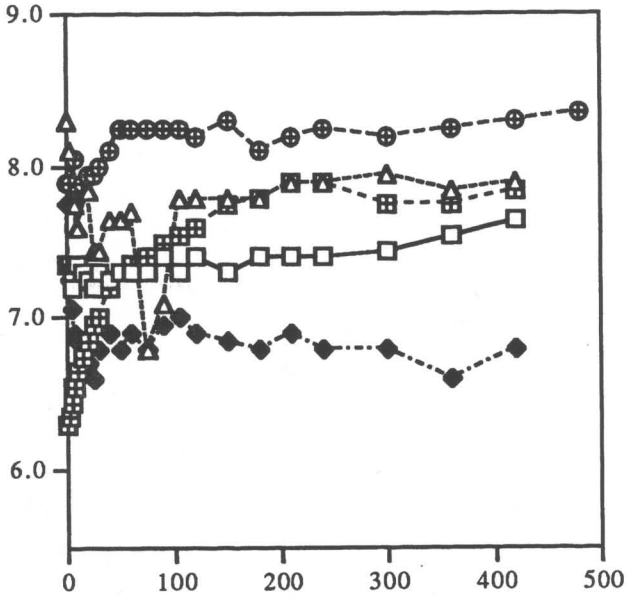
9.0
8.0
7.0
6.0
pH
0
100
200
300
400
500
time / min

Figure 39 : *In vivo* pH study of Carbopol 974P™ in the unaesthetized canine. Each curve represents a separate study.

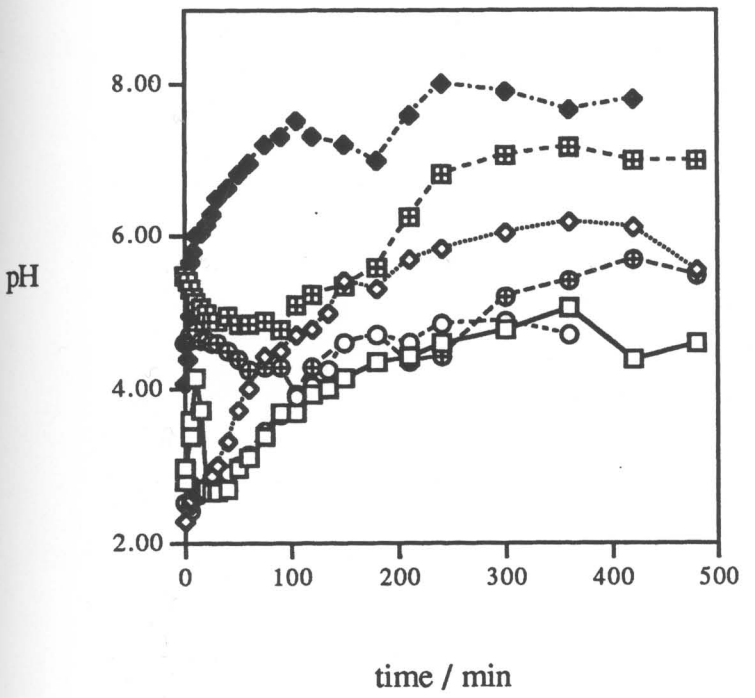
8.00
6.00
4.00
2.00
pH
0
100
200
300
400
500
time / min

Figure 40 : *In vivo* pH study of Noveon AA1™ (polycarbophil) in the unaesthetized canine. Each curve represents a separate study.

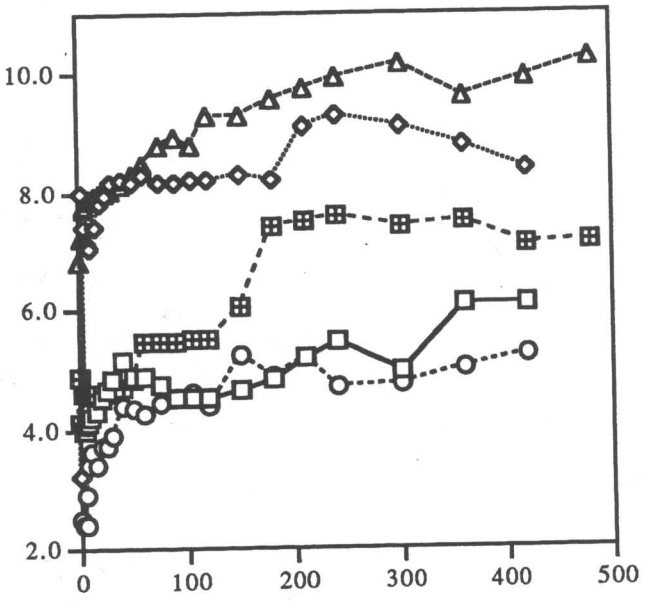
10.0
8.0
6.0
4.0
2.0
pH
0
100
200
300
400
500
time / min

phase I. Therefore, the phase III housekeeper wave arriving at different times could affect the study by polymer encountering gastric secretions at variable times; (2) contractions due to MMC may have massaged the microelectrode from the center of the polymer mass resulting in measuring not the pH of the polymer mass, but something more influenced by the lumenal contents; or most likely (3) the canines were almost always in an agitated emotional state during these studies. Evidence has shown that the emotional state of the subject may often affect the status of the gastrointestinal tract.[121,189-191] Therefore, it is probable that either the wire electrode hanging from the cannula or the reference electrode attached to canines' hind leg disturbed their normally quiet character. This altered emotional state may have caused the inconsistent results.

VI. COMPUTER MODEL

Numerical simulation can be used to predict and understand diverse phenomena. Simulation software allows the user to describe a complex system in bits and pieces, to draw a block diagram of the system, to enter mathematical descriptions of each block, and to observe how variables of the model change over time. Simulation software is used to study a system or process by allowing the user to observe the effect of parameter changes on different variables.[192] In our studies, we have used STELLA,™ a simulation software package, to describe the temporal and spatial movement of fluid in the human gastrointestinal tract and to imitate the swelling history of an orally ingested delivery system composed of the hydrogel polymers studied previously.

STELLA™ is designed for the construction of any process where a "component" is transferred from one compartment to another requiring a knowledge of the factors controlling the rate of transfer.[193] It is an icon-based simulator designed for the Apple™ Macintosh™ computer. These icons are shown in Figure 41. Through the use of these icons, one constructs a diagram of the process or system that is to be modeled. Each icon represents a tool that, once being put into the model, may be programmed as a numerical constant, a linear or non-linear relationship between two parameters or as a logic statement.[193]

The tools operate as the basic elements or building blocks of the model. Stocks are the containers or reservoirs which represent

Figure 41 : The STELLA™ toolbox. Symbols used by STELLA™ for each element of a model. From top to bottom they are stocks, flow control/flow path, input links, and converters.

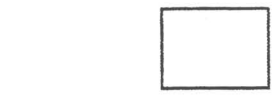

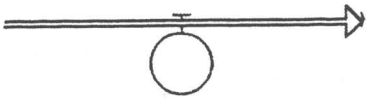

the time varying quantities, e.g., the accumulation of material over time. The Flow icon joins two stocks and represents the flux or physical movement of material into or out of the stock per unit time and are pictorially represented as pipes containing a source, a valve and a direction. Occasionally one end of the flow icon does not coincide with a stock and, as shown in Figure 42, the arrow will begin or end with a cloud. This cloud represents an infinite source or sink respectively. Flows have units of mass or concentration transferred per unit of time.[193-195]

Converters, represented by open circles, contain either constants or equations that convert input to results. The Converter modifies flow regulators or other converters. It allows the calculation of parameters using the values entered into the Stocks. Input links are used to connect the various elements of the model and direct the action between Stocks, Flows, and Converters. Without this connection, one element of the model cannot use the value of another element.[193,195]

The models set up using STELLA II™ software (High Performance Systems, Lyme, NH) were initially run on a Macintosh IIcx and later updated to a Macintosh Performa 636CD. The parameters and constants used in these models either originated from previously published reports[38,40,42-44,129,132,134-136,167,196-214] or were generated from the *in vivo* canine experiments discussed earlier in this thesis.

Figure 42 : The Flow icon represents the conversion or flow of material from one stock to another. Occasionally one end of the flow does not coincide with a stock and the arrow will begin or end with a cloud representing an infinite source or a sink, respectively.

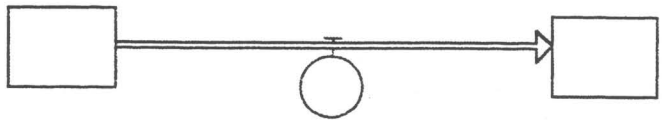

Stock Linked to another Stock

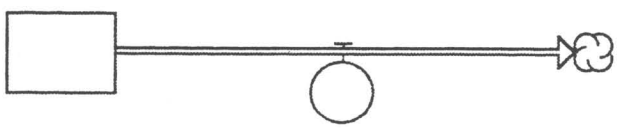

Stock Linked to a Cloud

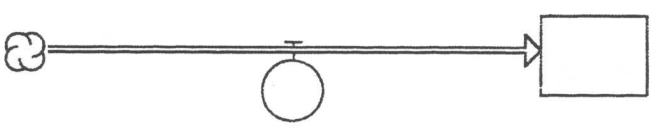

Cloud Linked to a Stock

VI.1 The Fasted Subject

The first model constructed described movement of fluid through the gastrointestinal tract of a fasted subject. The scheme of this model is presented in Figure 43. The model accounts for the gradual accumulation of gastric, pancreatic, and bile secretions before being released, as boluses, into the lumen of the small intestine at appropriate times in the fasted MMC. The model demonstrates the flow and reabsorption of material through the system from the stomach through the ileum.

The schematic was converted into the working STELLA™ computer model by the addition of Converters and Input Links as shown in Figure 44. In this model each rate constant was programmed as a Converter and all transfers were programmed as Flows. The equations and constants used in all of the computer model schemes are found in the Appendix. All constants used in this scheme were obtained from previously published studies.

The result of this model is depicted in Figure 45. As mentioned previously, the model was designed so that there is a gradual accumulation and storage of the gastric, pancreatic and bile juices which are released as boluses in a manner similar to their observed behavior under normal physiological conditions in human and canine subjects.[60,61,200]

The patterns of three MMC cycles are shown in Figure 45. Examination of the graphs indicates that the pattern produced by each of the three cycles is identical. The fluid secreted during a cycle is

Figure 43 : Full schematic representation of the model of fluid movement through the gastrointestinal tract of the fasted human.

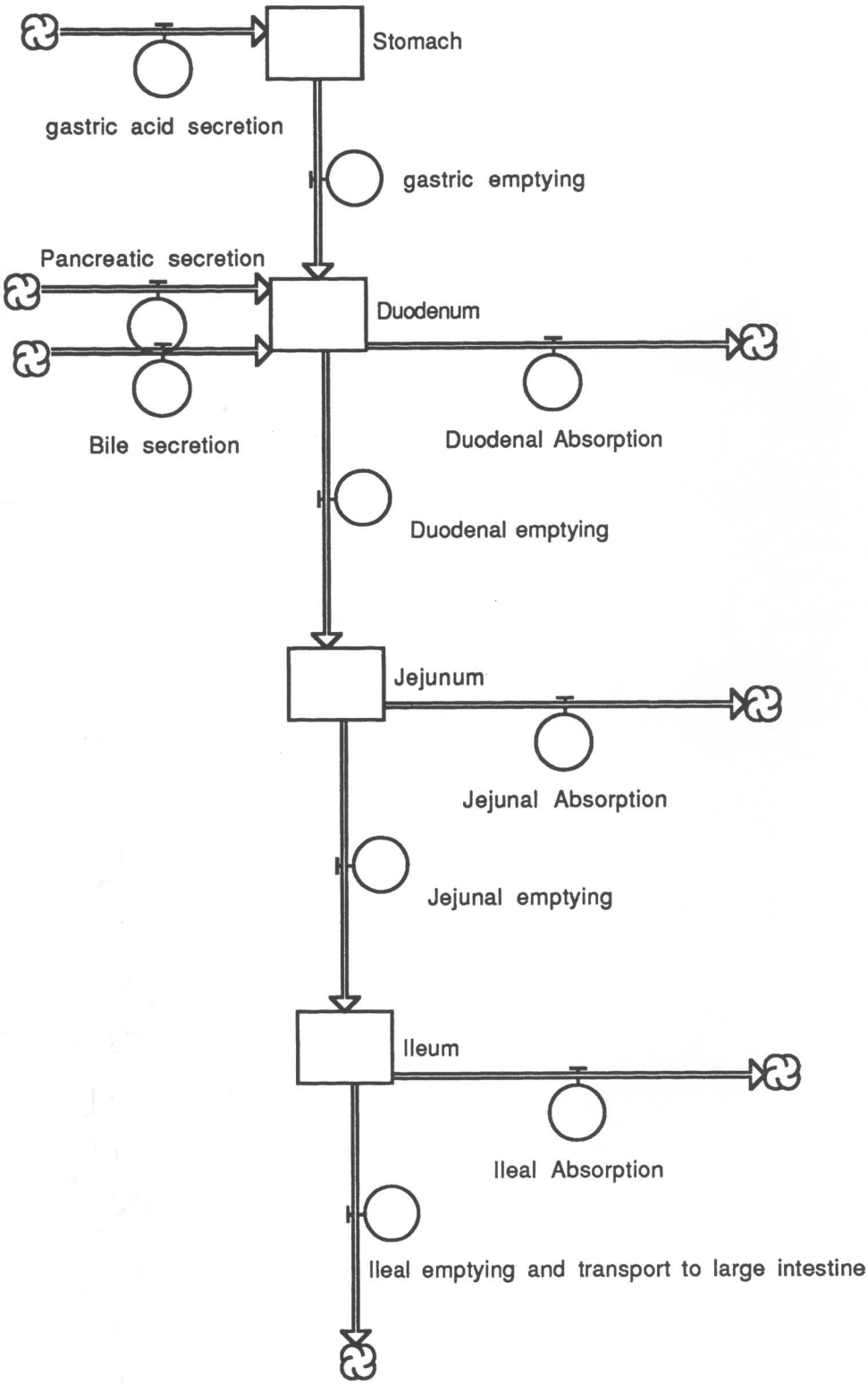
Stomach
gastric acid secretion
gastric emptying
Pancreatic secretion
Duodenum
Bile secretion
Duodenal Absorption
Duodenal emptying
Jejunum
Jejunal Absorption
Jejunal emptying
Ileum
Ileal Absorption
Ileal emptying and transport to large intestine

Figure 44 : Full schematic representation including converters and input links of the model of fluid movement through the gastrointestinal tract of the fasted human

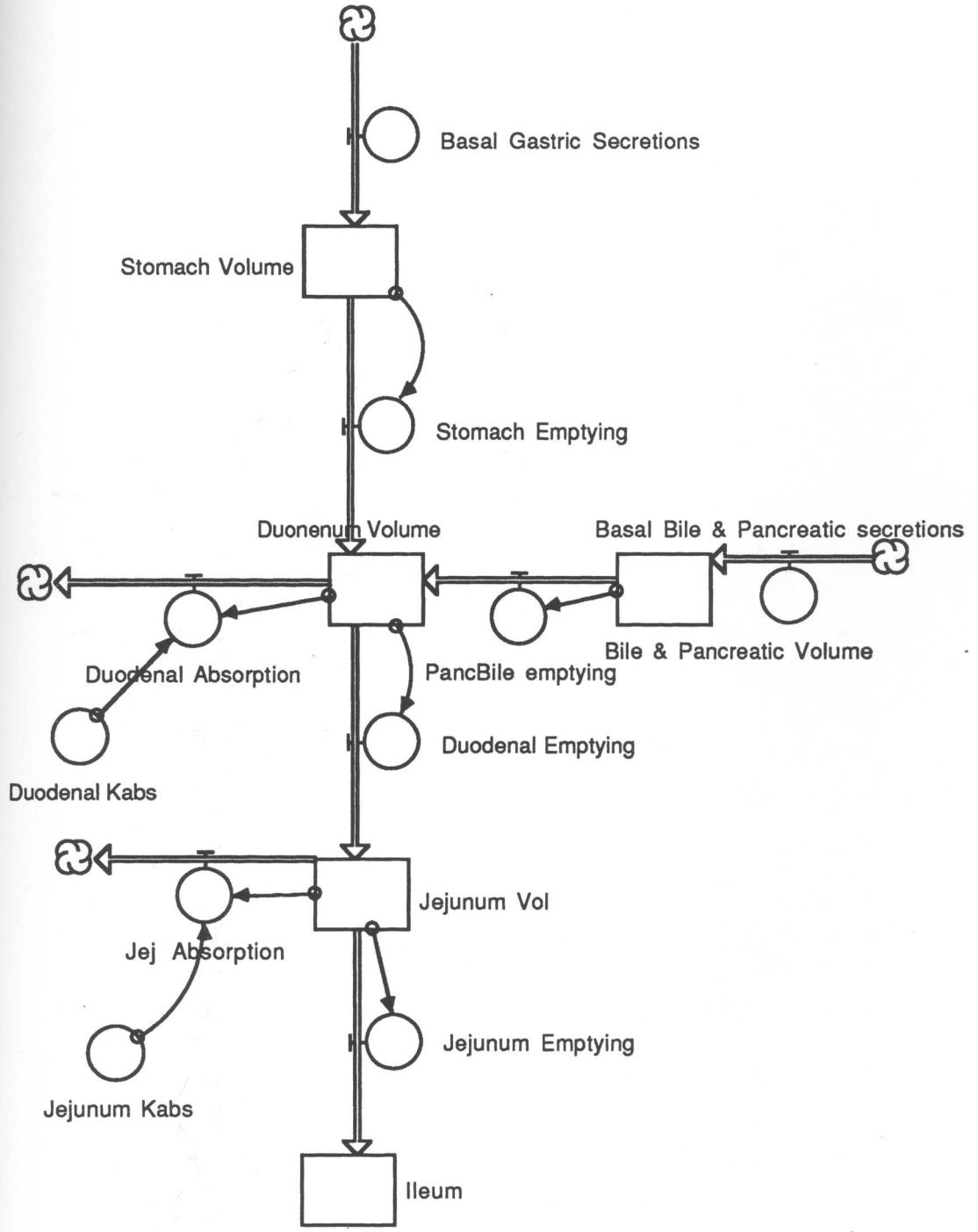
Basal Gastric Secretions
Stomach Volume
Stomach Emptying
Duonenum Volume
Basal Bile & Pancreatic secretions
Bile & Pancreatic Volume
Duodenal Absorption
PancBile emptying
Duodenal Emptying
Duodenal Kabs
Jejunum Vol
Jej Absorption
Jejunum Emptying
Jejunum Kabs
Ileum

Figure 45 : Simulation of fluid movement as it moves through the stomach, duodenum, jejunum and ileum in the fasted human. Curves represent the volume accumulation in each region of the gastrointestinal tract. 1-stomach, 3-duodenum, 4-jejunum, and 5-ileum. Curve #2 represents the secretion contribution of the bile and pancreas.

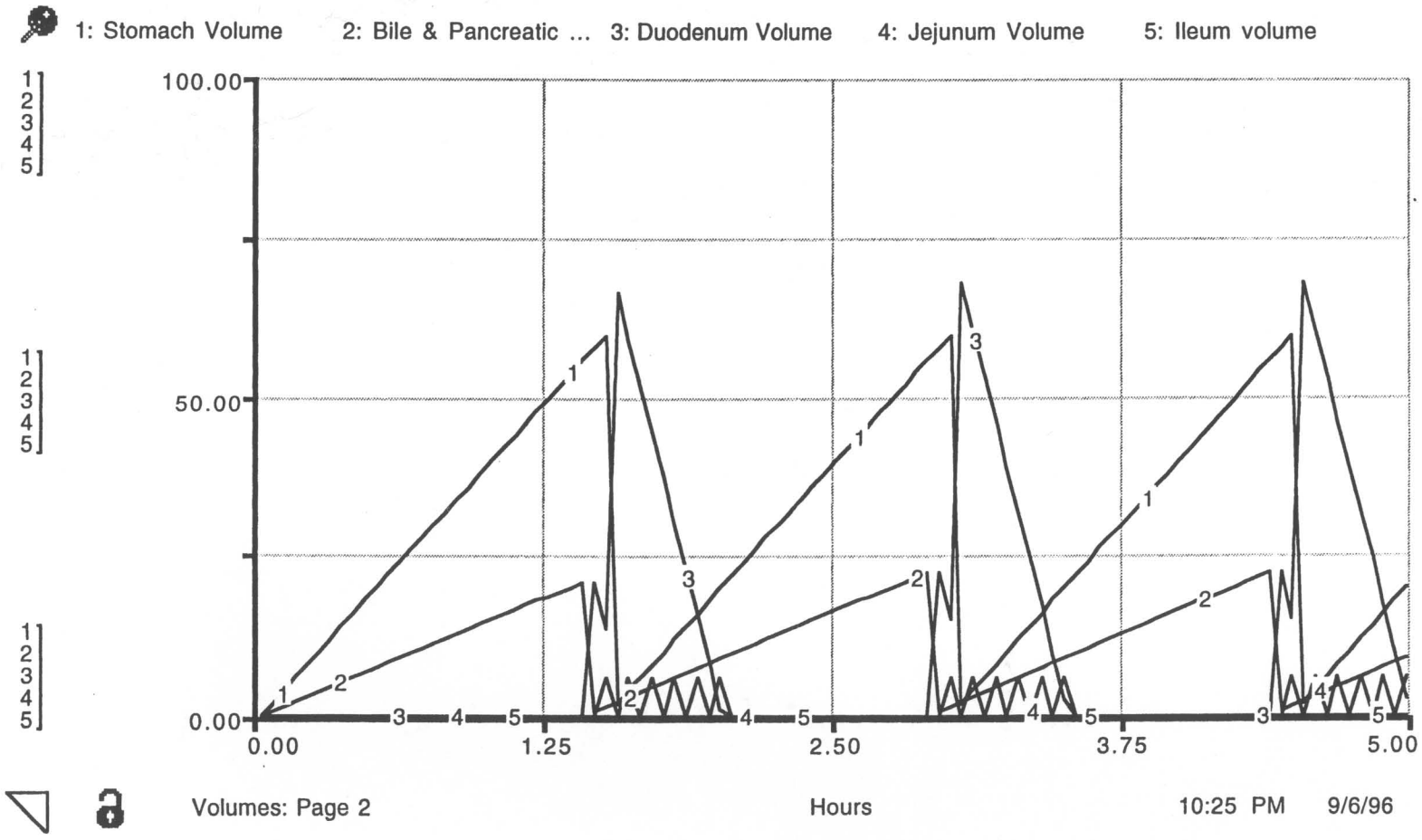
1: Stomach Volume
2: Bile & Pancreatic ...
3: Duodenum Volume
4: Jejunum Volume
5: Ileum volume
100.00
50.00
0.00
0.00
1.25
2.50
3.75
5.00
Volumes: Page 2
Hours
10:25 PM
9/6/96

reabsorbed before the onset of the next. Therefore, no residual fluid is seen to remain in the small intestine from the previous cycle.

In a closer examination of the model we see that all of the fluid that enters the small intestine is quickly reabsorbed. In fact, according to our model, all of the fluid is reabsorbed within approximately twenty minutes. Approximately 80% of the fluid presented is reabsorbed in the duodenum with the remaining 20% reabsorbed in the jejunum.

It is interesting to note that according to our model, none of the fluid secreted into the small intestine even came close to making it all the way through the small intestine into the ileum. All of the fluid was reabsorbed before the fluid passed the proximal jejunum.. This supports our observations in which fluid was never isolated from an opened ileal cannula of a fasted canine.

VI.2 The Water Fed Subject

The second computer model designed describes the movement of orally ingested 300 milliliters of water through the gastrointestinal tract of a fasted subject. The schematic of this study is shown in Figure 46. Essentially this scheme is the same as Figure 43 for the completely fasted subject with the exception of the addition of the Flow icon describing the oral ingestion of the water. As in the previous model, the schematic was transposed into the working STELLA™ model by addition of converters and Input links. The resulting scheme is shown in Figure 47. Many of the parameters and

Figure 46 : Full schematic representation of the model of fluid movement of an orally administered 300 ml water bolus through the gastrointestinal tract of the fasted human.

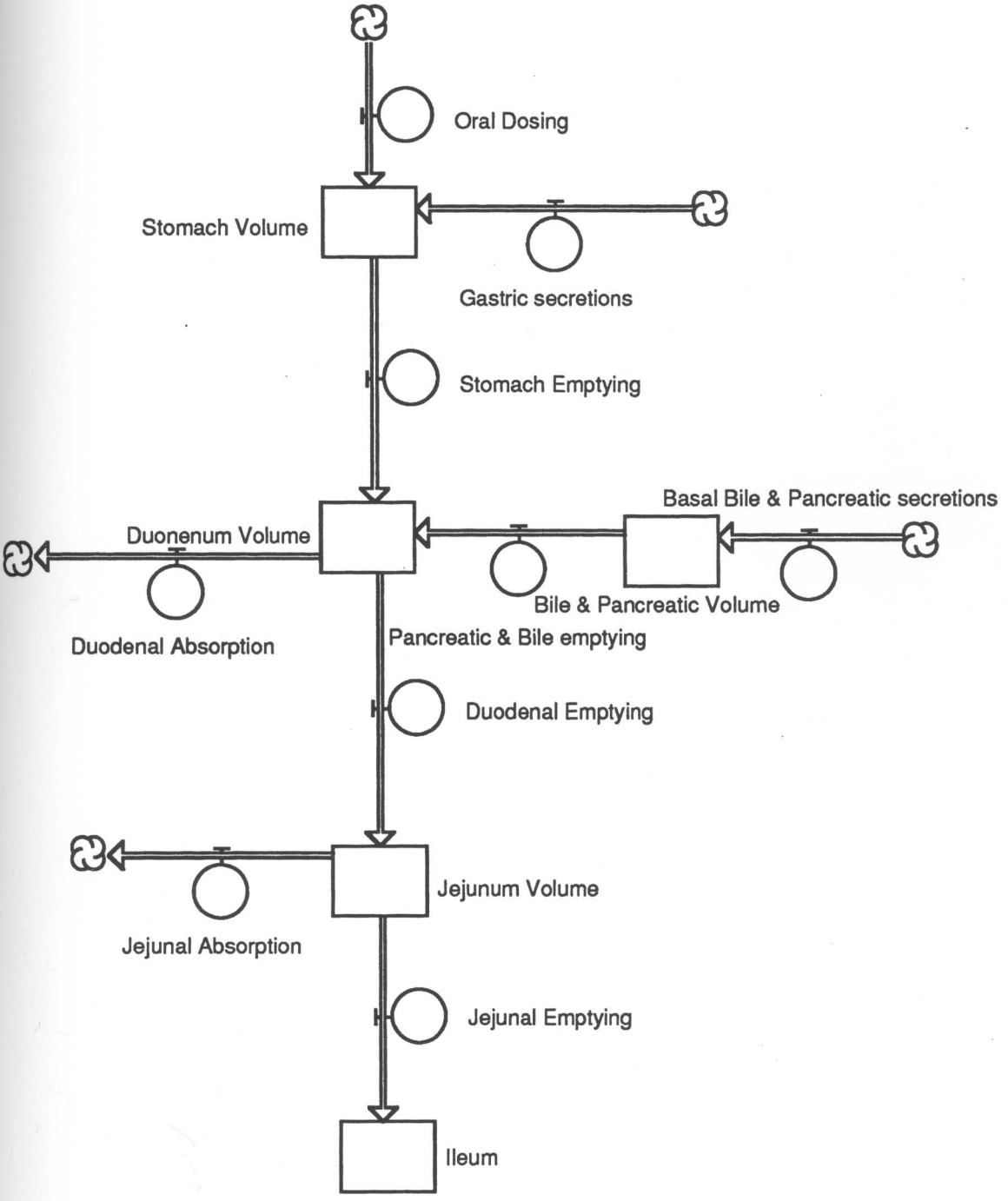
Oral Dosing
Stomach Volume
Gastric secretions
Stomach Emptying
Basal Bile & Pancreatic secretions
Duonenum Volume
Bile & Pancreatic Volume
Duodenal Absorption
Pancreatic & Bile emptying
Duodenal Emptying
Jejunum Volume
Jejunal Absorption
Jejunal Emptying
Ileum

Figure 47 : Full schematic representation including converters and input links of the model of fluid movement of an orally administered 300 ml water bolus through the gastrointestinal tract of the fasted human

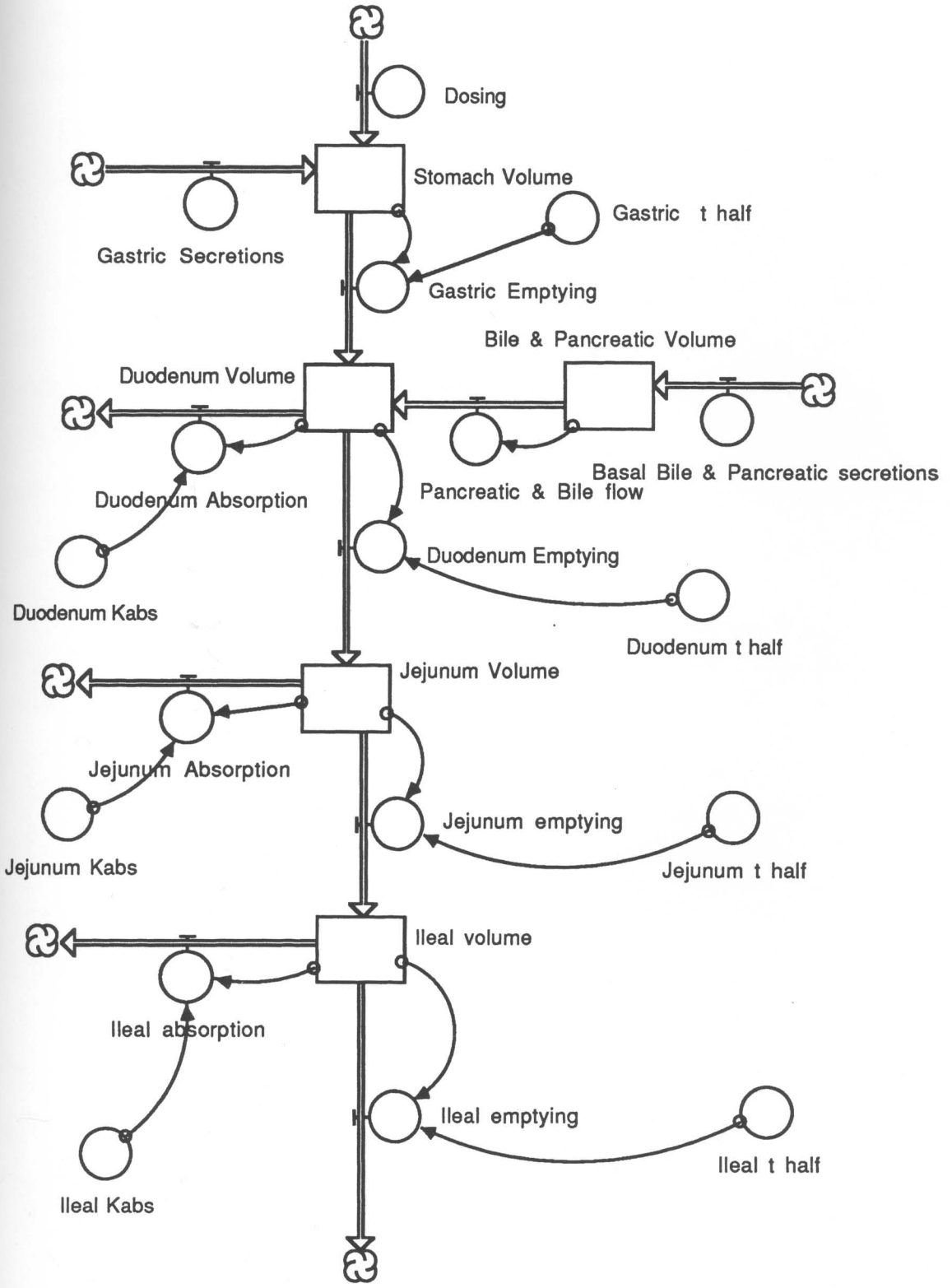
Dosing
Stomach Volume
Gastric Secretions
Gastric t half
Gastric Emptying
Bile & Pancreatic Volume
Duodenum Volume
Basal Bile & Pancreatic secretions
Duodenum Absorption
Pancreatic & Bile flow
Duodenum Emptying
Duodenum Kabs
Duodenum t half
Jejunum Volume
Jejunum Absorption
Jejunum emptying
Jejunum Kabs
Jejunum t half
Ileal volume
Ileal absorption
Ileal emptying
Ileal t half
Ileal Kabs

constants needed to be changed from the previous model to reflect conversion of the subject from fasted to fed conditions. These changes are shown in the equations for this model listed in the appendix.

In brief, the scheme accounts for the dosing of 300 milliliters of water directly into the stomach while the subject is in phase I of a fasting MMC. Water is seen to empty from the stomach into the duodenum, where it mixes with fluid from the pancreas and bile that have already been secreted. Some water is absorbed by the duodenum, however, a larger percentage of the dose passes through to the jejunum, where it is completely absorbed. Graphically this is shown in Figure 48, the plot generated by a running model. Again, as was observed in our *in vivo* canine studies, all fluid is absorbed in the duodenum and the jejunum. None appears to survive the length of the entire small intestine.

Reflecting what we saw *in vivo*, the model demonstrates that within approximately forty-five minutes most of the water is cleared from the stomach. In addition, the amount eluted corresponds closely to the volume administered, that is, duodenal secretions were seen to add very little extra volume. Our *in vivo* water fed studies showed that phasic activity returned approximately ninety minutes after a 300 milliliter gavage of water to the canines. Our model was designed to include all of these observations.

Since none of the 300 milliliters of water makes it through the entire small intestine and gets to the ileum, a question arose as to what volume of water would need to be ingested for some to appear in

Figure 48 : Simulation of fluid movement of an orally administered 300 ml water bolus as it moves through the stomach, duodenum, jejunum and ileum in the originally fasted human. Curves represent the volume accumulation in each region of the gastrointestinal tract. 1-stomach, 3-duodenum, 4-jejunum, and 5-ileum. Curve #2 represents the secretion contribution of the bile and pancreas.

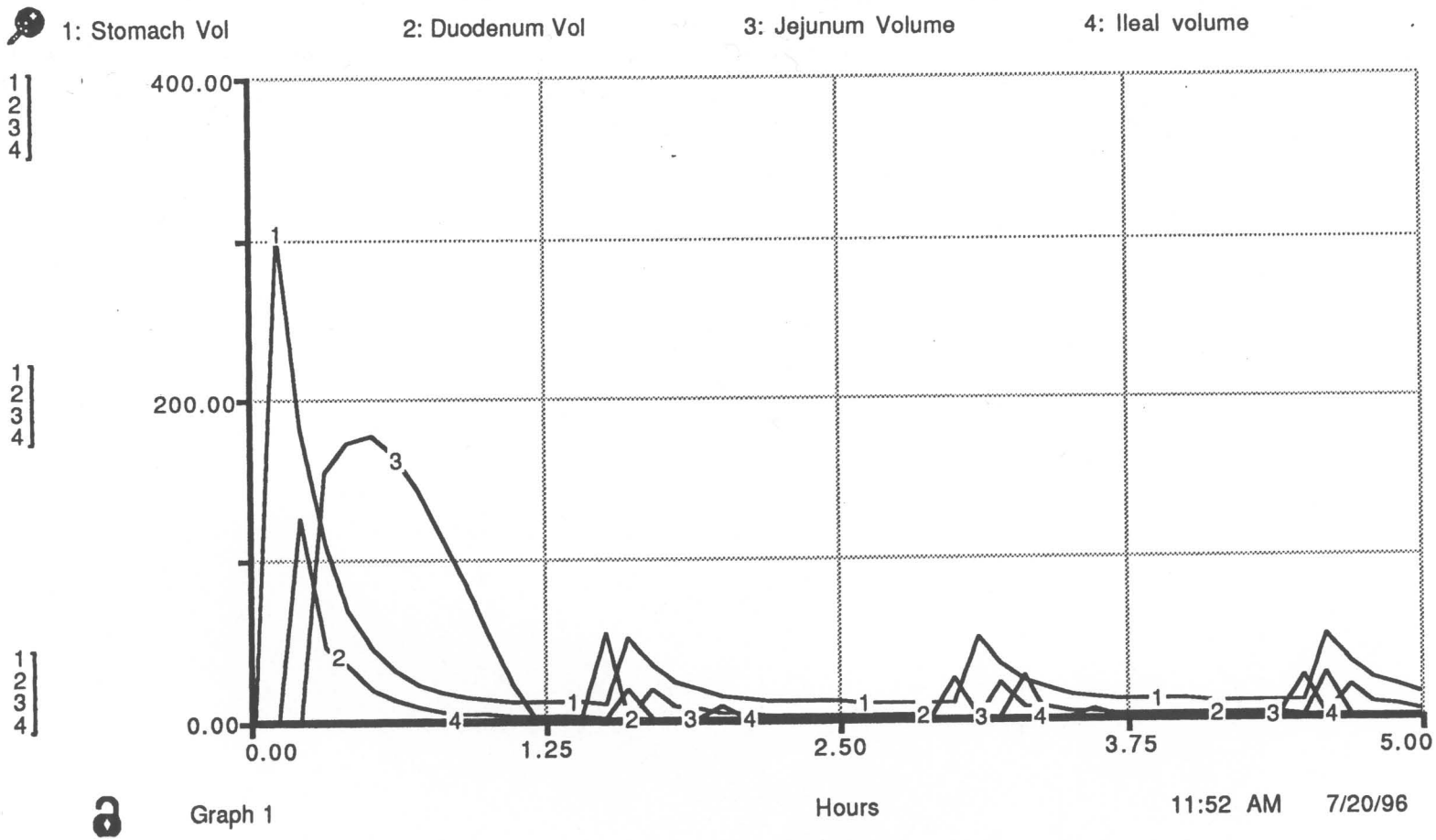
1: Stomach Vol
2: Duodenum Vol
3: Jejunum Volume
4: Ileal volume
400.00
200.00
0.00
0.00
1.25
2.50
3.75
5.00
Graph 1
Hours
11:52 AM 7/20/96

the ileum? By manipulating the model, we were able to discover that slightly more than 700 milliliters of water would need to be ingested as a bolus for any to make it to the ileal region. At this level the absorptive ability of the duodenum and the jejunum are overloaded. Therefore, some of the fluid presented to the small intestine via gastric emptying succeeds in making it to the ileum, where it is rapidly absorbed.

As mentioned earlier, phasic activity, i.e., the MMC, was seen to return ninety minutes after oral ingestion 300 milliliters of water. This was seen in our *in vivo* canine studies and was therefore programmed into our model. In the model it appeared that while the duodenum was empty at the onset of the phasic action, a residual volume of fluid remained in the jejunum. Upon onset of the gastric emptying phase III housekeeper wave, fluid passed through the duodenum and accumulated in the jejunum albeit much more proximal than where the residual volume would be expected to be. According to our computer generated model, it appears that the presence of fluid in the gastrointestinal tract does not absolutely preclude fasted gastric MMC patterns.

VI.3 The Pulmocare Fed Subject

The next model designed describes the action of Pulmocare™ through the small intestine of a fasted subject. The basic scheme shown in Figures 49 and 50 is essentially the same as that describing the movement of water in the model above. The only exception is that

Figure 49 : Full schematic representation of the model of fluid movement of orally administered Pulmocare ™ (240 ml bolus) through the gastrointestinal tract of the fasted human.

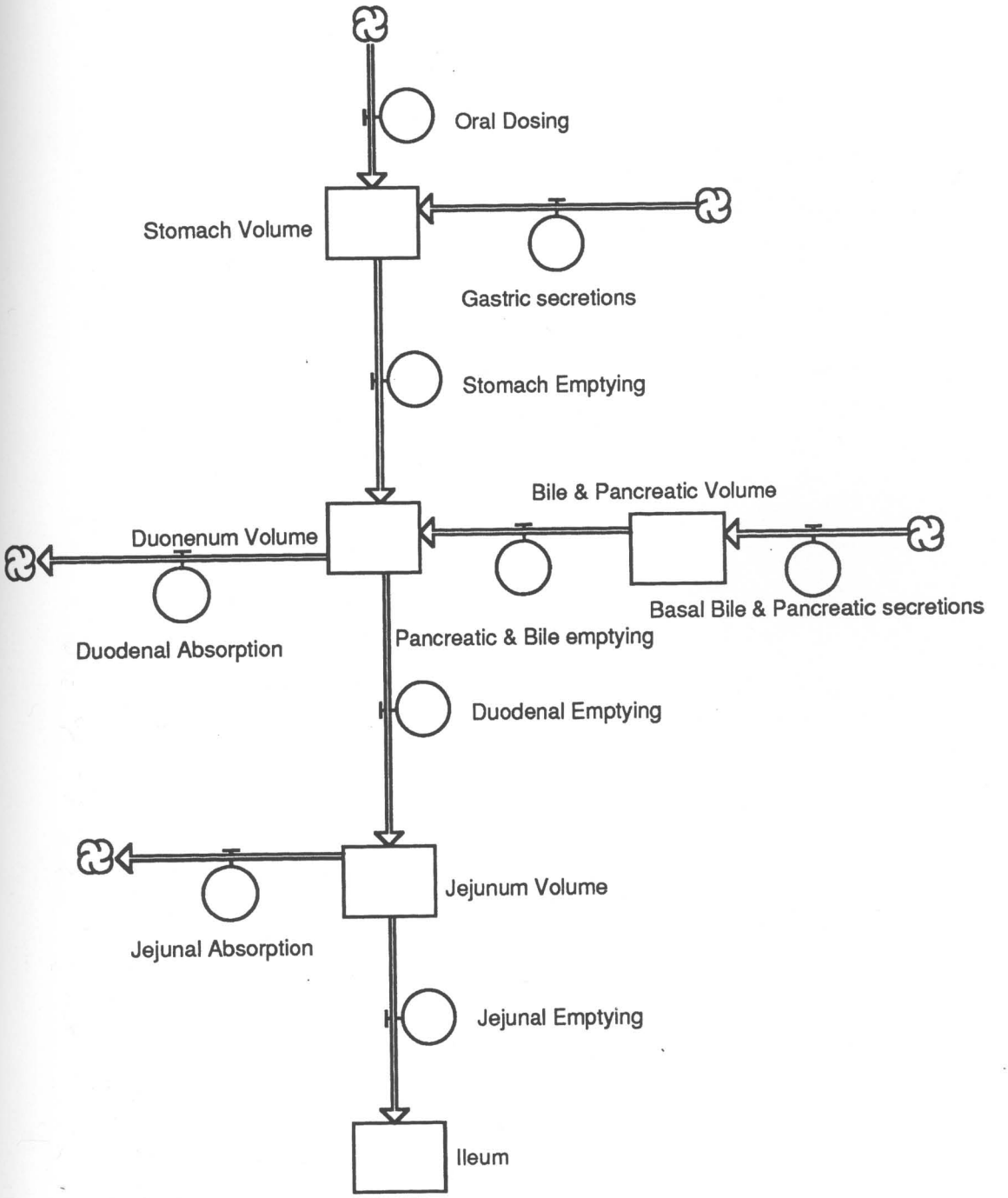
Oral Dosing
Stomach Volume
Gastric secretions
Stomach Emptying
Bile & Pancreatic Volume
Duonenum Volume
Basal Bile & Pancreatic secretions
Duodenal Absorption
Pancreatic & Bile emptying
Duodenal Emptying
Jejunum Volume
Jejunal Absorption
Jejunal Emptying
Ileum

Figure 50 : Full schematic representation including converters and input links of the model of fluid movement of orally administered Pulmocare ™ (240 ml bolus) bolus through the gastrointestinal tract of the fasted human

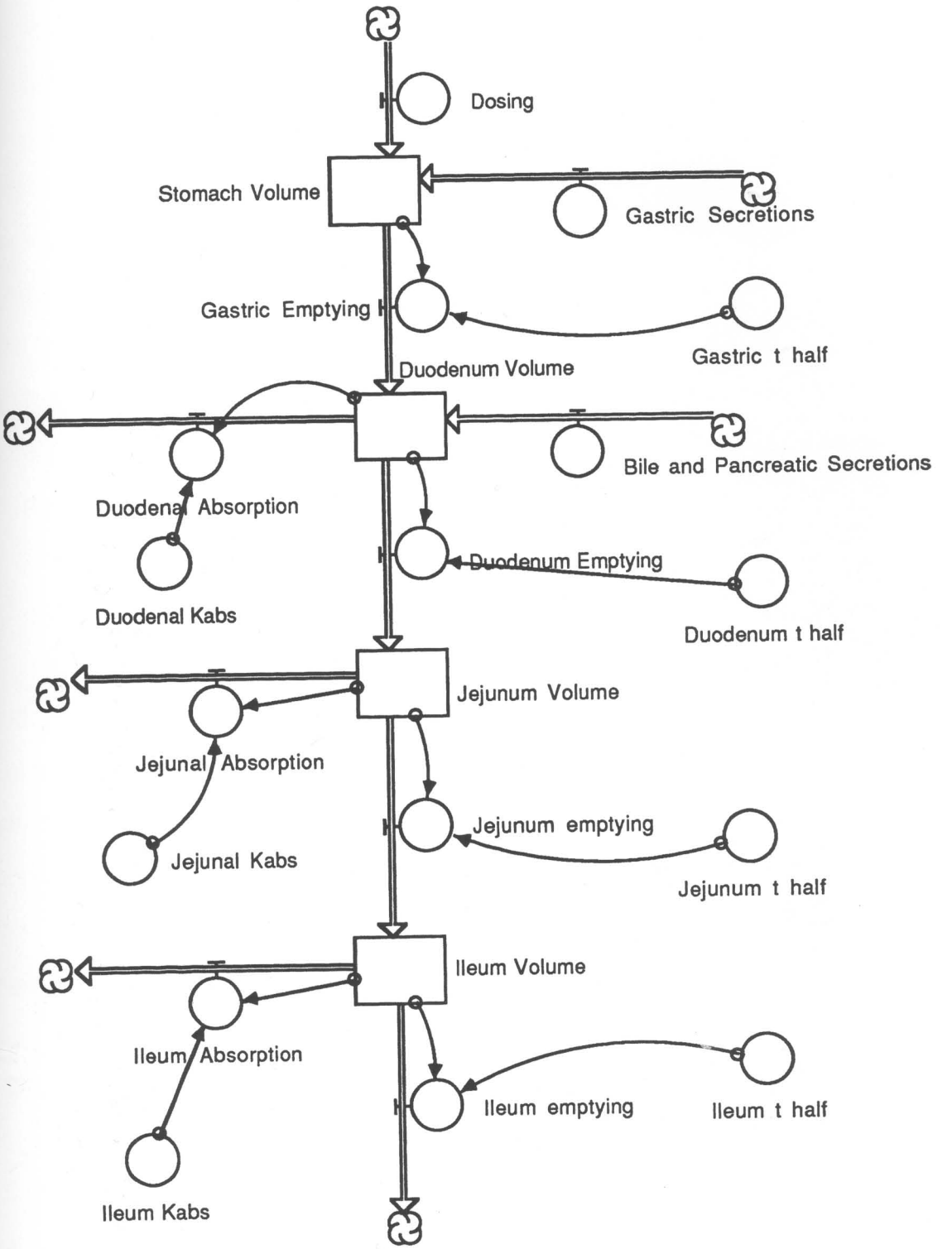
Dosing
Stomach Volume
Gastric Secretions
Gastric Emptying
Gastric t half
Duodenum Volume
Bile and Pancreatic Secretions
Duodenal Absorption
Duodenal Kabs
Duodenum Emptying
Duodenum t half
Jejunum Volume
Jejunal Absorption
Jejunal Kabs
Jejunum emptying
Jejunum t half
Ileum Volume
Ileum Absorption
Ileum Kabs
Ileum emptying
Ileum t half

no stock exists in the Pulmocare™ model for the accumulation of bile and pancreatic secretions.

The model was formulated by combining information gathered from the literature and the *in vivo* canine studies described earlier. In those five hour transit studies we saw that the fluid collected from the duodenal cannula was more than twice the volume that was administered. In addition, over the five hour period of the study, the animals' digestive patterns were not seen to revert to the fasted state as they had when they were fed water. This observation was incorporated into the model.

The migrating motor complex has been seen to be disrupted whenever a sufficiently large meal is ingested.[132,213] The duration of this disruption is directly related to the amount of calories taken for any of the three major food components, i.e., protein, carbohydrate, and fat.[213] Gastric effluent may enhance or slow stomach emptying by affecting duodenal receptors sensitive to acidity, fatty acids or osmotic effects.[40] In addition, depending upon the composition of the meal, feeding interrupts the interdigestive pancreatic secretions, converting it to a constant secretory pattern approximately 75% greater than peak secretory outputs observed during phase II.[129,214]

Pulmocare™ is a high fat, high calorie, hyperosmotic liquid nutrition supplement. These characteristics would be expected to elicit a strong influence upon the digestive pattern. For example, it would be expected to see a drastic reduction in the duodenal absorption rate, a decrease in gastric emptying rate, i.e., increase the

$t_{1/2}$ of emptying, and an increase in volume of gastric and duodenal secretions.

These factors were all accounted for in the model's design. To mimic what was seen *in vivo*, bile, pancreatic and gastric secretion inputs were all increased over their basal levels. The model was also modified to include the continuous secretion of bile and pancreatic secretions into the lumen that, as mentioned earlier, would be expected to occur in a fed subject. In addition to these increased secretions, the duodenal absorption rate was reduced to zero as would be expected as the body tries to convert the hyperosmotic contents of the lumen to approximate isoosmolality.

The result of this model is generated in the graph of Figure 51. It is apparent that stomach and duodenal emptying are prolonged relative to the previous models. In addition, since there is no absorption by the duodenum, all of the lumenal contents traverse into the jejunum where, according to the model, all but approximately fifty milliliters of fluid is absorbed. This fifty milliliters enters the ileum where it is quickly and completely absorbed. This supports the empirical observation that while the Pulmocare™ feeding *in vivo* results in a prolonged flow of fluid into the small intestine, no fluid was ever collected through the ileal cannula.

Since the five hour length of the canine Pulmocare™ study was not long enough to see a return of the interdigestive pattern, this model can only describe a fed subject. A reasonable assumption would be that upon return of the fasted state and the interdigestive

Figure 51 : Simulation of fluid movement of orally administered Pulmocare ™ (240 ml bolus) as it moves through the stomach, duodenum, jejunum and ileum in the originally fasted human. Curves represent the volume accumulation in each region of the gastrointestinal tract. 1-stomach, 3-duodenum, 4-jejunum, and 5-ileum. Curve #2 represents the secretion contribution of the bile and pancreas.

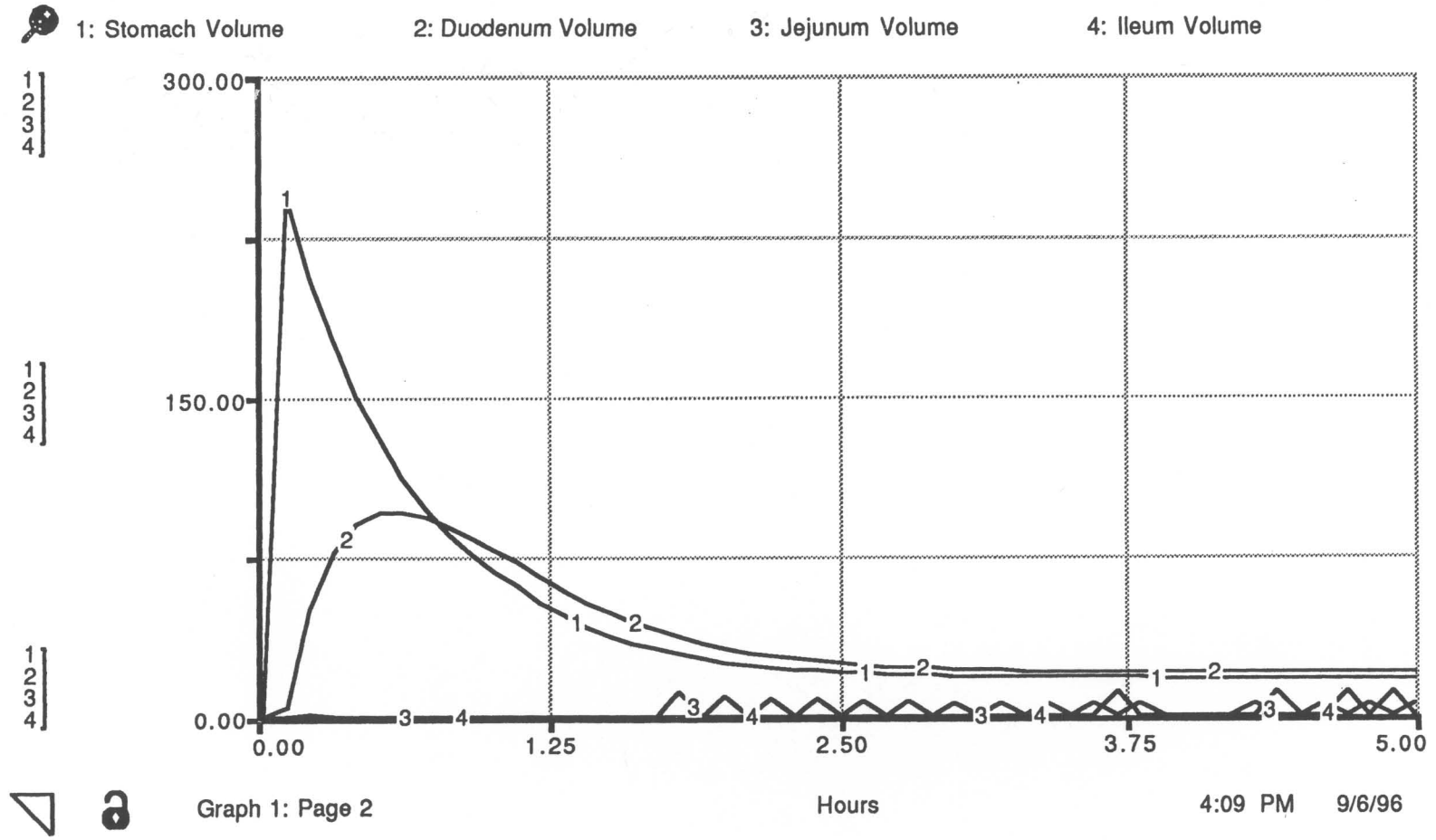
1: Stomach Volume
2: Duodenum Volume
3: Jejunum Volume
4: Ileum Volume
300.00
150.00
0.00
0.00
1.25
2.50
3.75
5.00
Graph 1: Page 2
Hours
4:09 PM
9/6/96

MMC, the subject, and therefore the model, would revert to the fasted state as described in the first model.

VI.4 The Swelling Model

The ultimate goal of the computer models was to describe the swelling kinetics of an orally ingested polymer delivery system through the human gastrointestinal tract. To achieve this, the model, shown in Figure 52, was designed for the fasted human. As in the previous models, it is assumed that the polymer system is ingested at the beginning of phase I of a migrating myoelectric complex (MMC) and was expelled from the stomach with the phase III housekeeper wave. It is also important to note that while this model is designed for the fasted subject, our *in vivo* studies have shown that the swelling kinetics of the hydrogel polymers was essentially identical whether our subjects are either fed or fasted. It is therefore assumed that this model describes hydrogel swelling under both conditions.

The values describing the swelling rates of the various polymers were gathered from *in vitro* studies performed in simulated gastric fluid (USP), simulated intestinal fluid (USP), and duodenal fluid collected from three fasted canines. The total length of the small bowel was taken to be approximately six meters divided between duodenum (30 cm), jejunum (2.5 meters), and ileum (3.5 meters).[38] The small intestinal transit time in fasted humans has been measured to be 5.5 ± 2.1 hours, not including a gastric emptying

Figure 52 : Full schematic representation of the model of polymer swelling as the delivery system moves through the gastrointestinal tract of a fasted human.

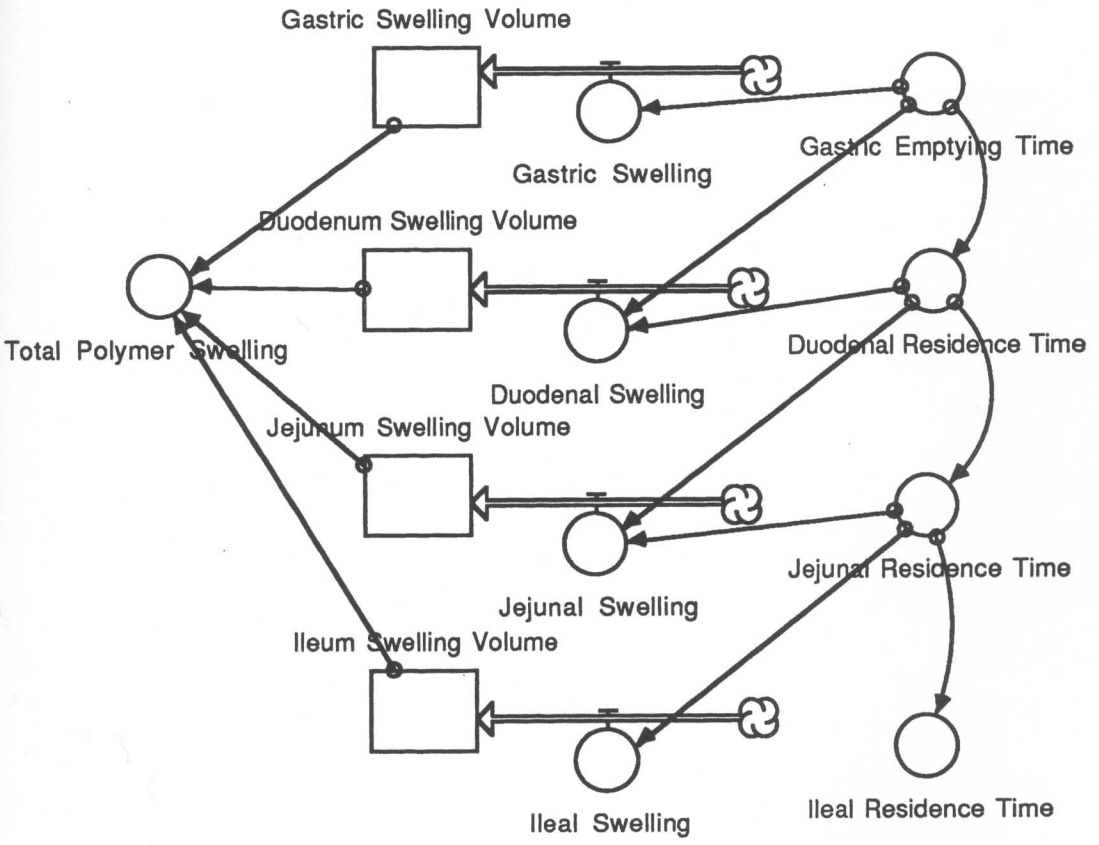
Gastric Swelling Volume
Gastric Swelling
Gastric Emptying Time
Duodenum Swelling Volume
Total Polymer Swelling
Duodenal Residence Time
Duodenal Swelling
Jejunum Swelling Volume
Jejunal Residence Time
Jejunal Swelling
Ileum Swelling Volume
Ileal Swelling
Ileal Residence Time

time of ninety minutes.[44] These values were incorporated into our model's development.

The graphic representation of the results of the model simulations for each of the four polymers studied is shown in Figures 53 through 56. In each graph, curve #5 represents total polymer swelling and is the simple sum of the regional swelling as the polymer moves through the gastrointestinal system. In addition, the equations and swelling data tables for each of these studies may be found in the Appendix of this thesis.

In each model clearly most of the fluid absorption occurs when the polymer is resident to the jejunal and ileal regions. This is due mainly to the relatively long time that the delivery system would be expected to reside in these regions as well as the less acidic pH innate to the jejunum and ileum. This factor is especially important for polyacid polymers. On the other hand, while all of the secretions either originate or pass through the duodenum, its effect on the swelling polymer is small due to its short 30 cm length. The polymer system would be expected to pass through the duodenum within approximately six minutes and thus, its relatively small contribution to the total swelling curve reflects this.

The gastric swelling contribution is smaller than would be expected if swelling was purely due to residence time. However, the pH of the region also plays a major role in the extent of swelling. Being lower than the pKa's of carboxymethyl cellulose, Carbopol and Noveon, the pH of the stomach enables the carboxylic acid functional groups of the polymers to be protonated. Since greatest swelling is

Figure 53 : Simulation of the swelling of hydroxypropyl methyl cellulose as it moves through the stomach, duodenum, jejunum and ileum in the originally fasted human. Curves represent the swelling in each of the indiviual regions of the gastrointestinal tract. 1-stomach, 2-duodenum, 3-jejunum, 4-ileum, and 5- total polymer swelling.

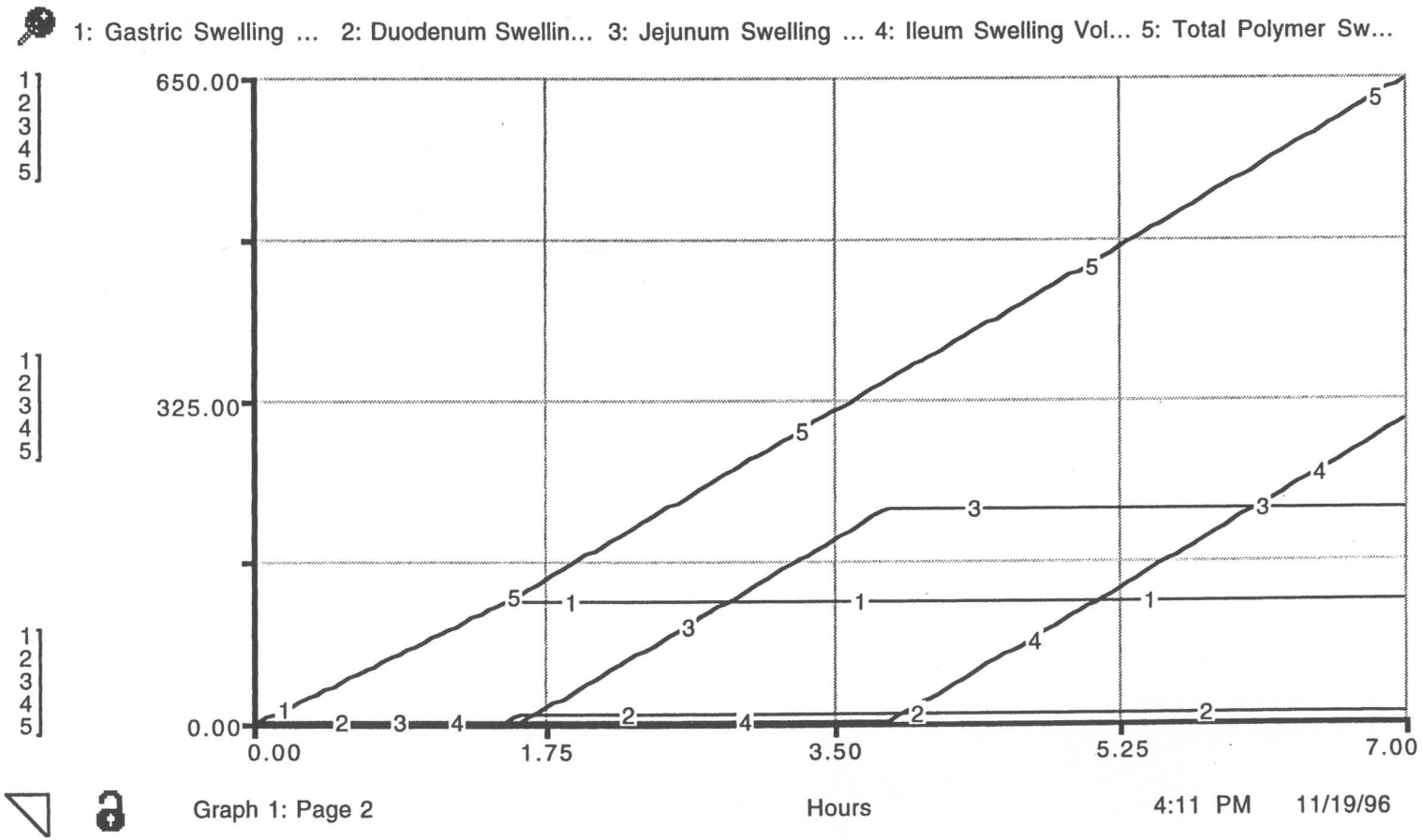
1: Gastric Swelling ...
2: Duodenum Swellin...
3: Jejunum Swelling ...
4: Ileum Swelling Vol...
5: Total Polymer Sw...
650.00
325.00
0.00
0.00
1.75
3.50
5.25
7.00
Graph 1: Page 2
Hours
4:11 PM
11/19/96

Figure 54 : Simulation of the swelling of carboxymethyl cellulose as it moves through the stomach, duodenum, jejunum and ileum in the originally fasted human. Curves represent the swelling in each of the indiviual regions of the gastrointestinal tract. 1-stomach, 2-duodenum, 3-jejunum, 4-ileum, and 5- total polymer swelling.

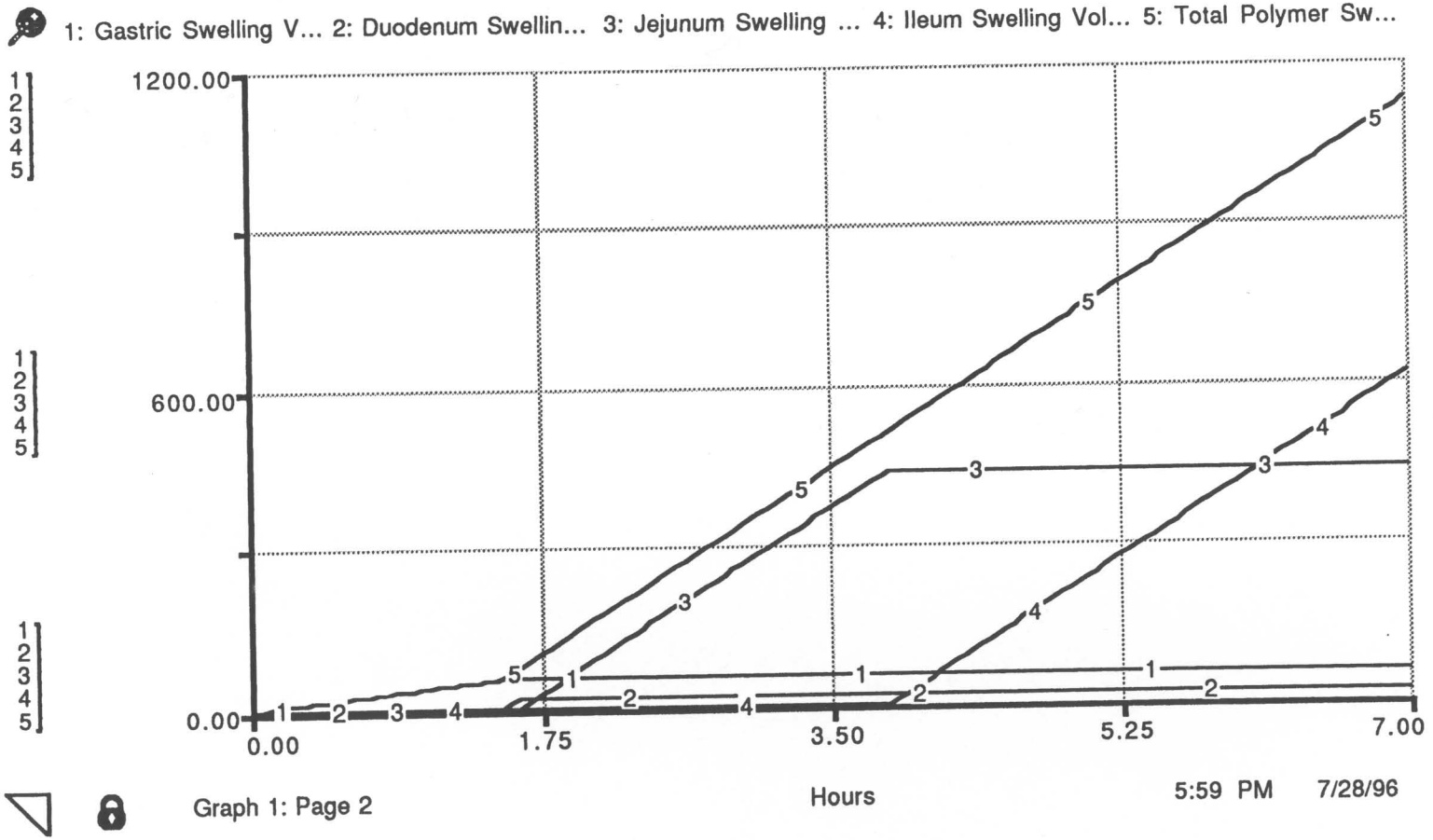
1: Gastric Swelling V... 2: Duodenum Swellin... 3: Jejunum Swelling ... 4: Ileum Swelling Vol... 5: Total Polymer Sw...
1200.00
600.00
0.00
0.00
1.75
3.50
5.25
7.00
Hours
Graph 1: Page 2
5:59 PM 7/28/96

Figure 55 : Simulation of the swelling of Carbopol 974P™ as it moves through the stomach, duodenum, jejunum and ileum in the originally fasted human. Curves represent the swelling in each of the indiviual regions of the gastrointestinal tract. 1-stomach, 2-duodenum, 3-jejunum, 4-ileum, and 5-total polymer swelling.

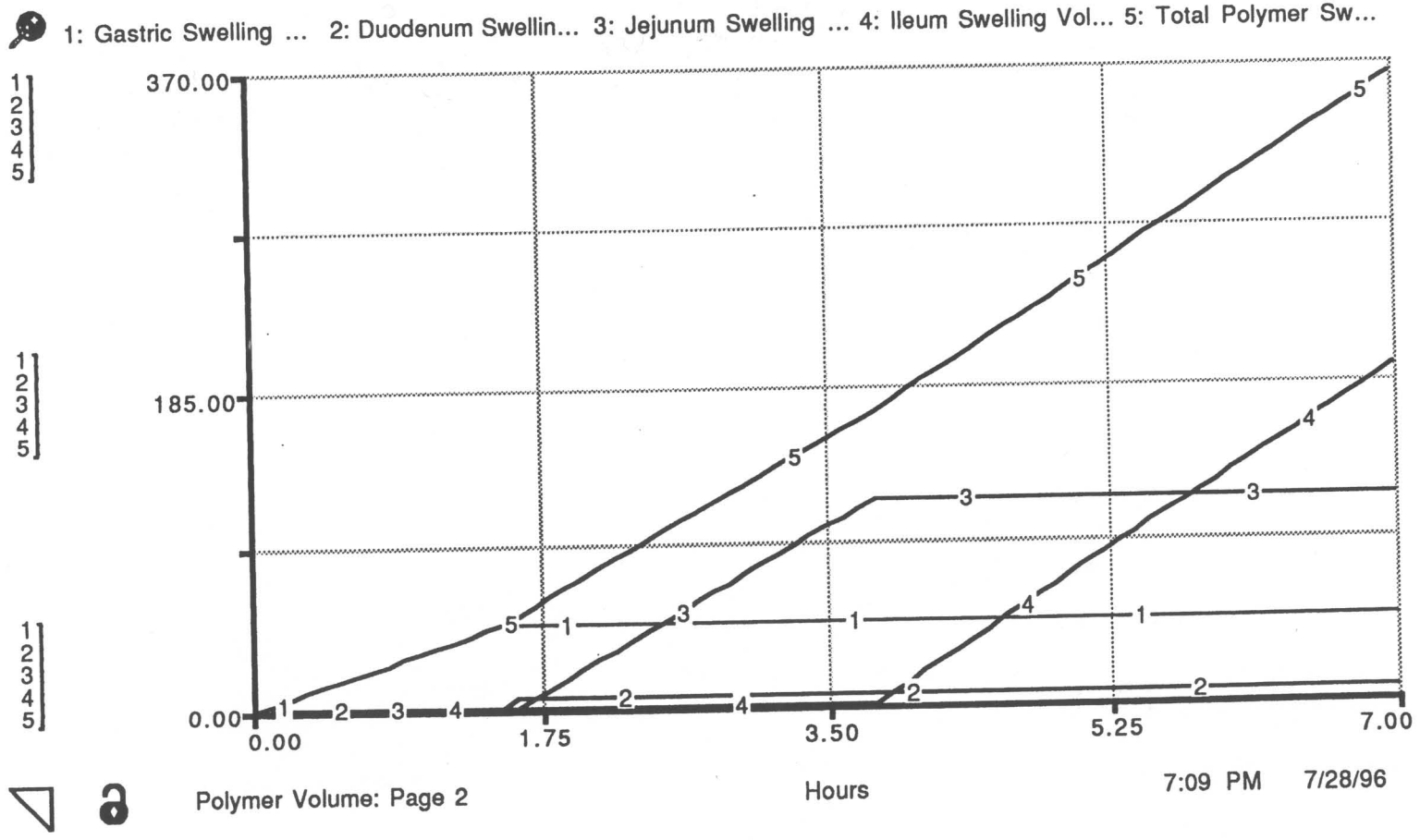
1: Gastric Swelling ...
2: Duodenum Swellin...
3: Jejunum Swelling ...
4: Ileum Swelling Vol...
5: Total Polymer Sw...
370.00
185.00
0.00
0.00
1.75
3.50
5.25
7.00
Hours
Polymer Volume: Page 2
7:09 PM
7/28/96

Figure 56 : Simulation of the swelling of Noveon AA1 (polycarbophil) as it moves through the stomach, duodenum, jejunum and ileum in the originally fasted human. Curves represent the swelling in each of the indiviual regions of the gastrointestinal tract. 1- stomach, 2-duodenum, 3-jejunum, 4-ileum, and 5- total polymer swelling.

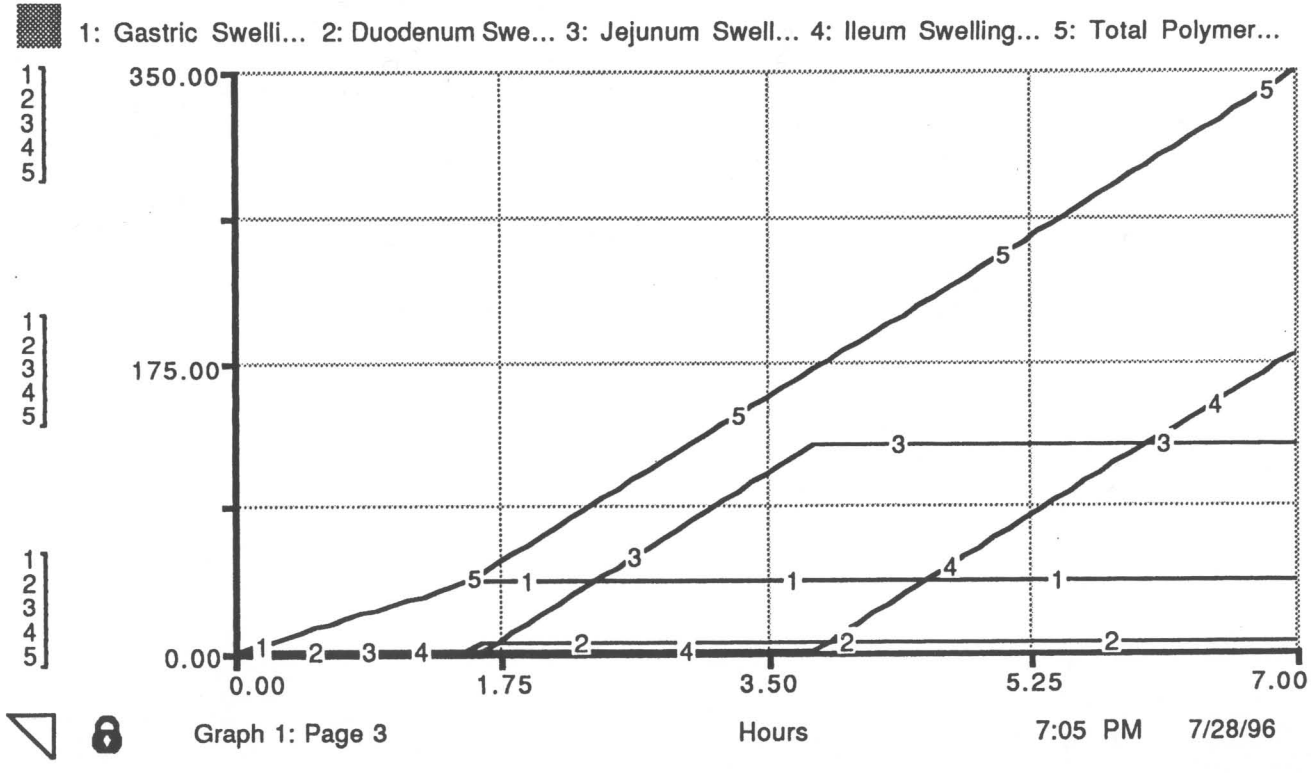
1: Gastric Swelli... 2: Duodenum Swe... 3: Jejunum Swell... 4: Ileum Swelling... 5: Total Polymer...
350.00
175.00
0.00
0.00
1.75
3.50
5.25
7.00
Graph 1: Page 3
Hours
7:05 PM
7/28/96

observed when the acid groups are in the ionized form, protonating these groups would result in the reduced swelling observed.

The exception to all this is seen in the case of the hydroxypropyl methyl cellulose study. Being electronically neutral, the effect of changes in gastrointestinal pH would be expected to be minimal. This, in fact, is what we saw in our *in vitro* experiments and therefore, was incorporated into our model.

Since the ultimate goal of the STELLA™ model is to estimate the *in vivo* behavior of the hydrogel polymer, a comparison of the model generated weight increase to the weight increase calculated from data from our canine experiments was performed. For our calculations we estimated the duodenal and ileal residence times of the polymer system to be 150 and 200 minutes, respectively and values corresponding to these times were taken directly from our canine studies.

The result of this comparison is shown in Table 14, showing the correspondence between the two methods for each of the polymers examined. Ranging from approximately a quarter of the canine generated values for the lightly cross-linked polyacrylic acids (carbopol and polycarbophil) to 73% for the neutral, straight chained hydroxypropyl methyl cellulose, the model generated value fell short of the canine generated value in each comparison. Perhaps with further study and expansion of the number and type of polymers studied a pattern will emerge from the correlations.

The conclusion from this study is that it appears that the STELLA™ model can be useful in describing the spatial and temporal

Table 14 : STELLA™ model and canine *in vivo* data comparison after 7 hours in the gastrointestinal tract. Values are expressed as weight increase in grams.

Polymer	*In vivo*	Model	*In vitro-in vivo* correlation factor #
Carbopol 974P™	1.510	0.354	0.234
Carboxymethyl cellulose	2.393	1.133	0.471
Hydroxypropyl methyl cellulose	0.890	0.648	0.728
Noveon AA1™ (polycarbophil)	1.269	0.350	0.276

in vitro -in vivo correlation factor = model */in vivo*

movement of fluid through the small intestine. In addition, it can, with the proper caveats, be useful in estimating the rate and extent of fluid uptake and swelling of ingested hydrogel based drug delivery systems. It must be remembered that since the STELLA™ model is developed from *in vitro* generated data, any *in vivo-in vitro* comparison will be only as good as the information at hand. As mentioned above, a scaling factor relating the behavior of the polymers under both conditions will most likely need to be generated before this model will become widely applicable. Meanwhile, until this calibration is available, the implication is that it is quite risky for researchers to assume they truly understand and can predict the behavior of a polymer *in vivo* solely based on *in vitro* observations.

VII. CONCLUSIONS

The goal of the above study was to add to our current understanding of the swelling behavior of hydrogel polymers. Hydrogel polymers are common components used in the design of orally administered delivery systems. Thus, a fuller understanding of their often unpredictable swelling nature in the gastrointestinal tract would assist in the design of more effective and efficient delivery systems.

The cannulated canine has been shown to be a good, albeit not ideal, model for gastrointestinal studies. Fasted motility patterns, gastric pH and gastric emptying of liquids in canines are very similar to what has been measured in humans. The main difference between the two species in the fasted state is a slightly higher intestinal pH seen in the canine.

While, in general, postprandial response is again similar in the two species, some differences are noted. Gastric and intestinal pH, at least just after eating, is seen to be more acidic in the canine. In addition, meal emptying rates and the return of fasted motility patterns have been seen to be somewhat slower in dogs. Therefore, with the proper caveats, information acquired from canine studies can help in the unraveling of what may be occurring *in vivo* in human subjects.

An attempt at studying the microclimate effect of influxing solutions into the polymer was not as conclusive as desired, but various trends were recognized. Comparison of pH changes during

polymer swelling studies in range of solutions showed that, except in the case of the very acidic simulated gastric fluid (pH 1.2), the influxing solution showed only a relatively small effect on the rate and extent of swelling. It appears that the ionic polymers used in this study can buffer the effect of the pH of the diffusing solution. As expected, this effect was absent in studies with hydroxypropyl methyl cellulose.

In vivo swelling studies have shown that, without exception, polymer swelling occurred to a greater extent in the duodenum as opposed to the ileum. In addition, swelling was found to be independent of whether the animal was fasted or fed water or Pulmocare.™ This demonstrated that gastric contents, as they pass through the small intestine, are not a major source of swelling promoting fluid.

The extent of swelling of the polymer system placed directly into the intestine through the cannulae was seen to be independent of the timing of the insertion relative to the migrating myoelectric complex (MMC). In addition, no difference was seen whether the polymer system was directly inserted into the intestine or ingested orally and then allowed to pass through the pylorus into the duodenum, naturally. The swelling kinetics was the same. Overall it appears that the MMC is seen not to exert much influence on the kinetics of swelling.

Swelling also does not appear to be affected by the presence or absence of gastrointestinal secretions. Through intravenous injections of atropine sulfate to shut down gastric and duodenal

secretions, and comparing the results to studies in non-atropinized canines, we saw that *in vivo* polymer swelling was independent of these secretions.

With these observations it appears that the source of swelling promoting fluid most likely is the mucous gel lining coating the small intestinal epithelial cells. A polymer delivery system residing in the gastrointestinal system can easily be envisioned in constant intimate contact with the mucous gel. Predominantly composed of water, this highly hydrated mucous lining could transfer whatever water the polymer would need for swelling. In addition, the difference in the swelling rate and extent in ileal and duodenal regions can be explained as being due to differences in the amount and thickness of mucous in the two regions.

A STELLA™ computer model describing the kinetics of polymer swelling and fluid movement through the gastrointestinal tract, spatially and temporally, was constructed. The model was assembled using literature available parameters as well as data generated by various *in vitro* studies. Comparison of model generated, *in vitro* based results with *in vivo* canine studies showed that, without exception, the rate and extent of swelling was consistently larger *in vivo.* While this study may help to understand the global picture of hydrogel polymer swelling, the most important implication is that researchers need to take care in assuming that they understand the behavior of a polymer delivery system solely based upon data generated by *in vitro* studies. Much more is going on in the gastrointestinal tract than we can model *in vitro.*

VIII. REFERENCES

1. Park K. Enzyme-digestible swelling hydrogels as platforms for long-term oral drug delivery: synthesis and characterization. *Biomaterials* 1988;**9**:435-441.

2. Peppas NA, Mikos AG. Preparation Methods and Structure of Hydrogels. In: Peppas NA, ed. Hydrogels in Medicine and Pharmacy. vol.I. Boca Raton, FL: CRC Press, Inc., 1986: 1-25.

3. Kudela V. Hydrogels. In: Kroschwitz JI, ed. Polymers: Biomaterials and Medical Applications. New York: John Wiley & Sons, 1989: 228-252.

4. Peppas NA, Khare AR. Preparation, structure and diffusional behavior of hydrogel in controlled release. *Advanced Drug Delivery Reviews* 1993;**11**(1/2):1-35.

5. Ratner BD. Biomedical Applications of Hydrogels; Review and Critical Appraisal. In: Williams DF, ed. Biocompatibility of Clinical Implant Materials. Boca Raton, FL: CRC Press, Inc., 1981: 145-175.

6. Wichterle O, Lim D. Hydrophilic gels for biological use. *Nature (London)* 1960;**185**:117-118.

7. Refojo MF. Polymers in Opthalmology: An Overview. In: Williams DF, ed. Biocompatibility in Clinical Practice. Boca Raton, Fl: CRC Press, Inc., 1981: 3-18.

8. Tollar M, Stol M, Kliment K. Surgical suture materials coated with a layer of hydrophilic hydron gel. *Journal of Biomedical Materials Research* 1969;**3**(2):305-313.

9. Kaganov AL, Stamberg J, Synek P. Hydrophilized polyethylene catheters. *Journal of Biomedical Materials Research* 1976;**10**(1):1-7.

10. Krejci L, Harrison R, Wichterle O. Hydroxyethyl methacrylate capillary strip: animal trials with a new glaucoma drainage device. *Archives of Ophthalmology* 1976;**84**(1):76.

11. Refojo MF. Contact lenses. In: Bikales RN, ed. Encyclopedia of Polymer Science and Technology, Suppl. 1. New York: John Wiley & Sons, 1979: 195-219.

12. Refojo MF. Artificial membranes for corneal surgery. *Journal of Biomedical Materials Research* 1969;**3**(3):333-347.

13. Kliment K, Stol M, Raab M, Stokr J. Study on a new soft denture liner of the Sofdent type. *Journal of Biomedical Materials Research* 1968;**2**(3):473-487.

14. Bray JC, Merrill EW. Poly(vinyl alcohol) hydrogels for synthetic articular cartilage materials. *Journal of Biomedical Materials Research* 1973;**7**(5):431-443.

15. Nathan P, Law EJ, MacMillan BG, et al. A new biomaterial for control of infection in the burn wound. *Transaction of the American Society of Artificial Internal Organs* 1976;**22**:30-41.

16. Rubin RM, Marshall JL. Porous hydrophilic polymer: good and bad news in orthopedic application of cruciate ligament substitution. *Journal of Biomedical Materials Research* 1975;**9**(3):375-380.

17. Kocvara S, Kliment C, Kubat J, Stol M, Ott Z, Dvorak J. Gel-fabric protheses of the ureter. *Journal of Biomedical Materials Research* 1967;**1**:325-336.

18. Ratner BD, Hoffman AS. Synthetic Hydrogels for Biomedical Applications. In: Andrade JD, ed. Hydrogels for Medical and Related Applications. Washington, D.C: American Chemical Society, 1976: 1-36.

19. Benson H, Harley B, Schmitt EE. Drug Applications. In: Kroschwitz JI, ed. Polymers: Biomaterials and Medical Applications. New York: John Wiley & Sons, 1989: 131-150.

20. Kim SW. Hydrogels as drug delivery systems. *Pharmacy International* 1983;**4**(April):90-91.

21. Siegel RA. pH-Sensitive Gels: Swelling Equilibria, Kinetics, and Applications for Drug Delivery. In: Kost J, ed. Pulsed and Self-Regulated Drug Delivery. Boca Raton, FL: CRC Press, Inc., 1990: 129-157.

22. Siegel RA. Hydrophobic Weak Polyelectrolyte Gels: Studies of Swelling Equilibria and Kinetics. In: Dusek K, ed. Responsive Gels: Volume Transitions I. Berlin Heidelberg: Springer-Verlag, 1993: 233-267.

23. Hirokawa Y, Tanaka T. Volume phase transition in a nonionic gel. *Journal of Chemical Physics* 1984;**81**(12):6379-6380.

24. Park H. Synthesis and Evaluation of Some Bioadhesive Hydrogels. Master of Science: University of Wisconsin-Madison, 1984.

25. Pradny M, Kopecek J. Hydrogels for site-specific oral delivery. *Macromolecular Chemistry* 1990;**191**:1887-1897.

26. Firestone BA, Siegel RA. Kinetics and mechanisms of water sorption in hydrophobic, ionizable copolymer gels. *Journal of Applied Polymer Science* 1991;**43**:901-914.

27. Tanaka T. Gels. In: Mark HF, Kroschwitz JI, eds. Encyclopedia of Polymer Science and Engineering. New York: John Wiley & Sons, 1985: 514-531.

28. Ricka J, Tanaka T. Swelling of ionic gels: Quantitative performance of the Donnan theory. *Macromolecules* 1984;**17**:2916-2921.

29. Hoffman AS. Applications of thermally reversible polymers and hydrogels in therapeutics and diagnostics. *Journal of Controlled Release* 1987;**6**:297-305.

30. Dong L-C, Hoffman AS. Synthesis and application of thermally reversible heterogels for drug delivery. *Journal of Controlled Release* 1990;**12**(1):21-31.

31. Yoshida R, Uchida K, Kaneko Y, et al. Comb-type grafted hydrogels with rapid de-swelling response to temperature changes. *Nature* 1995;**374**:240-242.

32. Tanaka T. Gels. *Scientific American* 1981;**244**(1):124-138.

33. Gerke SH, Andrews GP, Cussler EL. Chemical aspects of gel extraction. *Chemical Engineering Science* 1986;**41**:2153-2160.

34. Tanaka T. Phase transitions in gels and a single polymer. *Polymer* 1979;**20**:1404-1412.

35. Ilavsky M, Hrouz J, Ulbrich K. Phase transition in swollen gels. The temperature collapse and mechanical behaviour of poly (N,N-diethylyacrylamide) networks in water. *Polymer Bulletin* 1982;**7**:107-113.

36. Yoshida R, Sakai K, Okano T, Sakurai Y. Modulating the phase transition temperature and thermosensitivity in N-

isopropylacrylamide copolymer gels. *Journal of Biomaterials Science, Polymer Edition* 1994;**6**:585-598.

37. Rao S, Ritschel WA. Colonic drug delivery of small peptides. *S.T.P. Pharma Sciences* 1995;**5**(1):19-29.

38. Watson DW, Sodeman J William A. The Small Intestine. In: Sodeman J William A., Sodeman. WA, eds. Pathologic Physiology. Mechanisms of Disease. 5th ed. Philadephia, PA: W.B. Saunders Company, 1974: 734-766.

39. Ritschel WA. Targeting in the gastrointestinal tract: New approaches. *Methods and Findings in Experimental and Clinical Pharmacology* 1991;**13**(5):313-336.

40. Bass P. Gastric Emptying; differences among liquid, fiber, polymer and solid dosage forms of medications. Current status on targeted drug delivery to the gastrointestinal tract. Greenswood, S.C.: Capsugel Library, 1993: 23-33.

41. Youngberg CA, Berardi RR, Howatt WF, et al. Comparison of gastrointestinal pH in cystic fibrosis and healthy subjects. *Digestive Diseases and Sciences* 1987;**32**(5):472-480.

42. Sournac M, Maublant J-C, Aiache J-M, Vayre A, Bougaret J. Scintigraphic study of the gastro-intestinal transit and correlations with the drug absorption kinetics of a sustained release theophylline tablet. *Journal of Controlled Release* 1988;**7**:139-146.

43. Davis SS, Hardy JG, Fara JW. Transit of pharmaceutical dosage forms through the small intestine. *Gut* 1986;**27**:886-892.

44. Mundy MJ, Wilson CG, Hardy JG. The effect of eating on transit through the small intestine. *Nuclear Medicine Communications* 1989;**10**:45-50.

45. Davis SS, Hardy JG, Taylor MJ, Whalley DR, Wilson CG. A comparative study of the gastrointestinal transit of a pellet and tablet formulation. *International Journal of Pharmaceutics* 1984;**21**:167-177.

46. Davis SS, Hardy JG, Taylor MJ, Whalley DR, Wilson CG. The effect of food on the gastrointestinal transit of pellets and an osmotic device (Osmet). *International Journal of Pharmaceutics* 1984;**21**:331-340.

47. Malagelada J-R, Robertson JS, Brown ML, et al. Intestinal transit of solid and liquid components of a meal in health. *Gastroenterology* 1984;**87**:1255-1263.

48. Christiansen PM. The incidence of achlorhydria and hypochlorhydria in healthy subjects and patients with gastrointestinal diseases. *Scandinavian Journal of Gastoenterology* 1968;**3**:497-508.

49. Dressman JB, Berardi RR, Dermentzoglou LC, et al. Upper gastrointestinal (GI) pH in young, healthy men and women. *Pharmaceutical Research* 1990;**7**(7):756-761.

50. Evans DF, Pye G, Bramley R, Clark AG, Dyson TJ, Hardcastle JD. Measurement of gastrointesinal pH profiles in normal ambulant human subjects. *Gut* 1988;**29**:1035-1041.

51. Soergel KH, Hofman AF. Absorption. In: Frohlich ED, ed. Pathophysiology. Altered Regulatory Mechanisms in Disease. Philadelphia: J.B. Lippincott, 1972: 423-453.

52. Simon GL, Gorbach SL. Intestinal flora in health and disease. *Gastroenterology* 1984;**86**:174-193.

53. Shalaby WSW, Park K. Biochemical and mechanical characterization of enzyme-digestible hydrogel. *Pharmaceutical Research* 1990;**7**(8):816-823.

54. Shalaby WSW, Chen M, Park K. A mechanistic assessment of enzyme-induced degradation of albumin-crosslinked hydrogels. *Journal of Bioactive Compatible Polymers* 1992;**7**(3):257-274.

55. Tabata Y, Ikada Y. Synthesis of gelatin microspheres containing Interferon. *Pharmaceutical Research* 1989;**6**(5):422-427.

56. Yan C, Li X, Chen X, et al. Anticancer gelatin microspheres with multiple functions. *Biomaterials* 1991;**12**:640-644.

57. Heller J, Pangburn SH, Roskos KV. Development of enzymatically degradable protective coatings for use in triggered drug delivery systems: Derivatized starch hydrogels. *Biomaterials* 1990;**11**:345-350.

58. Laakso T, Sjoholm I. Biodegradable microspheres X: Some properties of polyacryl starch microparticles prepared From acrylic acid-esterified starch. *Journal of Pharmaceutical Sciences* 1987;**76**(12):962-939.

59. Pangburn SH, Trescony PV, Heller J. Lysozyme degradation of partially deacetylated chitin, its films and hydrogels. *Biomaterials* 1982;**3**:105-108.

60. Vander AJ, Sherman JH, Luciano DS. Human Physiology. The Mechanisms of Body Function. Fourth ed. New York: McGraw-Hill Book Company, 1985.

61. Guyton AC. Secretory Functions of the Alimentary Tract. Basic Human Physiology: Normal Function and Mechanisms of Disease. Philadelphia: W.B. Saunders Company, 1977: 670-685.

62. Allen A, Hutton D, McQueen S, Garner A. Dimensions of gastroduodenal surface pH gradient exceed those of adherent mucus gel layers. *Gastroenterology* 1983;**85**:463-476.

63. Litt M. Comparative studies of mucus and mucin physiochemistry. In: Nugent J, O'Connor M, eds. Mucus and Mucosa, Ciba Foundation Symposium 109. London: Pittman, 1984: 196.

64. MacAdam A. The effect of gastro-intestinal mucus on drug absorption. *Advanced Drug Delivery Reviews* 1993;**11**:201-220.

65. Furia TE. Cellulose derivatives-sodium carboxymethyl cellulose. In: Furia TE, ed. Handbook of Food Additives. 2nd ed. Boca Raton, FL: CRC Press, 1972: 320-2.

66. Keller JD. Sodium carboxymethyl cellulose (CMC). In: Glicksman M, ed. Food Hydrocolloids. Boca Raton, FL: CRC Press, Inc., 1986: 43-104.

67. Fedderson RL, Thorp SN. Sodium carboxymethyl cellulose. In: Whistle RL, ed. Industrial Gums. 3rd ed. New York: Academic Press, 1993: 573-578.

68. Chowdhury FH, Neale SM. Acid behavior of carboxylic derivatives of cellulose. Part I. Carboxymethylcellulose. *Journal of Polymer Science, Part A* 1963;**1**:2881-2891.

69. Doelker E. Water-Swollen Cellulose Derivatives in Pharmacy. In: Peppas NA, ed. Hydrogels in Medicine and Pharmacy. vol 2. Boca Raton, FL: CRC Press, Inc., 1987: 115-160.

70. Greminger Jr. GK, Sabage AB. Methylcellulose and Its Derivatives. In: Whistler RL, BeMiller JN, eds. Industrial Gums. Polysaccharides and Their Derivatives. New York: Academic Press, 1959: 565-596.

71. Freydberg N, Gortner WA. Cellulose Derivatives. The Food Additives Book. New York: Bantam Books, 1982: 508-511.

72. Bettini R, Columbo P, Massimo G, Catellani PL, Vitali T. Swelling and drug release in hydrogel matrices: polymer viscosity and matrix porosity effects. *European Journal of Pharmaceutical Sciences* 1994;**2**:213-219.

73. Scheffel KG. Methyl and Hydroxypropyl Methyl Cellulose Derivatives. In: Davidson RL, Sittig M, eds. Water-Soluble Resins. Second ed. New York: Reinhold Book Corporation, 1968: 50-62.

74. Methocel Cellulose Ethers. Technical Handbook: Dow Chemical Company.

75. Grover JA. Methylcellulose (MC) and Hydroxypropylmethylcellulose (HPMC). In: Glicksman M, ed. Food Hydrocolloids. Boca Raton, FL: CRC Press, Inc., 1986: 121-154.

76. Glicksman M. Utilization of Synthetic Gums in the Food Industry. In: Chichester CO, Mrak EM, Stewart GF, eds. Advances in Food Research. New York: Academic Press, 1963: 284-367.

77. Klose RE, Glicksman M. Gums. In: Furia TE, ed. Handbook of Food Additives. second ed. Cleveland, OH: CRC Press, 1972: 95-359.

78. Alderman DA. A review of cellulose ethers in hydrophilic matrices for oral controlled-release dosage forms. *International Journal of Pharmaceutical Technology and Product Manufacturing* 1984;**5**(3):1-9.

79. Glicksman M. Gum Technology in the Food Industry. New York: Academic Press, 1969.

80. Formulating for Controlled Release with Methocel Premium cellulose ethers: Dow Chemical Company, 1987.

81. Windover FE. Alkyl and Hydroxyalkylcellulose Derivatives. In: Davidson RL, Sittig M, eds. Water-Soluble Resins. New York: Reinhold Publishing Corporation, 1962: 52-68.

82. Carbopol: Bioadhesion: B.F. Goodrich Specialty Chemicals, 1995.

83. Carbopol: Toxicity of the Carbopol® Resins as a Class: B.F. Goodrich Specialty Chemicals, 1995.

84. Carbomer 934P. The United States Pharmacopeia. The National Formulary. Rockville, MD: United States Pharmacopeial Convention, Inc., 1994: 2226.

85. Danhof IE. Pharmacology, toxicology, clinical efficacy, and adverse effects of calcium polycarbophil, an enteral hydrosorptive agent. *Pharmacotherapy* 1982;**2**(1):18-28.

86. Rutledge ML, Willner MM, King JT. Calcium polycarbophil in acute childhood diarrhea. *Clinical Pediatrics* 1963;**2**(2):61-63.

87. Carbopol 971P NF for Pharmaceutical Applications: B.F. Goodrich Specialty Chemicals, 1994.

88. Lehr C-M, Bouwstra JA, Kok W, et al. Effects of the mucoadhesive polymer polycarbophil on the intestinal absorption of a peptide drug in the rat. *Journal of Pharmacy and Pharmacology* 1992;**44**:402-407.

89. Lueben HL, Lehr C-M, Rentel C-O, et al. Bioadhesive polymers for the peroral delivery of peptide drugs. *Journal of Conrolled Release* 1994;**29**:329-338.

90. Carbomer. In: Reynolds JEF, ed. Martindale. The Extra Pharmacopoeia. 29th ed. London: Pharmaceutical Press, 1989: 1433.

91. Noveon AA1 Polycarbophil: B.F. Goodrich Specialty Chemicals, 1991.

92. Carbopol® 971P NF Resin, Carbopol® 974P NF Resin: B.F. Goodrich Specialty Chemicals, 1994.

93. Roth JLA. Effect of polycarbophil as enteral hydrosorbent in diarrhea. *American Journal of Digestive Diseases* 1960;**5**(1):965-971.

94. Pimparker BD, Paustian FF, Roth JLA, Bockus HL. Effect of polycarbophil on diarrhea and constipation. *Gastroenterology* 1961;**41**:297-404.

95. Carbopol Resins, Noveon Polycarbophil, Pemulen Polymeric Emulsifiers, The Proven Polymers in Pharmaceuticals: B.F. Goodrich Specialty Chemicals, 1994.

96. Jimenez-Castellanos MR, Zia H, Rhodes CT. Mucoadhesive drug delivery systems. *Drug Development and Industrial Pharmacy* 1993;**19**(1 & 2):143-194.

97. Irons BK, Robinson JR. Bioadhesives in Drug Delivery. In: Pizzi A, Mittal KD, eds. Handbook of Adhesive Technology. New York: Marcel Dekker, Inc., 1994: 615-627.

98. Park H, Robinson JR. Mechanisms of mucoadhesion of poly(acrylic acid) hydrogels. *Pharmaceutical Research* 1987;**4**(6):457-464.

99. Polymers for Pharmaceutical Applications: B.F. Goodrich Specialty Chemicals.

100. Leung S-HS, Irons BK, Robinson JR. Polyanionic hydrogel as a gastric retentive system. *Journal of Biomaterials Science, Polymer Edition* 1993;**4**(5):483-492.

101. Testa B, Etter J-C. Apport de la rheologie l'eude des interactions entre les macromolecules de Carbopol® ainsi qu'a la determination semi-quantitative de la force ioinque de leurs dispersions. *Pharmaceutica Acta Helvetiae* 1973;**48**(6):378-388.

102. Woodard G, ed. Principles in Drug Administration. New York, NY: Academic Press, 1965.

103. Smyth RD, Danekar KA, Lee FH, DeLong AF, Polk A. Use of the Dog in Bioavailability and Bioequivalence Testing. In: Crouthamel W, Sarapu AC, eds. Animal Models for Oral Drug Delivery in Man: In Situ and In Vivo Approaches. Washington, D.C.: American Pharmaceutical Association, 1983: 125-148.

104. Purich ED, Hunt JP. The Use of Animal Models in New Drug Evaluation. In: Crouthamel W, Sarapu AC, eds. Animal Models for Oral Drug Delivery in Man: In Situ and In Vivo Approaches. Washington, D.C.: American Pharmaceutical Association, 1983: 162-177.

105. Crouthamel W, Bekersky I. Preclinical Evaluation of New Drug Candidates and Drug Delivery Systems in the Dog. In: Crouthamel W, Sarapu AC, eds. Animal Models for Oral Drug Delivery in Man: In Situ and In Vivo Approaches. Washington, D.C: American Pharmaceutical Association, 1983: 107-123.

106. Evans HE. Miller's Anatomy of the Dog. third ed. Philadelphia: W.B. Saunders Company, 1993.

107. Williams PL, Warwick R, Dyson M, Bannister LH, eds. Gray's Anatomy. thirty-seventh ed. London: Churchill Livingstone, 1989.

108. Schummer A, Nickel R, Sack WO. The Viscera of the Domestic Mammals. second revised ed. New York: Springer-Verlag, 1979.

109. Bradley OC, revised by Grahame T. Topographical Anatomy of the Dog. Sixth ed. New York: The Macmillan Company, 1959.

110. Wolvekamp WTC. Enteroclysis. A new radiographic technique for evaluation of the small intestine of the dog. Ames,IA: Iowa State University Press, 1989.

111. Bone JF. Animal Anatomy and Physiology. Third ed. Englewood Cliffs, New Jersey: A Reston Book, Prentice Hall, 1988.

112. Dressman JB, Yamada K. Animal Models for Oral Drug Absorption. In: Welling PG, Tse FLS, Dighe SV, eds. Pharmaceutical Bioequivalence. New York: Marcel Dekker Inc, 1991: 235-266.

113. Breazile JE. The Lower Alimentary Tract. In: Breazile JE, ed. Textbook of Veterinary Physiology. Philadelphia: Lea & Febiger, 1971: 395-412.

114. Ogata H, Aoyagi N, Kaniwa N, et al. Development and evaluation of a new peroral test agent GA-Test for assessment of gastric acidity. *Journal of Pharmacobio-Dynamics* 1984;**7**:656-664.

115. Borgstrom A, Dahlquist A, Lundh G, Sjovall J. Studies of intestinal digestion and absorption in the human. *Journal of Clinical Investigation* 1957;**36**:1521-1536.

116. Rhodes J, Prestwich CJ. Acidity at different sites in the proximal duodenum of normal subjects and patients with duodenal ulcer. *Gut* 1966;**7**:509-594.

117. Rovelstad RA, Maher FT. Problems associated with assessment of effects of diet, antacids, and anticholinergic agents on gastric and duodenal acidity, as measured by the glass electrode *in situ*. *Gastroenterology* 1962;**42**:588-591.

118. Russell TL, Berardi RR. Upper gastrointestinal pH in seventy-nine healthy, elderly, North American men and women. *Pharmaceutical Research* 1993;**10**(2):187-196.

119. Lui C Y,, Amidon GL, Berardi RR, Fleisher D, Youngberg C, Dressman JB. Comparison of gastrointestinal pH in dogs and humans: implications on the use of the beagle dog as a model for oral absorption in humans. *Journal of Pharmaceutical Sciences* 1986;**75**(3):271-4.

120. Dressman JB. Comparison of canine and human gastrointestinal physiology. *Pharmaceutical Research* 1986;**3**(3):123-131.

121. Youngberg CA, Wlodyga J, Schmaltz S, Dressman JB. Radiotelemteric determination of gastrointestinal pH in four healthy Beagles. *American Journal of Veterinary Research* 1985;**46**(7):1516-1521.

122. Bueno L, Fioramonti J, Ruckebusch Y. Gastric pH changes associated with duodenal motility in fasted dogs. *Journal of Physiology* 1981;**316**:319-325.

123. Ovesen L, Bendtsen F, Tage-Jensen U, Pedersen NT, Gram BR, Rune SJ. Intraluminal pH in the stomach, duodenum and proximal jejunum in

normal subjects and patients with exocrine pancreatic insufficiency. *Gastroenterology* 1986;**90**(4):958-962.

124. Davies B, Morris T. Physiological parameters in laboratory animal and humans. *Pharmaceutical Research* 1993;**10**(7):1093-1095.

125. Dressman JB, Amidon GL. Radiotelemetric method for evaluating enteric coatings. *Journal of Pharmaceutical Sciences* 1984;**73**(7):935-938.

126. Benn A, Cooke WT. Intraluminal pH of duodenum and jejunum in fasting subjects with normal and abnormal gastric or pancreatic function. *Scandinavian Journal of Gastroenterology* 1971;**6**:313-317.

127. Brooks AM, Grossman MI. Postprandial pH and neutralizing capacity of the proximal duodenum in dogs. *Gastroenterology* 1970;**59**:85-89.

128. Maxwell JD, Ferguson A, Watson WC. The effect of gastric secretory status on jejunal pH measured by radiotelemetering. *Dugestion* 1971;**4**:345-352.

129. Malagelada JR, Longstreth GF, Summerskill HJ, Go VLW. Measurement of gastric functions during digestion of ordinary solid meals in man. *Gastroenterology* 1976;**70**:203-210.

130. Ehrhardt L, Hartmann V, Patt L. *Deutsche Apotheker-Zeitung* 1972;**112**:2005.

131. Ehrlein HJ, Prove J. Effect of viscosity of test meals on gastric emptying in dogs. *Quarterly Journal of Experimental Physiology* 1982;**67**(3):419-425.

132. Code CF, Marlett JM. The interdigestive myo-electric complex of the stomach and small bowel of dogs. *Journal of Physiology, London* 1975;**246**:289-309.

133. Szurszewski JH. A migrating electric complex of the canine small intestine. *American Journal of Physiology* 1969;**217**:1757-1763.

134. Kerlin P, Zinmeister A, Phillips S. Relationship of motility to flow of contents in the human small intestine. *Gastroenterology* 1982;**82**:701-706.

135. Kerlin P, Phillips S. Differential transit of liquids and solid residue through the human ileum. *American Journal of Physiology* 1983;**245**:G38-G43.

136. Scratcherd T, Grundy D. The physiology of intestinal motility and secretion. *British Journal of Anaesthesiology* 1984;**56**:3-18.

137. Gleysteen JJ, Sarna SK, Myrvik AL. Canine cyclic motor activity of stomach and small bowel: The vagus is not the governor. *Gastroenterology* 1985;**88**:1926-1932.

138. Liaw J. Bioavailability Studies of Theo-Dur Tablets in the Fasted Cannulated Dog. Master of Science: University of Wisconsin-Madison, 1988.

139. Russell J, Bass P. Canine gastric emptying of polycarbophil: a indigestible particulate substance. *Gastroenterolgy* 1985;**89**:307-312.

140. Sarna SK. Cyclic motor activity: Migrating motor complex. *Gastroenterology* 1985;**89**:894-913.

141. Sarna SK, Gleysteen JJ, Lang IM. Is gastric cyclic motor activity a migrating motor complex? *Gastroenterology* 1985;**88**:1570.

142. Gupta PK. Processing of Liquids and Solids by the Fasted Canine Stomach. Doctor of Philosophy: University of Wisconsin-Madison, 1990.

143. Weisbrodt NW, Wiley JN, Overholt BF, Bass PA. A relation between gastroduodenal muscle contractions and gastric emptying. *Gut* 1969;**10**:543-548.

144. Rees WDW, Go VLW, Malagelada J-R. Simultaneous meaurement of antroduodenal motility, gastric emptying and duodenogastric reflux in man. *Gut* 1979;**20**:963-970.

145. Teeter BC, Bass P. Gastric emptying of liquid test meals of various temperatures in the dog. *Proceedings of the Society for Experimental Biology and Medicine* 1982;**169**:527-531.

146. Schmid H-R, Ehrlein H-J. Effects of enteral infusion of hypertonic saline and nutrients on canine jejunal motor patterns. *Digestive Diseases and Sciences* 1993;**38**(6):1062-1072.

147. Brener W, Hendrix TR, McHugh PR. Regulation of the gastric emptying of glucose. *Gastroenterology* 1983;**85**:76-82.

148. Stephens JR, Woolson RF, Cooke AR. Effects of essential and non-essential amino acids on gastric emptying in the dog. *Gastroenterology* 1975;**69**(4):920-927.

149. Moore JG, Christian PE, Brown JA, et al. Influence of age on gastric emptying of liquid-solid meals in man. *Digestive Diseases and Sciences* 1984;**29**:513-519.

150. Meyer JH, MacGregor MB, Gueller R, Martin P, Cavalieri R. 99mTc-tagged chicken liver as a marker of food in human stomach. *Digestive Diseases and Sciences* 1976;**21**(4):296-304.

151. Meyer JH, Dressman JB, Fink A, Amidon GL. Effect of size and density on canine gastric emptying of non-digestible solids. *Gastroenterology* 1985;**89**:805-813.

152. Hinder RA, Kelly KA. Canine gastric emptying of solids and liquids. *American Journal of Physiology* 1977;**233**:E335-E340.

153. Brown S, Moore J, Christian P, et al. Influence of meal weight and caloric content on gastric emptying of meals in man. *Gastroenterology* 1982;**82**:1026.

154. Holt S, Reid J, Taylor TV, Tothill P, Heading RC. Gastric emptying of solids in man. *Gut* 1982;**23**:292-296.

155. Meyer JH, Oshashi H, Jejn D, Thomson JB. Size of liver particles emptied from the human stomach. *Gastroenterology* 1981;**80**:1489-1496.

156. Meyer JH, Thomson JB, Cohen MB, Shadchehr A, Mandiola SA. Sieving of solid food by the canine stomach and sieving after gastric surgery. *Gastroenterology* 1979;**76**:804-813.

157. Meyer HH, Gu Y, Elashoff J, Reedy T, Dressman J, Amidon G. Effects of viscosity and fluid outflow on postcibal gastric emptying of solids. *American Journal of Physiology* 1986;**250**:G161-G164.

158. Mroz CT, Kelly KA. The role of the extrinsic antral nerves in the regulation of gastric emptying. *Surgery, Gynecology and Obstetrics* 1977;**145**:369-377.

159. Weisbrodt NW. Motility of the small intestine. In: Johnson LR, ed. Physiology of the Gastrintestinal Tract. second ed. New York: Raven Press, 1987: 631-663.

160. Sugito K, Ogata H, Goto H, et al. Gastrointestinal transit on non-distingrating solid formulations in humans. *International Journal of Pharmaceutics* 1990;**60**:89-97.

161. Christensen FN, Davis SS, Hardy JG, Taylor MJ, Whalley DR, Wilson CG. The use of gamma scintigraphy to follow the gastrointestinal transit of pharmaceutical formulations. *Journal of Pharmacy and Pharmacology* 1985;**37**(2):91-95.

162. Buffer Solutions. In: Sober HA, ed. Handbook of Biochemistry. Cleveland: The Chemical Rubber Co., 1970: J234-J237.

163. Gastric fluid, simulated TS. The United States Pharmacopeia. The National Formulary. Rockville,MD: United States Pharmacopeial Convention, Inc., 1994: 2053.

164. Intestinal fluid, simulated TS. The United States Pharmacopeia. The National Formulary. Rockville, MD: United States Pharmacopeial Convention, Inc., 1994: 2053.

165. Kaus LC, Fell JT, Sharma H, Taylor DC. On the intestinal transit of a single non-disintegrating object. *International Journal of Pharmaceutics* 1984;**20**:315-323.

166. Lennernas H, Ahrenstedt O, Ungell A-L. Intestinal drug absorption during induced net water absorption in man; a mechanistic study using antipyrine, atenolol and enalaprilat. *British Journal of Clinical Pharmacology* 1994;**37**:589-596.

167. Lennarnas H. Regional jejunal perfusion. A new approach to study oral drug absorption in man. *Pharmaceutical Research* 1992;**9**:1243-1251.

168. Thomas JE. An improved cannula for gastric and intestinal fistula. *Proceedings of the Society of Experimental Biology and Medicine* 1941;**46**:260-261.

169. Rubinstein A, Li VHK, Gruber P, Bass P, Robinson JR. Improved intestinal cannula for drug delivery studies in the dog. *Journal of Pharmacological Methods* 1988;**19**:213-217.

170. Li VHK. Gastric Emptying of Nondigestible Solids in the Fasted Dog. Doctor of Philosophy: Univeristy of Wisconsin, 1987.

171. Hunt JN. Regulation of gastric emptying. In: Code CF, ed^eds. Handbook of Physiology. Washington, D.C.: American Physiology Society, 1968: 1917-1937.

172. Atropine sulfate. In: McEvoy GK, ed. AHFS Drug Information. Bethesda, MD: American Society of Hospital Pharmacists, Inc., 1991: 653-656 and 1664-1665.

173. Lee KY, Shiratori K, Chen YF, Ta-Min C, Chey WY. A hormonal mechanism for the interdigestive pancreatic secretion in dogs. *American Journal of Physiology* 1986;**14**:G759-G764.

174. Konturek SJ, Thor P, Bilski J, Tasler J, Cieszkowski M. Cephalic phase of gastroduodenal alkaline secretion. *Scandanavian Journal of Gastroenterology* 1986;**21 (Suppl 125)**:100-105.

175. Konturek SJ, Thor P. Relation between duodenal alkaline secretion and motility in fasted and sham fed dogs. *American Journal of Physiology* 1986;**251**(5 Pt 1):G591-G506.

176. Pendleton RG, Bendesky RJ, Cook PG. Effects of Atropine upon various components mediating postprandial gastric acid secretions in dogs. *Journal of Pharmacology and Experimental Methods* 1987;**240**(2):396-399.

177. Beglinger C, Haecki W, Gyr K, Stalder GA. The release of pancreatic polypeptide by intraduodenal 1-phenylalanine in the dog. *Hepato-Gastroenterolgy* 1981;**28**(2):116-117.

178. Fox JET, Daniel EE, Jury J, Track NS, Chiu S. Cholinergic control mechanisms for immunoreactive motilin release and motility in the canine duodenum. *Canadian Journal of Physiology and Pharmacology* 1983;**61**:1042-1049.

179. Kayasseh L, Haecki WH, Gyr K, et al. The endogenous release of pancreatic polypeptide by acid and meal in dogs. Effect of somatostatin. *Scandinavian Journal of Gastroenterolgy* 1978;**13**(4):385-391.

180. Drug information sheet for Atropine sulfate injection: Eli Lilly and Company, 1992.

181. Litt M. Comparative studies of mucus and mucin physicochemisty. In: Jonathan N, O'Connor M, eds. Mucus and mucosa. Ciba Foundation symposium 109. London: Pittman, 1984: 196-211.

182. Allen A. Mucus-a protective secretion of complexity. *Trends in Biochemical Sciences* 1983;**8**(5):169-173.

183. Verdugo P. Hydration kinetic of exocytosed mucins in cultured secretory cells of the rabbit trachea: a new model. In: Jonathan N, O'Connor M, ed. Mucus and mucosa. Ciba Foundation symposium 109. London: Pittman, 1984: 212-225.

184. Creeth JM. Constituents of mucus and their separation. *British Medical Bulletin* 1982;**34**:17-24.

185. Chu KU, Tsuchiya T, Ishizuka J, Uchida T, Townsend Jr. CM, Thompson JC. Tropic response of gut and pancreas after ileojejunal transposition. *Annals of Surgery* 1995;**221**(3):249-256.

186. Rubinstein A, Tirosh B. Mucus gel thickness and turnover in the gastrointestinal tract of the rat: Response to cholinergic stimulus and implication for mucoadhesion. *Pharmaceutical Research* 1994;**11**(6):794-799.

187. Altmann CG, LeBlond CP. Factors influencing villus size in the small intestine of adult rats as revealed by transposition of intestinal segments. *American Journal of Anatomy* 1970;**127**:15-36.

188. Clarke RM. Mucosal architecture and epithelial cell production rate in the small intestine of the albino rat. *Journal of Anatomy* 1970;**107**:519-529.

189. Wolf S. The psyche and the stomach. A historical vignette. *Gastroenterology* 1981;**80**(3):605-614.

190. Wolf S. Effects of suggestion and conditioning on the action of chemical agents in human subjects-The pharmacology of placebos. *Journal of Clinical Investigation* 1950;**20**:100-109.

191. Wolf S, Wolff HG. Human Gastric Function. An Experimental Study of a Man and His Stomach. second ed. New York: Oxford University Press, 1947.

192. Bogen DK. Simulation software for the Macintosh. *Science* 1989;**246**:138-142.

193. Mikulecky DC. Modelling intestinal absorption and other nutrition related processes using PSPICE and STELLA. *Journal of Pediatric Gastroenterology and Nutrition* 1990;**11**:7-20.

194. Ramsey MW, Grass GM, Vallner JJ. Pharmacokinetic simulations using STELLA®: Prediction of in vivo performance of oral dosage forms. *European Journal of Pharmaceutics and Biopharmaceutics* 1991;**37**:192-197.

195. Washington C, Washington N, Wilson C. Pharmacokinetic Modelling using STELLA on the Apple™ Macintosh™. Chichester, West Essex, England: Ellis Horwood Limited, 1990.

196. Itoh Z, Honda R, Hiwatashi K. Biphasic secretory response of exocrine pancreas to feeding. *American Journal of Physiology* 1980;**238**:G332-G337.

197. Dillard RL, Eastman H, Fordtran JS. Volume-flow relationship during the transport of fluid through the human small intestine. *Gastroenterology* 1965;**49**:58-66.

198. Kerlin P, Phillips S. Variability of motility of the ileum and jejeunum in healthy man. *Gastroenterology* 1982;**82**:694-700.

199. Davenport HW. Mechanisms of Gastric and Pancreatic Secretion. In: Frohlich ED, ed. Pathophysiology. Philadelphia: J.B. Lippicott, Co., 1972: 407-422.

200. Davenport HW. A Digest of Digestion. Chicago: Year Book Medical Publishers, Inc., 1975.

201. Davenport HW. Physiology of the Digestive Tract. Fourth ed. Chicago: Year Book Medical Publishers, Inc., 1977.

202. Fordtran JS, Rector Jr. FC, Ewton MF, Soter N, Dinney J. Permeability characteristics of the human small intestine. *Journal of Clinical Investigation* 1965;**44**(12):1935-1944.

203. Price JM, Davis SS, Sparrow RA, Wilding IR. The effect of meal composition on the gastrocolonic response: Implications for drug delivery to the colon. *Pharmaceutical Research* 1993;**10**(5):722-726.

204. Yeo CJ, Bastidas JA, Schmieg Jr. RE, Zinner MJ. Meal-stimulated absorption of water and electrolytes in canine jejunum. *American Journal of Physiology* 1990;**259**:G402-G409.

205. Granger DN, Barrowman JA, Kvietys PR. Clinical Gastrointestinal Physiology. Philadelphia: W.B.Saunders Co., 1985.

206. Sarr MG, Kelly KA, Phillips SF. Canine jejunal absorption and transit during interdigestive and digestive motor states. *American Journal of Physiology* 1980;**239**:G167-G172.

207. Coupe AJ, Davis SS, Wilding IR. Variation in gastrointestinal transit of pharmaceutical dosage forms in healthy subjects. *Pharmaceutical Research* 1991;**8**:360-364.

208. Solomon TE. Regulation of pancreatic secretion. *Clinics in Gastroenterology* 1984;**13**(3):657-678.

209. Chang EB, Rao MC. Intestinal Water and Electrolyte Transport. In: Johnson LR, ed. Physiology of the Gastrointestinal Tract. Third ed. New York: Raven Press, 1994: 2027-2081.

210. Sarr MG, Kelly KA. Patterns of movement of liquids and solids through the canine jejunum. *American Journal of Physiology* 1980;**229**:G497-G503.

211. Brooks FP. Effect of diet on gastric secretion. *American Journal of Clinical Nutrition* 1985;**42**:1006-1019.

212. Ritschel WA. Handbook of Basic Pharmacokinetics. Third ed. Hamilton, IL: Drug Intelligence Publications, Inc., 1986.

213. DeWever I, Eeckhout C, Vantrappen G, Hellemans J. How does oil disrupt the interdigestive myoelectric complex. In: Christensen J, ed. Gastrointestinal Motility. New York: Raven Press, 1980: 295-297.

214. DiMagno EP, Go VLW, Sumerskill WHJ. Relations between pancreatic enzyme outputs and malabsorption in severe pancreatic insufficiency. *New England Journal of Medicine* 1973;**288**:813-815.

215. Grass GM, Bozarth CA, Vallner JJ. Evaluation of the performance of controlled release dosage forms of Ticlopidine using in vitro intestinal permeability and computer simulations. *Journal of Drug Targeting* 1994;**2**(1):23-33.

216. Grass GM, Lee VHL. A model to predict aqueous humor and plasma pharmacokinetics of ocularly applied drugs. *Investigative Ophthalmology and Visual Science* 1993;**34**:2251-2259.

217. Shatkin JA, Brown HS. Pharmacokinetics of the dermal route of exposure to volatile organic chemicals in water: A computer simulation model. *Environmental Research* 1991;**56**:90-108.

218. Brown HS, Hattis D. The role of skin absorption as a route of exposure to volatile organic compounds in household tap water: a simulated kinetic approach. *Journal of the American College of Toxicity* 1989;**8**(5):839-851.

219. Grass GM, Morehead WT. Evidence for site specific absorption of a novel ace inhibitor. *Pharmaceutical Research* 1989;**6**(9):759-765.

220. Knuutila-Jerku M, Robinson JR, Urtti A. Model for pharmacokinetics of ocularly applied Pilocarpine. *Pharmaceutical Research* 1996;**submitted for publication**.

IX. APPENDIX : COMPUTER MODEL

The use of STELLA II™ for the simulation of pharmacokinetic studies is well established.[44,194,215-220] The program uses the input values to calculate the kinetic outcome of interest. In our studies we were interested in (1) the availability and movement of fluid through and (2) the simulated swelling history of hydrogel polymers in the gastrointestinal tract.

The following are the equations used for the stocks, flows and converters which describe the schematic representations of each of the models presented in the text. The equations are presented as they appear in the equation window of the STELLA™ program. In addition, a table pad has been included for each of the models. This table documents, as a function of time, the volume of fluid present in the specific region of the gastrointestinal tract of interest or the extent of swelling, depending upon which model is being studied.

All simulations were performed using the Euler's integration method with a time interval (dt) of 0.1 hour. The terms and units of the equation parameters are described in Table A-1.

Table A-1 : Terms and units used in the STELLA™ kinetic model

Symbols

Flows	ml/hr	
• absorption		
• dosing		
• emptying		(unless bolus/pulse then ml)
• secretion		
Volume	ml	
Time	hr	
•t half		(time to empty 1/2 of volume)
Swelling	mg/hr	(water uptake by polymer)
Pulse (X,Y,Z)	Pulse(amplitude, first time, repetition time)	
Pulse	Bolus	
amplitude	ml	

Figure A-1 : Full schematic representation of the model of fluid movement through the gastrointestinal tract of the fasted human.

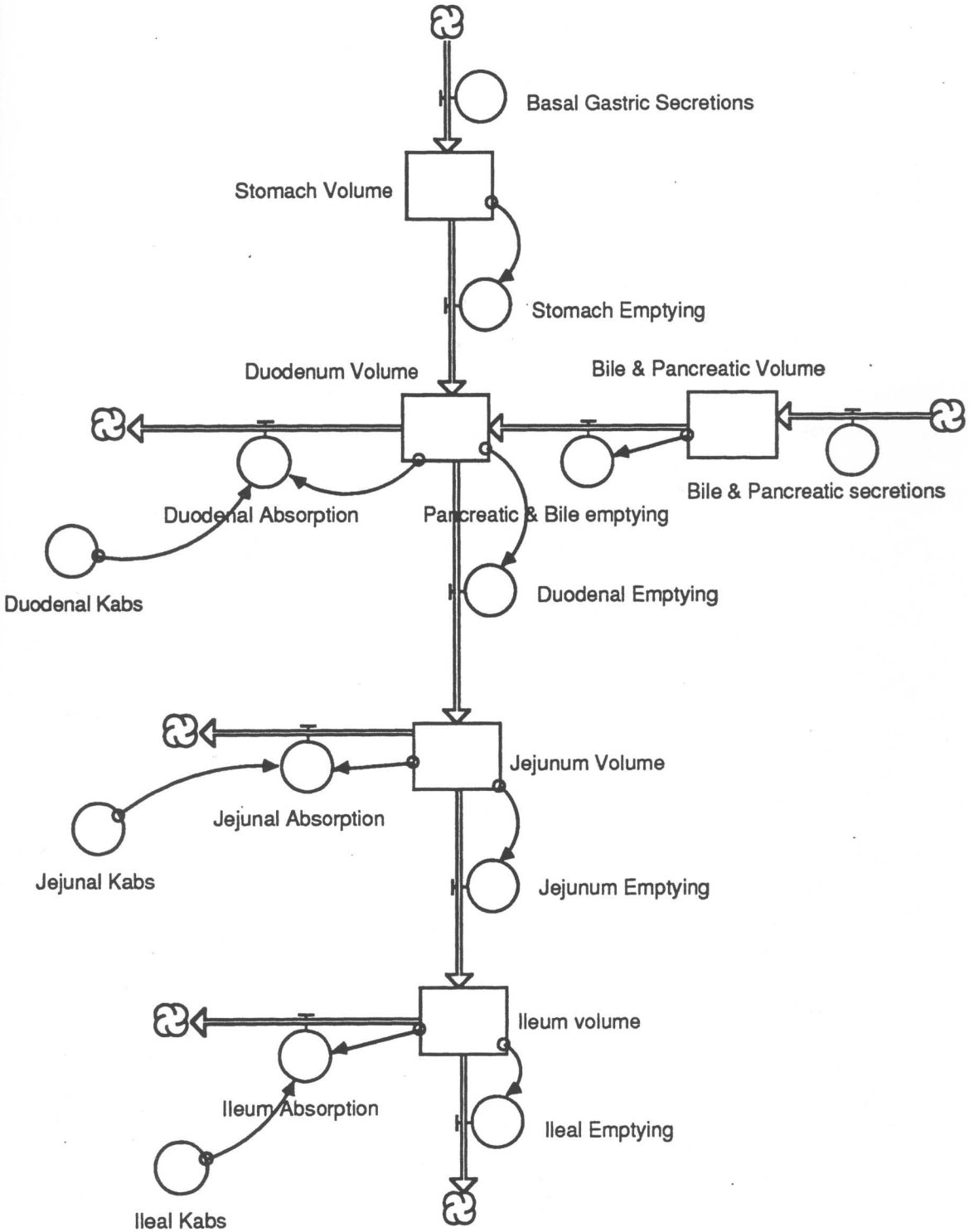
Basal Gastric Secretions
Stomach Volume
Stomach Emptying
Duodenum Volume
Bile & Pancreatic Volume
Duodenal Absorption
Pancreatic & Bile emptying
Bile & Pancreatic secretions
Duodenal Kabs
Duodenal Emptying
Jejunum Volume
Jejunal Absorption
Jejunal Kabs
Jejunum Emptying
Ileum volume
Ileum Absorption
Ileal Emptying
Ileal Kabs

Figure A-2 : Structural equations and program listing for the model of fluid movement through the gastrointestinal tract of the fasted human as printed out in the equation window of STELLA II™.

```
Bile_&_Pancreatic_Volume(t) = Bile_&_Pancreatic_Volume(t - dt) +
(Bile_&_Pancreatic_secretions - Pancreatic_&_Bile_emptying) * dt
INIT Bile_&_Pancreatic_Volume = 0

INFLOWS:
Bile_&_Pancreatic_secretions = 15

OUTFLOWS:
Pancreatic_&_Bile_emptying =
Pulse(Bile_&_Pancreatic_Volume,1.4,1.5)
Duodenum_Volume(t) = Duodenum_Volume(t - dt) +
(Stomach_Emptying + Pancreatic_&_Bile_emptying -
Duodenal_Absorption - Duodenal_Emptying) * dt
INIT Duodenum_Volume = 0

INFLOWS:
Stomach_Emptying = Pulse(Stomach_Volume,1.5,1.5)
Pancreatic_&_Bile_emptying =
Pulse(Bile_&_Pancreatic_Volume,1.4,1.5)

OUTFLOWS:
Duodenal_Absorption = If (Duodenum_Volume>0) then Duodenal_Kabs
else 0
Duodenal_Emptying = If Duodenum_Volume>0 then 120 else 0
Ileum_volume(t) = Ileum_volume(t - dt) + (Jejunum_Emptying -
Ileum_Absorption - Ileal_Emptying) * dt
INIT Ileum_volume = 0

INFLOWS:
Jejunum_Emptying = If (Jejunum_Volume>0) then 120 else 0
OUTFLOWS:
Ileum_Absorption = IF(Ileum_volume > 0) THEN (Ileal_Kabs) ELSE(0)
Ileal_Emptying = IF(Ileum_volume>0) THEN(120) else 0
Jejunum_Volume(t) = Jejunum_Volume(t - dt) + (Duodenal_Emptying -
Jejunal_Absorption - Jejunum_Emptying) * dt
INIT Jejunum_Volume = 0

INFLOWS:
Duodenal_Emptying = If Duodenum_Volume>0 then 120 else 0
OUTFLOWS:
```

```
Jejunal_Absorption = If (Jejunum_Volume>0) then (Jejunal_Kabs)
else 0
Jejunum_Emptying = If (Jejunum_Volume>0) then 120 else 0
Stomach_Volume(t) = Stomach_Volume(t - dt) +
(Basal_Gastric_Secretions - Stomach_Emptying) * dt
INIT Stomach_Volume = 0

INFLOWS:
Basal_Gastric_Secretions = 40
OUTFLOWS:
Stomach_Emptying = Pulse(Stomach_Volume,1.5,1.5)
Duodenal_Kabs = 25
Ileal_Kabs = 270
Jejunal_Kabs = 360
```

Figure A-3 : Time course of fluid volume movement and distribution through the stomach, duodenum, jejunum and ileum in the fasted human.

Time/hr	Gastric Volume	Duodenum Volume	Jejunum Volume	Ileum Volume
0	0.00	0.00	0.00	0.00
0.1	4.00	0.00	0.00	0.00
0.2	8.00	0.00	0.00	0.00
0.3	12.00	0.00	0.00	0.00
0.4	16.00	0.00	0.00	0.00
0.5	20.00	0.00	0.00	0.00
0.6	24.00	0.00	0.00	0.00
0.7	28.00	0.00	0.00	0.00
0.8	32.00	0.00	0.00	0.00
0.9	36.00	0.00	0.00	0.00
1	40.00	0.00	0.00	0.00
1.1	44.00	0.00	0.00	0.00
1.2	48.00	0.00	0.00	0.00
1.3	52.00	0.00	0.00	0.00
1.4	56.00	0.00	0.00	0.00
1.5	60.00	21.00	0.00	0.00
1.6	4.00	66.50	12.00	0.00
1.7	8.00	52.00	0.00	0.00
1.8	12.00	37.50	12.00	0.00
1.9	16.00	23.00	0.00	0.00
2	20.00	8.50	12.00	0.00
2.1	24.00	0.00	0.00	0.00
2.2	28.00	0.00	0.00	0.00
2.3	32.00	0.00	0.00	0.00
2.4	36.00	0.00	0.00	0.00
2.5	40.00	0.00	0.00	0.00
2.6	44.00	0.00	0.00	0.00
2.7	48.00	0.00	0.00	0.00
2.8	52.00	0.00	0.00	0.00
2.9	56.00	0.00	0.00	0.00
3	60.00	22.50	0.00	0.00
3.1	4.00	68.00	12.00	0.00
3.2	8.00	53.50	0.00	0.00
3.3	12.00	39.00	12.00	0.00
3.4	16.00	24.50	0.00	0.00
3.5	20.00	10.00	12.00	0.00
3.6	24.00	0.00	0.00	0.00
3.7	28.00	0.00	0.00	0.00
3.8	32.00	0.00	0.00	0.00
3.9	36.00	0.00	0.00	0.00
4	40.00	0.00	0.00	0.00
4.1	44.00	0.00	0.00	0.00
4.2	48.00	0.00	0.00	0.00

4.3	52.00	0.00	0.00	0.00
4.4	56.00	0.00	0.00	0.00
4.5	60.00	22.50	0.00	0.00
4.6	4.00	68.00	12.00	0.00
4.7	8.00	53.50	0.00	0.00
4.8	12.00	39.00	12.00	0.00
4.9	16.00	24.50	0.00	0.00
Final	20.00	10.00	12.00	0.00

Figure A-4 : Full schematic representation of the model of fluid movement of an orally administered 300 ml water bolus through the gastrointestinal tract of the originally fasted human.

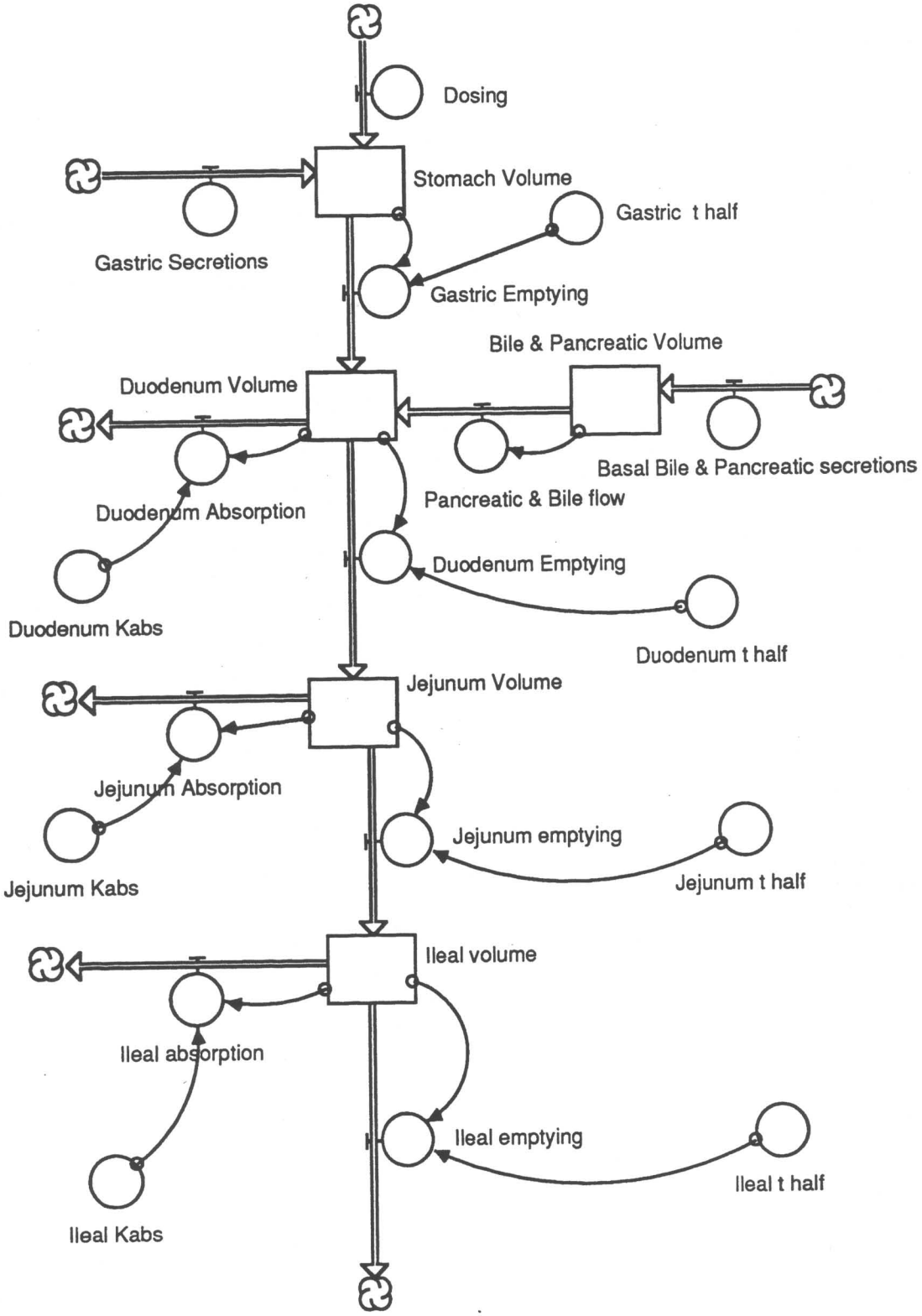
Dosing
Stomach Volume
Gastric t half
Gastric Secretions
Gastric Emptying
Bile & Pancreatic Volume
Duodenum Volume
Basal Bile & Pancreatic secretions
Duodenum Absorption
Pancreatic & Bile flow
Duodenum Emptying
Duodenum Kabs
Duodenum t half
Jejunum Volume
Jejunum Absorption
Jejunum emptying
Jejunum Kabs
Jejunum t half
Ileal volume
Ileal absorption
Ileal emptying
Ileal t half
Ileal Kabs

Figure A-5 : Structural equations and program listing for the model of fluid movement of an orally administered 300 ml water bolus through the gastrointestinal tract of the originally fasted human as printed out in the equation window of STELLA II™.

```
Bile_Pancreatic_Vol(t) = Bile_Pancreatic_Vol(t - dt) +
(Basal_BP_secretions - PancBile) * dt
INIT Bile_Pancreatic_Vol = 30

INFLOWS:
Basal_BP_secretions = 15

OUTFLOWS:
PancBile = PULSE(Bile_Pancreatic_Vol, 1.4, 1.5)
Duodenum_Vol(t) = Duodenum_Vol(t - dt) + (Gastric_Emptying +
PancBile - Duo_Absorption - Duodenum_Emptying) * dt
INIT Duodenum_Vol = 0

INFLOWS:
Gastric_Emptying = If Stomach_Vol>0 then
(Stomach_Vol*0.693/Gastric_t12) else PULSE(Stomach_Vol, 1.5, 1.5)
PancBile = PULSE(Bile_Pancreatic_Vol, 1.4, 1.5)

OUTFLOWS:
Duo_Absorption = If (Duodenum_Vol>0) then Duo_Kabs else 0
Duodenum_Emptying = If (Duodenum_Vol>0) then
(Duodenum_Vol*0.693/Duodenum_t_half) else 0
Ileal_volume(t) = Ileal_volume(t - dt) + (Jejunum_emptying -
Ileal_absorption - Ileal_emptying) * dt
INIT Ileal_volume = 0

INFLOWS:
Jejunum_emptying = If time < 3.5 then 0 else If Jejunum_Volume > 0
then Jejunum_Volume*0.693/Jejunum_t_half else 0

OUTFLOWS:
Ileal_absorption = if Ileal_volume > 0 then Ileal_Kabs ELSE (0)
Ileal_emptying = if TIME < 4.5 then 0 else if Ileal_volume > 0 then
Ileal_volume*.693/Ileal_t_half else 0
Jejunum_Volume(t) = Jejunum_Volume(t - dt) + (Duodenum_Emptying
- Jej_Absorption - Jejunum_emptying) * dt
INIT Jejunum_Volume = 0

INFLOWS:
Duodenum_Emptying = If (Duodenum_Vol>0) then
(Duodenum_Vol*0.693/Duodenum_t_half) else 0
```

OUTFLOWS:
Jej_Absorption = If (Jejunum_Volume>0) then Jej_Kabs else 0
Jejunum_emptying = If time < 3.5 then 0 else If Jejunum_Volume > 0 then Jejunum_Volume*0.693/Jejunum_t_half else 0
Stomach_Vol(t) = Stomach_Vol(t - dt) + (Gastric_Secretions + Dosing - Gastric_Emptying) * dt
INIT Stomach_Vol = 0

INFLOWS:
Gastric_Secretions = 40
Dosing = if TIME < 1then Pulse (300,0,10000) else PULSE(40, 1.5,1.5)

OUTFLOWS:
Gastric_Emptying = If Stomach_Vol>0 then (Stomach_Vol*0.693/Gastric_t12) else PULSE(Stomach_Vol, 1.5, 1.5)
Duodenum_t_half = 0.0567
Duo_Kabs = 25
Gastric_t12 = 0.167
Ileal_Kabs = 270
Ileal_t_half = .00000716
Jejunum_t_half = .0000117
Jej_Kabs = 360

Figure A-6 : Time course of fluid volume movement and distribution of an orally administered 300 ml water bolus through the duodenum, jejunum and ileum in the originally fasted human.

Hours	Stomach Volume	Duodenum Volume	Jejunum Volume	Ileal Volume
0	0.00	0.00	0.00	0.00
0.1	304.00	0.00	0.00	0.00
0.2	181.85	126.15	0.00	0.00
0.3	110.39	44.93	154.18	0.00
0.4	68.58	33.32	173.10	0.00
0.5	44.12	18.55	177.83	0.00
0.6	29.81	11.69	164.50	0.00
0.7	21.44	7.27	142.78	0.00
0.8	16.54	4.78	115.68	0.00
0.9	13.68	3.30	85.52	0.00
1	12.00	2.44	53.56	0.00
1.1	11.02	1.94	20.54	0.00
1.2	10.45	1.64	0.00	0.00
1.3	10.11	1.47	0.00	0.00
1.4	9.92	1.37	1.80	0.00
1.5	9.80	52.31	0.00	0.00
1.6	49.73	0.00	17.88	0.00
1.7	33.10	18.14	0.00	0.00
1.8	23.36	7.20	0.00	0.00
1.9	17.67	5.59	0.00	0.00
2	14.34	3.59	6.84	0.00
2.1	12.39	2.65	0.00	0.00
2.2	11.25	2.05	0.00	0.00
2.3	10.58	1.71	0.00	0.00
2.4	10.19	1.51	2.09	0.00
2.5	9.96	1.39	0.00	0.00
2.6	9.83	1.32	1.70	0.00
2.7	9.75	1.28	0.00	0.00
2.8	9.70	1.26	1.57	0.00
2.9	9.68	1.25	0.00	0.00
3	9.66	23.74	0.00	0.00
3.1	49.65	0.00	0.00	0.00
3.2	33.05	20.60	0.00	0.00
3.3	23.33	6.64	25.18	0.00
3.4	17.65	5.71	0.00	0.00
3.5	14.33	3.56	0.00	0.00
3.6	12.38	2.65	4.35	0.00
3.7	11.24	2.05	0.00	0.00
3.8	10.58	1.71	0.00	0.00
3.9	10.19	1.51	0.00	0.00
4	9.96	1.39	0.00	0.00
4.1	9.83	1.32	0.00	0.00
4.2	9.75	1.28	0.00	0.00
4.3	9.70	1.26	0.00	0.00

4.4	9.68	1.25	1.54	0.00
4.5	9.66	23.74	0.00	0.00
4.6	49.65	0.00	25.25	0.00
4.7	33.05	18.10	0.00	0.00
4.8	23.33	7.19	0.00	0.00
4.9	17.65	5.58	0.00	0.00
Final	14.33	3.58	0.00	0.00

Figure A-7 : Full schematic representation of the model of fluid movement of orally administered Pulmocare ™ (240 ml bolus) through the gastrointestinal tract of the originally fasted human.

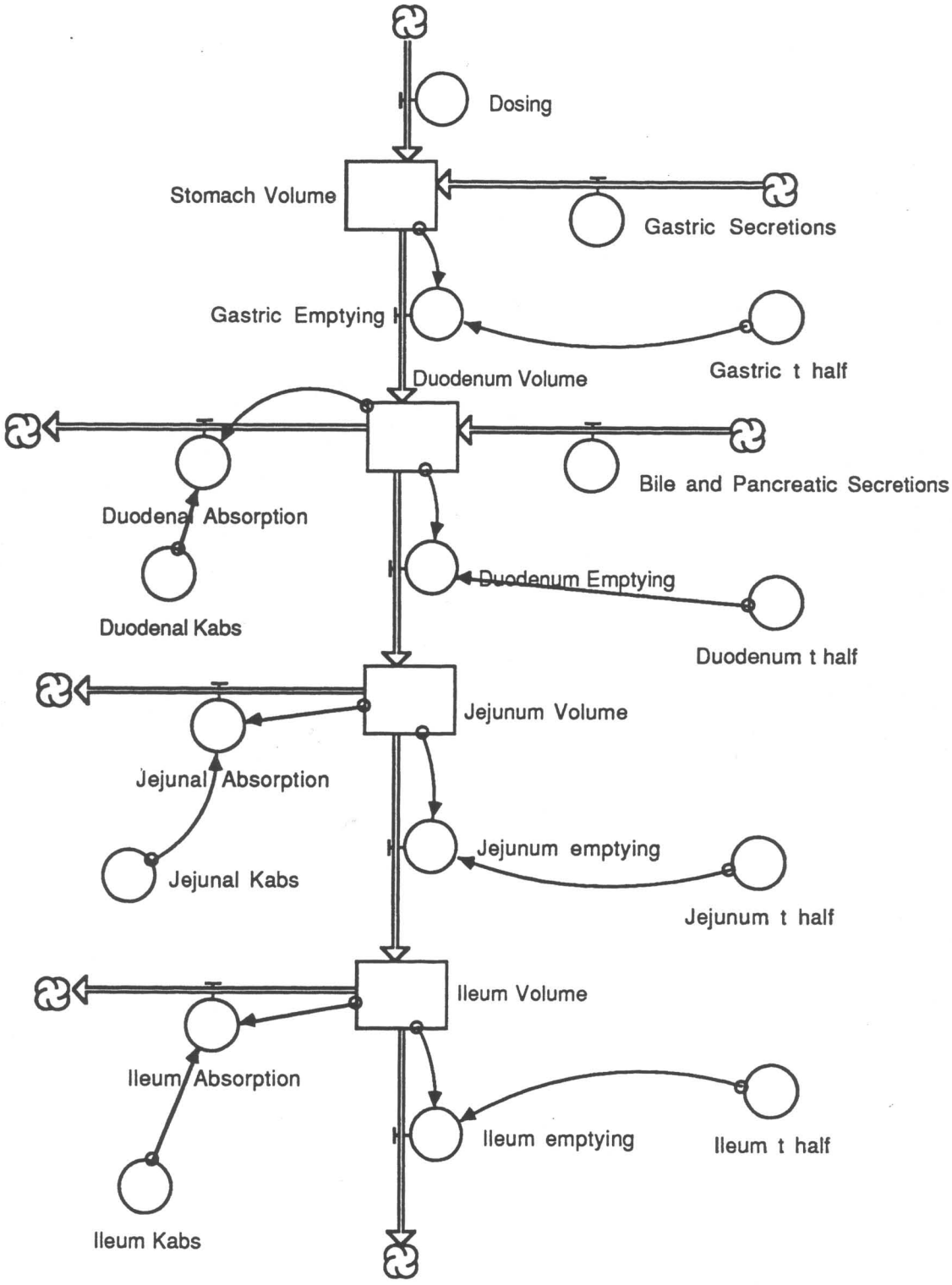
Dosing
Stomach Volume
Gastric Secretions
Gastric Emptying
Gastric t half
Duodenum Volume
Bile and Pancreatic Secretions
Duodenal Absorption
Duodenal Kabs
Duodenum Emptying
Duodenum t half
Jejunum Volume
Jejunal Absorption
Jejunal Kabs
Jejunum emptying
Jejunum t half
Ileum Volume
Ileum Absorption
Ileum Kabs
Ileum emptying
Ileum t half

Figure A-8 : Structural equations and program listing for the model of fluid movement of orally administered Pulmocare ™ (240 ml bolus) through the gastrointestinal tract of the originally fasted human as printed out in the equation window of STELLA II™.

```
Duodenum_Volume(t) = Duodenum_Volume(t - dt) + (Gastric_Emptying
+ Bile_and_Pancreatic_Secretions - Duodenal_Absorption -
Duodenum_Emptying) * dt
INIT Duodenum_Volume = 0

INFLOWS:
Gastric_Emptying = If (Stomach_Volume>0 ) then
Stomach_Volume*0.693/Gastric_t_half  else  0
Bile_and_Pancreatic_Secretions = IF(TIME < 1) THEN(45) ELSE(25)

OUTFLOWS:
Duodenal_Absorption = If (Duodenum_Volume>0) then Duodenal_Kabs
else 0
Duodenum_Emptying = If (Duodenum_Volume>0) then
Duodenum_Volume*0.693/Duodenum_t_half  else  0
Ileum_Volume(t) = Ileum_Volume(t - dt) + (Jejunum_emptying -
Ileum_Absorption - Ileum_emptying) * dt
INIT Ileum_Volume = 0

INFLOWS:
Jejunum_emptying = IF(Jejunum_Volume > 0) AND(TIME > 3.5) THEN
(Jejunum_Volume*.693/Jejunum_t_half)  ELSE  (0)

OUTFLOWS:
Ileum_Absorption = IF(Ileum_Volume > 0) then Ileum_Kabs else 0
Ileum_emptying = IF(Ileum_Volume > 0) AND(TIME > 4.5) THEN
(Ileum_Volume*.693/Ileum_t_half)  Else  0
Jejunum_Volume(t) = Jejunum_Volume(t - dt) + (Duodenum_Emptying
- Jejunal_Absorption - Jejunum_emptying) * dt
INIT Jejunum_Volume = 0

INFLOWS:
Duodenum_Emptying = If (Duodenum_Volume>0) then
Duodenum_Volume*0.693/Duodenum_t_half  else  0

OUTFLOWS:
Jejunal_Absorption = If (Jejunum_Volume>0) then Jejunal_Kabs else
0
Jejunum_emptying = IF(Jejunum_Volume > 0) AND(TIME > 3.5) THEN
(Jejunum_Volume*.693/Jejunum_t_half)  ELSE  (0)
```

```
Stomach_Volume(t) = Stomach_Volume(t - dt) + (Dosing +
Gastric_Secretions - Gastric_Emptying) * dt
INIT Stomach_Volume = 0

INFLOWS:
Dosing = Pulse (240,0,10000)
Gastric_Secretions = IF(TIME < 1) then 50 else 30

OUTFLOWS:
Gastric_Emptying = If (Stomach_Volume>0 ) then
Stomach_Volume*0.693/Gastric_t_half  else  0
Duodenal_Kabs = 0
Duodenum_t_half = .25
Gastric_t_half = .4
Ileum_Kabs = 270
Ileum_t_half = .00000716
Jejunal_Kabs = 360
Jejunum_t_half = .0000117
```

Figure A-9: Time course of fluid volume movement and distribution of orally administered Pulmocare ™ (240 ml bolus) through the duodenum, jejunum and ileum in the originally fasted human.

Time/hr	Stomach Volume	Duodenum Volume	Jejunum Volume	Ileum Volume
0	0.00	0.00	0.00	0.00
0.1	245.00	4.50	0.00	0.00
0.2	207.55	50.20	1.25	0.00
0.3	176.60	76.74	0.00	0.00
0.4	151.00	90.56	0.00	0.00
0.5	129.84	96.12	0.00	0.00
0.6	112.34	96.47	0.00	0.00
0.7	97.88	93.69	0.00	0.00
0.8	85.92	89.18	0.00	0.00
0.9	76.04	83.84	0.00	0.00
1	67.86	78.28	0.00	0.00
1.1	61.11	72.84	0.00	0.00
1.2	53.52	65.73	0.00	0.00
1.3	47.25	59.28	0.00	0.00
1.4	42.06	53.54	0.00	0.00
1.5	37.77	48.48	0.00	0.00
1.6	34.23	44.09	0.00	0.00
1.7	31.30	40.30	0.00	0.00
1.8	28.88	37.05	11.17	0.00
1.9	26.87	34.28	0.00	0.00
2	25.22	31.94	9.50	0.00
2.1	23.85	29.95	0.00	0.00
2.2	22.72	28.28	8.30	0.00
2.3	21.78	26.88	0.00	0.00
2.4	21.01	25.70	7.45	0.00
2.5	20.37	24.72	0.00	0.00
2.6	19.84	23.89	6.85	0.00
2.7	19.40	23.21	0.00	0.00
2.8	19.04	22.64	6.43	0.00
2.9	18.74	22.16	0.00	0.00
3	18.49	21.76	6.14	0.00
3.1	18.29	21.44	0.00	0.00
3.2	18.12	21.16	5.94	0.00
3.3	17.98	20.94	0.00	0.00
3.4	17.87	20.75	5.80	0.00
3.5	17.77	20.59	0.00	0.00
3.6	17.69	20.46	5.71	0.00
3.7	17.63	20.36	0.00	11.38
3.8	17.57	20.27	5.64	0.00
3.9	17.53	20.19	0.00	0.00
4	17.49	20.13	0.00	0.00
4.1	17.46	20.08	0.00	0.00
4.2	17.44	20.04	0.00	0.00
4.3	17.42	20.01	5.56	0.00

4.4	17.40	19.98	0.00	11.10
4.5	17.38	19.95	0.00	0.00
4.6	17.37	19.93	5.53	0.00
4.7	17.36	19.92	0.00	11.06
4.8	17.35	19.91	5.52	0.00
4.9	17.35	19.89	0.00	11.04
Final	17.34	19.88	5.51	0.00

Figure A-10 : Full schematic representation of the model of polymer swelling as it moves through the gastrointestinal tract of a fasted human.

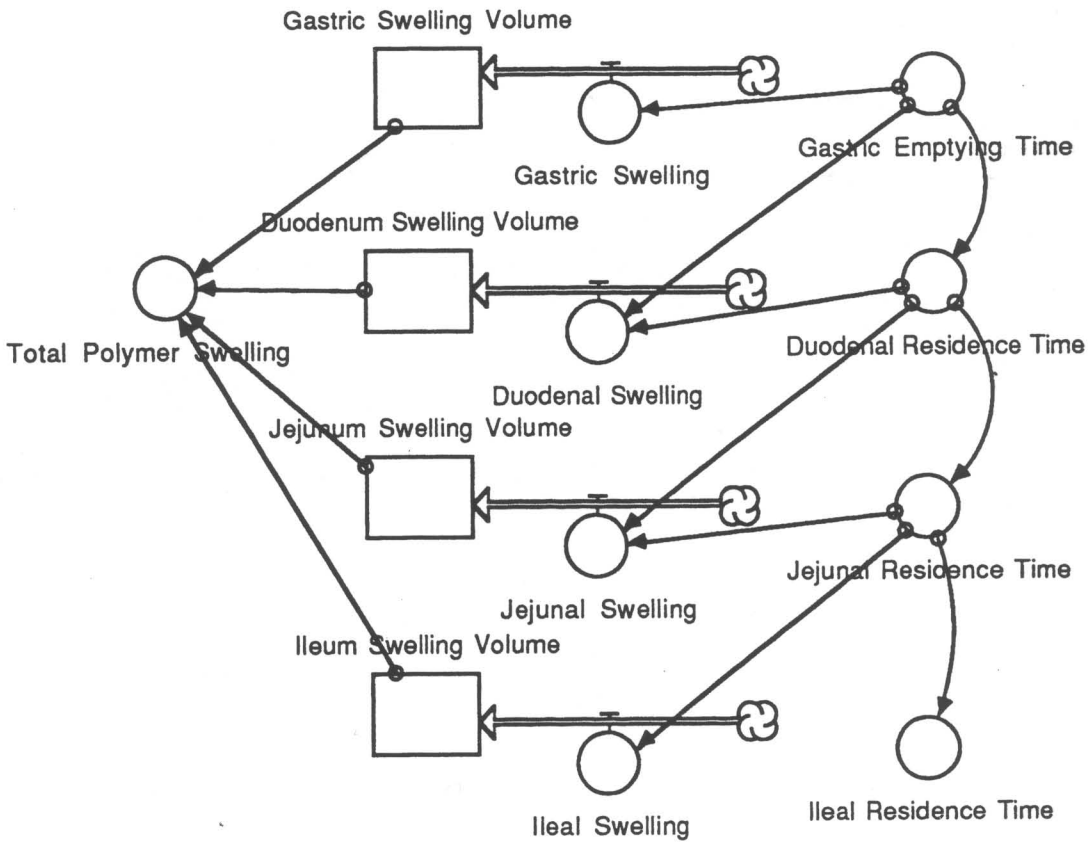
Gastric Swelling Volume
Gastric Swelling
Gastric Emptying Time
Duodenum Swelling Volume
Total Polymer Swelling
Duodenal Swelling
Duodenal Residence Time
Jejunum Swelling Volume
Jejunal Swelling
Jejunal Residence Time
Ileum Swelling Volume
Ileal Swelling
Ileal Residence Time

Figure A-11 : Structural equations and program listing for the model of hydroxypropyl methyl cellulose swelling as it moves through the gastrointestinal tract of the originally fasted human as printed out in the equation window of STELLA II™.

```
Duodenum_Swelling_Volume(t) = Duodenum_Swelling_Volume(t - dt)
+ (Duodenal_Swelling) * dt
INIT Duodenum_Swelling_Volume = 0

INFLOWS:
Duodenal_Swelling = If (Time >Gastric_Emptying_Time And
Time<Duodenal_Residence_Time) then 85 else 0
Gastric_Swelling_Volume(t) = Gastric_Swelling_Volume(t - dt) +
(Gastric_Swelling) * dt
INIT Gastric_Swelling_Volume = 0

INFLOWS:
Gastric_Swelling = If Time < Gastric_Emptying_Time then 81 else 0
Ileum_Swelling_Volume(t) = Ileum_Swelling_Volume(t - dt) +
(Ileal_Swelling) * dt
INIT Ileum_Swelling_Volume = 0

INFLOWS:
Ileal_Swelling = If Time > Jejunal_Residence_Time then 96 else 0
Jejunum_Swelling_Volume(t) = Jejunum_Swelling_Volume(t - dt) +
(Jejunal_Swelling) * dt
INIT Jejunum_Swelling_Volume = 0

INFLOWS:
Jejunal_Swelling = If Time > Duodenal_Residence_Time and Time <
Jejunal_Residence_Time then 96 else 0
Duodenal_Residence_Time = Gastric_Emptying_Time + 0.1
Gastric_Emptying_Time = 1.5
Ileal_Residence_Time = Jejunal_Residence_Time + 3.3
Jejunal_Residence_Time = Duodenal_Residence_Time + 2.2

Total_Polymer_Swelling = Gastric_Swelling_Volume +
Duodenum_Swelling_Volume + Jejunum_Swelling_Volume +
Ileum_Swelling_Volume
```

Figure A-12 : Time course of hydroxypropyl methyl cellulose swelling as it moves through the stomach, duodenum, jejunum and ileum in the originally fasted human.

Time/hr	Gastric Swelling Volume	Duodenum Swelling Volume	Jejunum Swelling Volume	Ileum Swelling Volume	Total Polymer Swelling
0	0.00	0.00	0.00	0.00	0.00
0.1	8.10	0.00	0.00	0.00	8.10
0.2	16.20	0.00	0.00	0.00	16.20
0.3	24.30	0.00	0.00	0.00	24.30
0.4	32.40	0.00	0.00	0.00	32.40
0.5	40.50	0.00	0.00	0.00	40.50
0.6	48.60	0.00	0.00	0.00	48.60
0.7	56.70	0.00	0.00	0.00	56.70
0.8	64.80	0.00	0.00	0.00	64.80
0.9	72.90	0.00	0.00	0.00	72.90
1	81.00	0.00	0.00	0.00	81.00
1.1	89.10	0.00	0.00	0.00	89.10
1.2	97.20	0.00	0.00	0.00	97.20
1.3	105.30	0.00	0.00	0.00	105.30
1.4	113.40	0.00	0.00	0.00	113.40
1.5	121.50	0.00	0.00	0.00	121.50
1.6	121.50	8.50	0.00	0.00	130.00
1.7	121.50	8.50	9.60	0.00	139.60
1.8	121.50	8.50	19.20	0.00	149.20
1.9	121.50	8.50	28.80	0.00	158.80
2	121.50	8.50	38.40	0.00	168.40
2.1	121.50	8.50	48.00	0.00	178.00
2.2	121.50	8.50	57.60	0.00	187.60
2.3	121.50	8.50	67.20	0.00	197.20
2.4	121.50	8.50	76.80	0.00	206.80
2.5	121.50	8.50	86.40	0.00	216.40
2.6	121.50	8.50	96.00	0.00	226.00
2.7	121.50	8.50	105.60	0.00	235.60
2.8	121.50	8.50	115.20	0.00	245.20
2.9	121.50	8.50	124.80	0.00	254.80
3	121.50	8.50	134.40	0.00	264.40
3.1	121.50	8.50	144.00	0.00	274.00
3.2	121.50	8.50	153.60	0.00	283.60
3.3	121.50	8.50	163.20	0.00	293.20
3.4	121.50	8.50	172.80	0.00	302.80
3.5	121.50	8.50	182.40	0.00	312.40
3.6	121.50	8.50	192.00	0.00	322.00
3.7	121.50	8.50	201.60	0.00	331.60
3.8	121.50	8.50	211.20	0.00	341.20
3.9	121.50	8.50	211.20	9.60	350.80
4	121.50	8.50	211.20	19.20	360.40
4.1	121.50	8.50	211.20	28.80	370.00
4.2	121.50	8.50	211.20	38.40	379.60
4.3	121.50	8.50	211.20	48.00	389.20

4.4	121.50	8.50	211.20	57.60	398.80
4.5	121.50	8.50	211.20	67.20	408.40
4.6	121.50	8.50	211.20	76.80	418.00
4.7	121.50	8.50	211.20	86.40	427.60
4.8	121.50	8.50	211.20	96.00	437.20
4.9	121.50	8.50	211.20	105.60	446.80
5	121.50	8.50	211.20	115.20	456.40
5.1	121.50	8.50	211.20	124.80	466.00
5.2	121.50	8.50	211.20	134.40	475.60
5.3	121.50	8.50	211.20	144.00	485.20
5.4	121.50	8.50	211.20	153.60	494.80
5.5	121.50	8.50	211.20	163.20	504.40
5.6	121.50	8.50	211.20	172.80	514.00
5.7	121.50	8.50	211.20	182.40	523.60
5.8	121.50	8.50	211.20	192.00	533.20
5.9	121.50	8.50	211.20	201.60	542.80
6	121.50	8.50	211.20	211.20	552.40
6.1	121.50	8.50	211.20	220.80	562.00
6.2	121.50	8.50	211.20	230.40	571.60
6.3	121.50	8.50	211.20	240.00	581.20
6.4	121.50	8.50	211.20	249.60	590.80
6.5	121.50	8.50	211.20	259.20	600.40
6.6	121.50	8.50	211.20	268.80	610.00
6.7	121.50	8.50	211.20	278.40	619.60
6.8	121.50	8.50	211.20	288.00	629.20
6.9	121.50	8.50	211.20	297.60	638.80
Final	121.50	8.50	211.20	307.20	648.40

Figure A-13 : Structural equations and program listing for the model of Carboxymethyl cellulose sodium salt swelling as it moves through the gastrointestinal tract of the originally fasted human as printed out in the equation window of STELLA II™.

```
Duodenum_Swelling_Volume(t) = Duodenum_Swelling_Volume(t - dt)
+ (Duodenal_Swelling) * dt
INIT Duodenum_Swelling_Volume = 0

INFLOWS:
Duodenal_Swelling = If (Time >Gastric_Emptying_Time And Time <
Duodenal_Residence_Time) then 196 else 0
Gastric_Swelling_Volume(t) = Gastric_Swelling_Volume(t - dt) +
(Gastric_Swelling) * dt
INIT Gastric_Swelling_Volume = 0

INFLOWS:
Gastric_Swelling = If Time < Gastric_Emptying_Time then 36.3 else 0
Ileum_Swelling_Volume(t) = Ileum_Swelling_Volume(t - dt) +
(Ileal_Swelling) * dt
INIT Ileum_Swelling_Volume = 0

INFLOWS:
Ileal_Swelling = If Time > Jejunal_Residence_Time then 196 else 0

Jejunum_Swelling_Volume(t) = Jejunum_Swelling_Volume(t - dt) +
(Jejunal_Swelling) * dt
INIT Jejunum_Swelling_Volume = 0

INFLOWS:
Jejunal_Swelling = If Time > Duodenal_Residence_Time and Time <
Jejunal_Residence_Time then 196 else 0

Duodenal_Residence_Time = Gastric_Emptying_Time + 0.1
Gastric_Emptying_Time = 1.5
Ileal_Residence_Time = Jejunal_Residence_Time + 3.3
Jejunal_Residence_Time = Duodenal_Residence_Time + 2.2

Total_Polymer_Swelling = Gastric_Swelling_Volume +
Duodenum_Swelling_Volume + Jejunum_Swelling_Volume +
Ileum_Swelling_Volume
```

Figure A-14 : Time course of carboxymethyl cellulose swelling as it moves through the stomach, duodenum, jejunum and ileum in the originally fasted human.

Time/hr	Gastric Swelling Volume	Duodenum Swelling Volume	Jejunum Swelling Volume	Ileum Swelling Volume	Total Polymer Swelling
0	0.00	0.00	0.00	0.00	0.00
0.1	3.63	0.00	0.00	0.00	3.63
0.2	7.26	0.00	0.00	0.00	7.26
0.3	10.89	0.00	0.00	0.00	10.89
0.4	14.52	0.00	0.00	0.00	14.52
0.5	18.15	0.00	0.00	0.00	18.15
0.6	21.78	0.00	0.00	0.00	21.78
0.7	25.41	0.00	0.00	0.00	25.41
0.8	29.04	0.00	0.00	0.00	29.04
0.9	32.67	0.00	0.00	0.00	32.67
1	36.30	0.00	0.00	0.00	36.30
1.1	39.93	0.00	0.00	0.00	39.93
1.2	43.56	0.00	0.00	0.00	43.56
1.3	47.19	0.00	0.00	0.00	47.19
1.4	50.82	0.00	0.00	0.00	50.82
1.5	54.45	0.00	0.00	0.00	54.45
1.6	54.45	19.60	0.00	0.00	74.05
1.7	54.45	19.60	19.60	0.00	93.65
1.8	54.45	19.60	39.20	0.00	113.25
1.9	54.45	19.60	58.80	0.00	132.85
2	54.45	19.60	78.40	0.00	152.45
2.1	54.45	19.60	98.00	0.00	172.05
2.2	54.45	19.60	117.60	0.00	191.65
2.3	54.45	19.60	137.20	0.00	211.25
2.4	54.45	19.60	156.80	0.00	230.85
2.5	54.45	19.60	176.40	0.00	250.45
2.6	54.45	19.60	196.00	0.00	270.05
2.7	54.45	19.60	215.60	0.00	289.65
2.8	54.45	19.60	235.20	0.00	309.25
2.9	54.45	19.60	254.80	0.00	328.85
3	54.45	19.60	274.40	0.00	348.45
3.1	54.45	19.60	294.00	0.00	368.05
3.2	54.45	19.60	313.60	0.00	387.65
3.3	54.45	19.60	333.20	0.00	407.25
3.4	54.45	19.60	352.80	0.00	426.85
3.5	54.45	19.60	372.40	0.00	446.45
3.6	54.45	19.60	392.00	0.00	466.05
3.7	54.45	19.60	411.60	0.00	485.65
3.8	54.45	19.60	431.20	0.00	505.25
3.9	54.45	19.60	431.20	19.60	524.85
4	54.45	19.60	431.20	39.20	544.45
4.1	54.45	19.60	431.20	58.80	564.05
4.2	54.45	19.60	431.20	78.40	583.65
4.3	54.45	19.60	431.20	98.00	603.25

4.4	54.45	19.60	431.20	117.60	622.85
4.5	54.45	19.60	431.20	137.20	642.45
4.6	54.45	19.60	431.20	156.80	662.05
4.7	54.45	19.60	431.20	176.40	681.65
4.8	54.45	19.60	431.20	196.00	701.25
4.9	54.45	19.60	431.20	215.60	720.85
5	54.45	19.60	431.20	235.20	740.45
5.1	54.45	19.60	431.20	254.80	760.05
5.2	54.45	19.60	431.20	274.40	779.65
5.3	54.45	19.60	431.20	294.00	799.25
5.4	54.45	19.60	431.20	313.60	818.85
5.5	54.45	19.60	431.20	333.20	838.45
5.6	54.45	19.60	431.20	352.80	858.05
5.7	54.45	19.60	431.20	372.40	877.65
5.8	54.45	19.60	431.20	392.00	897.25
5.9	54.45	19.60	431.20	411.60	916.85
6	54.45	19.60	431.20	431.20	936.45
6.1	54.45	19.60	431.20	450.80	956.05
6.2	54.45	19.60	431.20	470.40	975.65
6.3	54.45	19.60	431.20	490.00	995.25
6.4	54.45	19.60	431.20	509.60	1014.85
6.5	54.45	19.60	431.20	529.20	1034.45
6.6	54.45	19.60	431.20	548.80	1054.05
6.7	54.45	19.60	431.20	568.40	1073.65
6.8	54.45	19.60	431.20	588.00	1093.25
6.9	54.45	19.60	431.20	607.60	1112.85
Final	54.45	19.60	431.20	627.20	1132.45

Figure A-15 : Structural equations and program listing for the model of Carbopol 974P swelling as it moves through the gastrointestinal tract of the originally fasted human as printed out in the equation window of STELLA II™.

```
Duodenum_Swelling_Volume(t) = Duodenum_Swelling_Volume(t - dt)
+ (Duodenal_Swelling) * dt
INIT Duodenum_Swelling_Volume = 0

INFLOWS:
Duodenal_Swelling = If (Time >Gastric_Emptying_Time And Time <
Duodenal_Residence_Time) then 53.5 else 0
Gastric_Swelling_Volume(t) = Gastric_Swelling_Volume(t - dt) +
(Gastric_Swelling) * dt
INIT Gastric_Swelling_Volume = 0

INFLOWS:
Gastric_Swelling = If Time < Gastric_Emptying_Time then 31.4 else 0
Ileum_Swelling_Volume(t) = Ileum_Swelling_Volume(t - dt) +
(Ileal_Swelling) * dt
INIT Ileum_Swelling_Volume = 0

INFLOWS:
Ileal_Swelling = If Time > Jejunal_Residence_Time then 60.6 else 0

INFLOWS:
Jejunum_Swelling_Volume(t) = Jejunum_Swelling_Volume(t - dt) +
(Jejunal_Swelling) * dt
INIT Jejunum_Swelling_Volume = 0

INFLOWS:
Jejunal_Swelling = If Time >Duodenal_Residence_Time and Time<
Jejunal_Residence_Time then 53.5 else 0

Duodenal_Residence_Time = Gastric_Emptying_Time + 0.055
Gastric_Emptying_Time = 1.5
Ileal_Residence_Time = Jejunal_Residence_Time + 3.3
Jejunal_Residence_Time = Duodenal_Residence_Time + 2.2

Total_Polymer_Swelling = Gastric_Swelling_Volume +
Duodenum_Swelling_Volume + Jejunum_Swelling_Volume +
Ileum_Swelling_Volume
```

Figure A-16 : Time course of Carbopol 974P™ swelling as it moves through the stomach, duodenum, jejunum and ileum in the originally fasted human.

Time/hr	Gastric Swelling Volume	Duodenum Swelling Volume	Jejunum Swelling Volume	Ileum Swelling Volume	Total Polymer Swelling
0.00	0.00	0.00	0.00	0.00	0.00
0.10	3.14	0.00	0.00	0.00	3.14
0.20	6.28	0.00	0.00	0.00	6.28
0.30	9.42	0.00	0.00	0.00	9.42
0.40	12.56	0.00	0.00	0.00	12.56
0.50	15.70	0.00	0.00	0.00	15.70
0.60	18.84	0.00	0.00	0.00	18.84
0.70	21.98	0.00	0.00	0.00	21.98
0.80	25.12	0.00	0.00	0.00	25.12
0.90	28.26	0.00	0.00	0.00	28.26
1.00	31.40	0.00	0.00	0.00	31.40
1.10	34.54	0.00	0.00	0.00	34.54
1.20	37.68	0.00	0.00	0.00	37.68
1.30	40.82	0.00	0.00	0.00	40.82
1.40	43.96	0.00	0.00	0.00	43.96
1.50	47.10	0.00	0.00	0.00	47.10
1.60	47.10	5.35	0.00	0.00	52.45
1.70	47.10	5.35	5.35	0.00	57.80
1.80	47.10	5.35	10.70	0.00	63.15
1.90	47.10	5.35	16.05	0.00	68.50
2.00	47.10	5.35	21.40	0.00	73.85
2.10	47.10	5.35	26.75	0.00	79.20
2.20	47.10	5.35	32.10	0.00	84.55
2.30	47.10	5.35	37.45	0.00	89.90
2.40	47.10	5.35	42.80	0.00	95.25
2.50	47.10	5.35	48.15	0.00	100.60
2.60	47.10	5.35	53.50	0.00	105.95
2.70	47.10	5.35	58.85	0.00	111.30
2.80	47.10	5.35	64.20	0.00	116.65
2.90	47.10	5.35	69.55	0.00	122.00
3.00	47.10	5.35	74.90	0.00	127.35
3.10	47.10	5.35	80.25	0.00	132.70
3.20	47.10	5.35	85.60	0.00	138.05
3.30	47.10	5.35	90.95	0.00	143.40
3.40	47.10	5.35	96.30	0.00	148.75
3.50	47.10	5.35	101.65	0.00	154.10
3.60	47.10	5.35	107.00	0.00	159.45
3.70	47.10	5.35	112.35	0.00	164.80
3.80	47.10	5.35	117.70	0.00	170.15
3.90	47.10	5.35	117.70	6.06	176.21
4.00	47.10	5.35	117.70	12.12	182.27
4.10	47.10	5.35	117.70	18.18	188.33
4.20	47.10	5.35	117.70	24.24	194.39

4.30	47.10	5.35	117.70	30.30	200.45
4.40	47.10	5.35	117.70	36.36	206.51
4.50	47.10	5.35	117.70	42.42	212.57
4.60	47.10	5.35	117.70	48.48	218.63
4.70	47.10	5.35	117.70	54.54	224.69
4.80	47.10	5.35	117.70	60.60	230.75
4.90	47.10	5.35	117.70	66.66	236.81
5.00	47.10	5.35	117.70	72.72	242.87
5.10	47.10	5.35	117.70	78.78	248.93
5.20	47.10	5.35	117.70	84.84	254.99
5.30	47.10	5.35	117.70	90.90	261.05
5.40	47.10	5.35	117.70	96.96	267.11
5.50	47.10	5.35	117.70	103.02	273.17
5.60	47.10	5.35	117.70	109.08	279.23
5.70	47.10	5.35	117.70	115.14	285.29
5.80	47.10	5.35	117.70	121.20	291.35
5.90	47.10	5.35	117.70	127.26	297.41
6.00	47.10	5.35	117.70	133.32	303.47
6.10	47.10	5.35	117.70	139.38	309.53
6.20	47.10	5.35	117.70	145.44	315.59
6.30	47.10	5.35	117.70	151.50	321.65
6.40	47.10	5.35	117.70	157.56	327.71
6.50	47.10	5.35	117.70	163.62	333.77
6.60	47.10	5.35	117.70	169.68	339.83
6.70	47.10	5.35	117.7	175.74	345.89
6.80	47.10	5.35	117.7	181.8	351.95
6.90	47.10	5.35	117.7	187.86	358.01
Final	47.10	5.35	117.7	193.92	364.07

Figure A-17 : Structural equations and program listing for the model of Noveon AA1 (polycarbophil) swelling as it moves through the gastrointestinal tract of the originally fasted human as printed out in the equation window of STELLA II™.

```
Duodenum_Swelling_Volume(t) = Duodenum_Swelling_Volume(t - dt)
+ (Duodenal_Swelling) * dt
INIT Duodenum_Swelling_Volume = 0

INFLOWS:
Duodenal_Swelling = If (Time >Gastric_Emptying_Time And Time <
Duodenal_Residence_Time) then 56.1 else 0
Gastric_Swelling_Volume(t) = Gastric_Swelling_Volume(t - dt) +
(Gastric_Swelling) * dt
INIT Gastric_Swelling_Volume = 0

INFLOWS:
Gastric_Swelling = If Time < Gastric_Emptying_Time then 27.5 else 0
Ileum_Swelling_Volume(t) = Ileum_Swelling_Volume(t - dt) +
(Ileal_Swelling) * dt
INIT Ileum_Swelling_Volume = 0

INFLOWS:
Ileal_Swelling = If Time > Jejunal_Residence_Time then 56.1 else 0

Jejunum_Swelling_Volume(t) = Jejunum_Swelling_Volume(t - dt) +
(Jejunal_Swelling) * dt
INIT Jejunum_Swelling_Volume = 0

INFLOWS:
Jejunal_Swelling = If Time >Duodenal_Residence_Time and
Time<Jejunal_Residence_Time then 56.1 else 0

Duodenal_Residence_Time = Gastric_Emptying_Time + 0.1
Gastric_Emptying_Time = 1.5
Ileal_Residence_Time = Jejunal_Residence_Time + 3.3
Jejunal_Residence_Time = Duodenal_Residence_Time + 2.2

Total_Polymer_Swelling = Gastric_Swelling_Volume +
Duodenum_Swelling_Volume + Jejunum_Swelling_Volume +
Ileum_Swelling_Volume
```

Figure A-18 : Time course of Noveon AA1 (polycarbophil) swelling as it moves through the stomach, duodenum, jejunum and ileum in the originally fasted human.

Time/hr	Gastric Swelling Volume	Duodenum Swelling Volume	Ileum Swelling Volume	Jejunum Swelling Volume	Total Polymer Swelling
0.00	0.00	0.00	0.00	0.00	0.00
0.10	2.75	0.00	0.00	0.00	2.75
0.20	5.50	0.00	0.00	0.00	5.50
0.30	8.25	0.00	0.00	0.00	8.25
0.40	11.00	0.00	0.00	0.00	11.00
0.50	13.75	0.00	0.00	0.00	13.75
0.60	16.50	0.00	0.00	0.00	16.50
0.70	19.25	0.00	0.00	0.00	19.25
0.80	22.00	0.00	0.00	0.00	22.00
0.90	24.75	0.00	0.00	0.00	24.75
1.00	27.50	0.00	0.00	0.00	27.50
1.10	30.25	0.00	0.00	0.00	30.25
1.20	33.00	0.00	0.00	0.00	33.00
1.30	35.75	0.00	0.00	0.00	35.75
1.40	38.50	0.00	0.00	0.00	38.50
1.50	41.25	0.00	0.00	0.00	41.25
1.60	41.25	5.61	0.00	0.00	46.86
1.70	41.25	5.61	0.00	5.61	52.47
1.80	41.25	5.61	0.00	11.22	58.08
1.90	41.25	5.61	0.00	16.83	63.69
2.00	41.25	5.61	0.00	22.44	69.30
2.10	41.25	5.61	0.00	28.05	74.91
2.20	41.25	5.61	0.00	33.66	80.52
2.30	41.25	5.61	0.00	39.27	86.13
2.40	41.25	5.61	0.00	44.88	91.74
2.50	41.25	5.61	0.00	50.49	97.35
2.60	41.25	5.61	0.00	56.10	102.96
2.70	41.25	5.61	0.00	61.71	108.57
2.80	41.25	5.61	0.00	67.32	114.18
2.90	41.25	5.61	0.00	72.93	119.79
3.00	41.25	5.61	0.00	78.54	125.40
3.10	41.25	5.61	0.00	84.15	131.01
3.20	41.25	5.61	0.00	89.76	136.62
3.30	41.25	5.61	0.00	95.37	142.23
3.40	41.25	5.61	0.00	100.98	147.84
3.50	41.25	5.61	0.00	106.59	153.45
3.60	41.25	5.61	0.00	112.20	159.06
3.70	41.25	5.61	0.00	117.81	164.67
3.80	41.25	5.61	0.00	123.42	170.28
3.90	41.25	5.61	5.61	123.42	175.89
4.00	41.25	5.61	11.22	123.42	181.50
4.10	41.25	5.61	16.83	123.42	187.11
4.20	41.25	5.61	22.44	123.42	192.72

4.30	41.25	5.61	28.05	123.42	198.33
4.40	41.25	5.61	33.66	123.42	203.94
4.50	41.25	5.61	39.27	123.42	209.55
4.60	41.25	5.61	44.88	123.42	215.16
4.70	41.25	5.61	50.49	123.42	220.77
4.80	41.25	5.61	56.10	123.42	226.38
4.90	41.25	5.61	61.71	123.42	231.99
5.00	41.25	5.61	67.32	123.42	237.60
5.10	41.25	5.61	72.93	123.42	243.21
5.20	41.25	5.61	78.54	123.42	248.82
5.30	41.25	5.61	84.15	123.42	254.43
5.40	41.25	5.61	89.76	123.42	260.04
5.50	41.25	5.61	95.37	123.42	265.65
5.60	41.25	5.61	100.98	123.42	271.26
5.70	41.25	5.61	106.59	123.42	276.87
5.80	41.25	5.61	112.20	123.42	282.48
5.90	41.25	5.61	117.81	123.42	288.09
6.00	41.25	5.61	123.42	123.42	293.70
6.10	41.25	5.61	129.03	123.42	299.31
6.20	41.25	5.61	134.64	123.42	304.92
6.30	41.25	5.61	140.25	123.42	310.53
6.40	41.25	5.61	145.86	123.42	316.14
6.50	41.25	5.61	151.47	123.42	321.75
6.60	41.25	5.61	157.08	123.42	327.36
6.70	41.25	5.61	162.69	123.42	332.97
6.80	41.25	5.61	168.30	123.42	338.58
6.90	41.25	5.61	173.91	123.42	344.19
Final	41.25	5.61	179.52	123.42	349.80